Title
KINETICS OF A DENSE CULTURE FERMENTATION

Authors
Sortland, Lyman Dale
Wilke, Charles R.

Publication Date
1968-06-24

UCRL-18340

cy. 2

University of California

Ernest O. Lawrence Radiation Laboratory

KINETICS OF A DENSE CULTURE FERMENTATION

Lyman Dale Sortland and Charles R. Wilke

June 24, 1968

Berkeley, California

DISCLAIMER

Submitted as (Ph. D. Thesis)
by
Lyman Dale Sortland

UCRL-18340

UNIVERSITY OF CALIFORNIA

Lawrence Radiation Laboratory
Berkeley, California

AEC Contract No. W-7405-eng-48

KINETICS OF A DENSE CULTURE FERMENTATION

Lyman Dale Sortland and Charles R. Wilke

June 24, 1968

KINETICS OF A DENSE CULTURE FERMENTATION

Lyman Dale Sortland and Charles R. Wilke

Lawrence Radiation Laboratory
University of California
Berkeley, California

June 24, 1968

ABSTRACT

A fermentation system was designed and constructed to study the growth characteristics of micro-organisms at low and high cell concentrations. The technique used to develop high cell densities utilized a rotating micro-filtration unit to permit the removal of cell-free product from the fermenter. The fermenter volume and the filter were contained in a single unit composed of a series of concentric cylinders. The annuli served as the fermenter volume while the second outermost cylinder supported a micro-filtration membrane. Feed to the system was pumped at constant rates and the internal pressure built up to a value which would effect the required filtration rate. The system was operated batchwise and continuously with and without filtration.

The anaerobic growth characteristics of Streptococcus faecalus were determined at 37°C and pH 7.0 for batch, continuous and continuous with filtration modes of operation. Cell concentrations 45 times more concentrated than could be produced in batch culture were obtained using the filtration technique.

I. INTRODUCTION

Investigators have, in recent years, switched much of their efforts from studying the growth of micro-organisms in batch culture to investigating their growth in continuous culture. Batch culture by its very nature yields information on microbial processes which are in a state of flux and change. Only crude information as to the effect of various nutritional requirements on the physiology and metabolism of the cell can be determined since exhaustion of a necessary nutrient or product inhibition causes growth to cease. For these reasons one can only determine whether a certain nutrient recipe does or does not support growth and to a certain extent, how well.

The physiological state of micro-organisms grown in batch culture can be divided into three main regimes: (1) the lag period after innoculation where metabolic machinery of the cells is being organized to cope with the new environment, (2) the period of exponential growth or log phase where the organism is reproducing at the maximum rate possible under the prevailing growth conditions, and (3) finally the stationary phase where an essential nutrient is exhuasted or a metabolic product is formed which stops further multiplication. The largest number of cells and the largest amount of nutrient consumed occurs in the log phase, where the cell is under no restrictions as to growth rate except those imposed by its genetic heritage. This contrasts very strongly with the situation of the cell during continuous culture where the organism is always grown under conditions of a nutrient limitation (or product inhibition) except where the fermenter is operated near washout. Some investigators have attempted to use batch data to predict the performance of continuous fermenters and have succeeded fairly well with a given organism. Luedeking's[1] work with Lactobacillus delbruckii showed that batch data would indeed predict continuous performance and his results have been confirmed by Reilly.[2] Contrary results reported by Rosenberger and Elsden[3] for Streptococcus faecalus suggested that the metabolic pathways utilized by these bacteria during batch growth were different than those used during some conditions of continuous growth. Therefore, it would be difficult to predict continous performance from batch data alone.

Continuous fermentation allows the investigator to study cells under a variety of growth conditions and nutrient limitations on a steady state basis where the interference by transient behavioral characteristics is absent. The dynamic response of cells when subjected to sudden or cyclical changes in environment can be studied in a manner which is impossible to batch culture. Thus, continuous culture offers advantages in studying dynamics, nutrition and metabolic pathways in the microbial cell.

One of the main disadvantages of studying continuous fermentation is the time involved in going from one steady state to the next, a time which may stretch into many hours or even days if the dilution rate in the fermenter is small. Useful savings in time may be realized by employing batch culture for preliminary screening and testing of nutrient and growth characteristics.

The study of continuous fermentation has been in progress for some time and the various interactions of microbe and medium have been investigated by many workers. Few people have investigated the influence of cell density upon growth characteristics. Suppose a fermenter is operated continuously with two outlet streams, (1) an overflow stream having the same composition as the fermenter contents and (2) a cell-free product stream. At steady state the growth rates of cells is equal to their rate of removal and the concentration of cells is related to the rate of supply of the limiting nutrient. At a constant cell removal rate in the overflow, the microbial concentration is proportional to the ratio of cell-free product withdrawal to cell overflow rate. It should be possible to study the effect of cell interaction as a function of cell packing without the interference of medium and growth rate changes. From a practical point of view, growing micro-organisms in concentrated culture would increase the productivity per unit fermenter volume and could be of industrial importance if separation of cells from the broth could be done economically.

In order to investigate the continuous fermentation of dense bacterial cultures, an experimental fermenter was designed and built in which a rotating cylindrical microfilter separated cells from the broth

and allowed the removal of a cell-free effluent from the fermenter. Using this apparatus an investigation of the growth characteristics of Streptococcus faecalus was undertaken. Batch experiments were performed to obtain data on nutrient requirements and to obtain preliminary information about the conversion yields of substrate (glucose) to new cells. Following the development of a satisfactory nutrient recipe, continuous fermentation experiments with and without the removal of cell-free product were conducted.

A. A Brief Review of Fermentation Literature

Early studies of bacterial kinetics were made by Monod.[4] He demonstrated that micro-organisms growing with a single limiting substrate would utilize the substrate in direct proportion to the rate of growth. The growth of micro-organisms is autocatalytic in nature so that the growth rate is proportional to the number present multiplied by a specific growth rate constant. The second characteristic of microbial growth which Monod elucidated was the relation between this specific growth rate and the concentration of limiting substrate. He proposed an equation for the specific growth rate in terms of substrate concentration which was similar to that developed for enzyme kinetics by Michaelis and Menten.[5] Monod's model can be summarized by the following three equations:

$$\frac{dN}{dt} = \mu N \qquad (1)$$

$$\frac{dN}{dt} = - Y \frac{dS}{dt} \qquad (2)$$

$$\mu = \mu M \frac{S}{K_s + S} \qquad (3)$$

where:

N = cell concentration

t = time

μ = specific growth rate

μ_M = maximum specific growth rate

S = substrate concentration

K_s = saturation constant

Y = cell yield per unit substrate

Equation (1) is the expression for autocatalytic growth, Eq. (2) relates the substrate consumption to growth and Eq. (3) is the Michaelis-Menten form relating the growth rate to substrate concentration. This model has no provision for lags which do occur in microbial systems so that under transient growth conditions these equations may not be valid. Monod's model has been widely used to interpret microbial growth although it is not universally applicable.

Herbert[6] developed equations for continuous fermentations based on the Monod kinetic model. He showed that Aerobacter aerogenes and Torulu utilis followed the theoretical predictions fairly closely and that a stable steady state with substrate limitation could be established in continuous culture. Herbert also demonstrated the presence of an endogenous metabolism term for A. aerogenes. Luedeking and Piret[7] demonstrated that steady state conditions could be achieved in a single vessel continuous fermenter where toxic products of the fermentation limited growth in a particular manner. Northam[8] showed that steady state could be maintained under less stringent assumptions concerning the mechanism of product limited growth.

These early developments in continuous culture have been reviewed by Malek and Fencil[9] following two important symposia in 1960, the first in London in April dealing with continuous cultivation of micro-organisms and the second in Rome where the First International Fermentation Symposium was held in June. A comprehensive review of the mathematical models which have been developed to describe microbial processes has been compiled more recently by Edwards and Wilke.[10]

An interesting concept was used by Shu[11] during his development of a model to describe product accumulation in microbial processes. He incorporated into his model the concept of cell age, the time since the cell was formed by division from its parent. Using a series of exponential decay functions to represent the accumulation of product per unit weight of cell as a function of cell age, and coupled with a cell age distribution function, he developed equations for product accumulation for batch and continuous culture. Fredrickson and Tsuchiya[12] extended Shu's concept of cell age to develop a stochastic (probabilistic) model for microbial growth. Their model is, unfortunately, not very well suited to practical applications due to the difficulty in obtaining experimental values for the constants appearing in the distribution functions for growth and product formation. Tsuchiya et al.[13] have published a more detailed analysis of microbial dynamics where they attempt a number of approaches and models. They classify a model of population dynamics as being either distributed or segregated depending upon whether the culture is treated as a collection of individuals or as a unit of bio-mass. These models can be further divided into cases where the cell is assumed to have a structure, e.g. genetic fraction, a protein fraction, etc., or to have no structure. Furthermore, the models maybe either stochastic (probabilistic) or deterministic. The deterministic distributed models have the greater advantage for practical application since stochastic and segregated models impose considerable experimental difficulties.

Dynamics of microbial populations was the topic for a Seminar held in Japan in October 1965. The full procedings have been published.[14]

B. Previous Work Done on High Density Bacterial Fermentations

The concentration of micro-organisms grown in batch and continuous culture is usually on the order of a few grams dry weight per liter of broth. If the bio mass is considered to play the role of a catalyst in the conversion of substrate to product, then major

advantages in productivity would result from techniques whereby cell-free product could be removed from the fermentation system. Growth of micro-organisms is usually limited by one of two mechanisms; an essential nutrient is depleted in the medium or an inhibitory product of the metabolism is increased to a level which halts growth. To increase bacterial concentration beyond that possible in batch or continuous culture necessitates the continuous feeding of fresh medium and the removal of cell-free product from the fermentation system. There are a number of techniques to accomplish product removal. A possible method for large scale operation would be the continuous centrifugation of broth coupled with the recycle of cells to the fermenter. The use of a centrifuge for small scale experimentation is not too practical because of the large volumes of broth associated with the external lines and the centrifuge. Furthermore, an examination of the growth kinetics is made more difficult due to the changes undergone by the cells during their trip through the centrifuge and back to the fermenter. These changes are in response to the changing conditions of the medium in which they are residing. During the time spent in the external loop, the medium would be depleted of nutrients, and growth of cells would stop to be started again when the cells re-entered the fermenter. This cycling of the cell growth would hinder the investigation of steady state kinetics.

Exchange of nutrients and products between a growing culture separated from an external reservoir by a dialysis membrane is another method of producing dense cultures. Gerhardt and Gallup[15] developed a dialysis flask to grow high density cultures. Their apparatus consisted of a vessel partitioned by a dialysis membrane with fresh medium on one side and a growing culture on the other. The solutes were free to diffuse through the membrane while the micro-organisms were restricted to their compartment. As far as the cells were concerned, they were grown batch-wise and the apparatus was basically a batch fermenter with provision to exchange a cell-free product with the surroundings. Using this apparatus, Gerhardt and Gallup investigated a number of organisms and a variety of dialysis membranes. They found considerable increases in cell concentration when the growing culture was supplemented with nutrients derived

from the reservoir. They investigated the effect of bacterial concentration on the yield of cells per unit of substrate by using different ratios of fermenter volume to reservoir volume. Using Serratia marcescens, they found that cell concentration increased directly with increasing reservoir to fermenter volume ratios up to 10:1. Beyond this point, little increase in cell concentration occurred.

Using a more elaborate fermenter-dialysis system, Gallup and Gerhardt[16] investigated more fully the relationship between the yield constant of cells per unit of substrate and bacterial density. Their experimental apparatus consisted of a fermenter and a remote supply system which were interconnected using a plate and frame dialyser. Their test organism was S. marsescens and by combining various combinations of fermenter and reservoir volumes, they showed that conversion of substrate to cells was constant. The maximum concentration of cells achieved was 2 times 10^{12}/ml by total count which corresponded to 50% packed cell volume. Compared to batch culture, the concentration factor was approximately 10.

Development and testing of fermenter-dialysis systems has been a major effort of Gerhardt et al.[17,18,19,20] since the original work in 1963. They have developed a sterilizable plate and frame dialyser which reduces the holdup of liquid in the apparatus while increasing the fluid turbulance next to the membrane in order to increase the rate of mass transfer. A theoretical analysis of dialysis culture was made by Schultz and Gerhardt[21] based on Monod kinetics relating cell growth rate to substrate concentration and on simple models for membrane transport. Both the reservoir and the fermenter were operated in steady state, i.e., fresh medium from external sources flowed directly into both the fermenter and the reservoir. They concluded that at low flow rates, steady state concentration levels of cells should be inversely proportional to flow rate. Much higher cell production per unit of fermenter volume occurred, but at the expense of a lower yield of cells per unit of substrate. This lower yield was not due to changes in cell metabolism resulting from a concentration effect. It was caused by the loss of substrate via the reservoir effluent when operated at steady state.

C. Proposed Micro-filtration Technique

The use of dialysis poses two major difficulties for the investigation of high density cultures. The most important limitation is the slow rate of mass transfer through a dialysis membrane. Gerhardt and co-workers were restricted to concentration increase factors over batch of 10 or less. The mechanism of transfer is by diffusion and each molecular species in the broth will diffuse at different rates giving rise to medium compositions different than those in corresponding batch or continuous culture without dialysis. These problems led us to the present investigation of micro-filtration to separate cells from the liquid medium. The filter membranes which are manufactured by Millipore Corp. consist of a cellulose ester sheet with uniform pores comprising a large fraction of the filter membrane. The membrane used in the experiments was type WH with pore sizes of 0.45 microns. To improve the handling characteristics of regular Millipore membranes, type WH had incorporated in it a mono-filament weave of nylon. The void fraction and flow rates of pure water through the membrane are reduced somewhat due to the nylon micro-web.

If a sample of cells is filtered through a Millipore membrane, a cake of cells is built up next to the surface which rapidly reduces the rate of filtration to almost zero. To see if the rate of cake build-up could be reduced, an experimental apparatus similar to the plate and frame dialyser of Gerhardt et al. was constructed. The membrane and a support screen were constrained between two blocks of lucite with channels 1 cm x 1 cm x 100 cm machined into their surfaces. Culture medium containing cells was pumped through the channel on one side of the membrane at a high velocity and returned to the fermenter. Cell-free product passed through the membrane into the corresponding channel in the other lucite block and drained into a receiving vessel. A 5 to 10 psi pressure drop was maintained in the filter holder by adjusting a valve on the broth line down-stream of the filter. Preliminary data showed that after an initial large rate of filtration, the buildup of cake reduced the flow to a steady state value of approximately 3 ml/cm^2 hr.

Apparently further build-up of cake was halted by the liquid shear. The steady state filtration rate was quite small and it became clear that a scale-up of the plate and frame model to generate sufficient filtration capacity for a high density culture was not feasible. The broth hold-up in the filter and associated lines placed a severe restriction on the maximum cell concentration possible in the fermenter. Furthermore, the pumping rates required to limit cake build-up were quite large and heating problems were caused by the recycle pump.

To circumvent the problems caused by an external filtering system, a scheme was proposed whereby filtration and growth occurred in the same vessel. The proposed apparatus consisted of two concentric cylinders with a Millipore membrane fastened to the inner cylinder. The annulus would serve as the growth chamber and the inner cylinder would be rotated to supply the shear to reduce cake formation. The filtrate would flow through the membrane and pass from the system via a hollow shaft supporting the rotating filter. Calculations, based on the filtration rates previously determined, showed that by minimizing the annular gap and by reducing the volume at each end of the fermenter, very concentrated cultures of micro-organism could be developed.

One of the restrictions which was imposed by the construction of the fermenter was that fermentations in which gas was evolved could be very difficult to handle because of high rates of gas evolution in dense cultures which would cause excessive carry-over of the broth into the exit line by entrainment in the narrow annular space.

An experimental investigation of the rates of filtration as a function of time and rotational speed was carried out by Bhagat and Wilke[22] using polystyrene spheres which approximated the size and density of bacteria. Their results paralleled those obtained by the plate and frame filter using micro-organisms. The equipment was operated at a constant pressure in the annulus with the filtrate rate measured as a function of time. High initial flows decreased asymptotically to a steady state. Bhagat and Wilke found that the steady state value of the filtration rate varied with square of the rotational speed while the

pressure drop across the membrane had little effect. They found that an increase in pressure drop caused a momentary flow increase which slowly decayed to the previous steady state value. Since the resistance to flow through the cake built up on the filter was directly proportional to the cake thickness, the cake must have increased in thickness to a point proportional to the pressure drop across the membrane. The mechanism proposed to explain the filtration characteristics assumed that a concentration gradient of particles was present in the near vicinity of the cake surface and that dynamic equilibrium was established between the drag forces imposed on the particles by the flow of fluid through the cake and the back diffusion of particles due to the concentration gradient. If the steady state was disturbed by the increased flow due to a pressure increase, then more cake would build up until equilibrium was again established.

D. Review of S. faecalus Literature

The growth of dense cultures indicated the desirability of studying anaerobic organisms so that the transfer of oxygen would not be necessary. The homo-fermentative lactic acid bacteria offered a fairly well defined system for investigation since the limiting nutrient, glucose, is metabolized primarily to a single product, lactic acid. A disadvantage in working with these organisms is their stringent nutritional requirements. We chose a laboratory strain of Streptococcus faecalus obtained from the Department of Bacteriology at the University of California, Berkeley. This strain had been originally procurred from I. C. Gunsalus of the University of Illinois but had undergone several re-isolations during its residence at Berkeley, including one made by this experimenter. The isolate which was used in this work was labeled A5. One of the first investigations of S. faecalus by Gunsalus and Niven[23] indicated that this organism ferments glucose by the Embden-Meyerhof pathway to lactic acid with a 90-95% yield. Gibbs, Sokatch and Gunsalus[24] using C^{14}- labelled glucose confirmed this finding. While lactate is the major product from the catabolism of glucose, Gunsalus

and Niven[23] showed that under pH conditions above 6.5, the yield of lactate decreased and the presence of small quantities of formate, acetate, ethanol and CO_2 were detected. Other investigators[25] have also observed this phenomenon. Beauchop and Elsden,[26] using C^{14}-labelled glucose, have shown that virtually none of the glucose catabolized appears in the cell material. Their studies, which were primarily devoted to the growth of micro-organisms in relation to their energy supply, showed that, for S. faecalus and a number of other organisms grown under conditions of glucose limitation, the production of new cells was directly proportional to the glucose supplied in the medium. The yield appeared to remain constant for S. faecalus when grown in complex as well as defined media. Furthermore, they were able to correlate the cell yield with the known pathways for the production of energy in the various organisms. They found that the rate of synthesis of new cells per mole of ATP produced was fairly constant and independent of the organism.

Rosenberger and Elsden[3] have studied the yields of S. faecalus grown in continuous culture in a semi-defined medium under conditions of glucose and of tryptophan limitation. With glucose acting as the limiting substrate, the yield of cells per mole of glucose consumed remained fairly constant with growth rate. When tryptophan was limiting, the yield constant was lower. Furthermore, the yield was not constant, but decreased with increasing concentrations of glucose until a limiting value was reached. With an excess of glucose available, the specific consumption rate of glucose was not dependent upon the growth rate of the organism and, in fact, remained roughly constant. Since some organisms are known to accumulate large amounts of polysaccharides when grown at slow rates in continuous culture with the nitrogen source as the limiting factor, Rosenberger and Elsden investigated the possibility of such storage in S. faecalus. They estimated the total carbohydrate in the cells from cultures of differing cell yield constants and found that the differences observed could not explain the large change in the yield. The fact that the rate of catabolism is not controlled by the

rate of growth led them to postulate the presence of an ATPase which disposed of the accumulated high energy phosphate produced from the glycolysis pathway.

A second interesting observation, which appeared from their study, concerned the products formed from the fermentation of glucose. Previously, Gunsales and Niven[23] had observed that at pH levels higher than 6.5, the yield of lactate became smaller while ethanol, acetic and formic acid made their appearance. Rosenberger and Elsden also found that formic and acetic acids were produced but not ethanol. They found no dependence on pH but rather a strong dependence on growth rate. The conversion of glucose to lactate became much lower as the growth rate decreased. An extrapolation of their data indicates that most of the glucose would show up in formic and acetic acids as the rate of growth approached zero. Their material balances accounted for nearly 100% of glucose at the higher rates and only 90% at lower growth.

Mahler and Cordes[27] in their discussion of the metabolism of carbohydrates, point out that in a large number of micro-organisms growing under anaerobic conditions, pyruvate (the direct precursor of lactate in the glycolytic pathway) can be converted to acetate and formate. This reaction sequence has not been completely ascertained but the steps involved appear to begin with the decarboxylation of pyruvate to acetate with the production of acetyl CoA. This product can either be converted to acetyl phosphate in the "phosphoroclastic" reaction, and then to acetate with the production of one mole of ATP or participate as acetyl CoA in a large number of reactions leading to incorporation of carbon into cell material. That the latter incorporation does not occur has been demonstrated by Beauchop and Elsden.[26] The fate of the pairs of electrons produced in the above reaction differ. Clostridia transfer them to protons and liberate them as molecular hydrogen. Other bacteria transfer them to the CO_2 produced in the decarboxylation step and produce formate. This latter reaction appears to occur in S. faecalus since formate is produced and the presence of hydrogen has never been reported. In any event, each mole undergoing the clastic reaction to formate is capable of producing an additional mole of ATP.

Toennies and Shockman[28] have summarized a number of their results dealing with the growth chemistry of S. faecalus. The main objective of their investigations was to determine the influence of various amino acids and vitamins which are required by the cell. They showed that the depletion of essential growth factors required for cell wall formation tends to produce cells which are subject to autolysis and, therefore, death, while depletion of essential factors which are not critically involved in wall synthesis can produce a variety of modified forms, which differ from exponentially growing cells by the possession of additional wall substance.

II. EXPERIMENTAL APPARATUS AND PROCEDURES

A schematic diagram of the fermentation system is shown in Fig. 1. The system consists of a fermenter designed to remove cell-free product via a rotating filter, feed pumps and supply vessels for both sterile nutrient and NaOH addition, and a recycle line to an external pH electrode holder. The lines were either 1/8" o.d. stainless steel tubing or 1/8" i.d. natural rubber tubing. The rubber tubing had a 1/8" wall which would withstand pressures in excess of 50 psi. A peristaltic pump was used in the recycle line to circulate broth through the electrode holder. This line also contained a glass section with a small rubber serum cap through which the experimental samples were withdrawn from the system.

This experimental set up was used for all modes of operation; batch, continuous stirred tank (CST) and continuous stirred tank with filtration. During batch and CST operation, the filter was removed and replaced by a stirring shaft. During the continuous modes of operation, the effluent containing the micro-organisms was removed through the bleed line in the top of the fermenter. This effluent was allowed to flow freely during the CST operation and went to drain via exit point A. When operating in the filtration mode, cell-containing effluent was pumped in controlled amounts through the peristaltic pump in the bleed line to the measuring buret.

The feed pumps were positive displacement, so that during filtration the difference in volume flow rate between the bleed and feed rates was forced through the filter membrane of the rotor and out to drain via the hollow central shaft of the rotor. The pressure in the fermenter was allowed to fluctuate to supply the driving force needed to affect the filtration. During the initial phases of operation before much of a pressure drop through the membrane was built up, the internal pressure was maintained above atmospheric by means of a pressure regulator in the filtrate exit line.

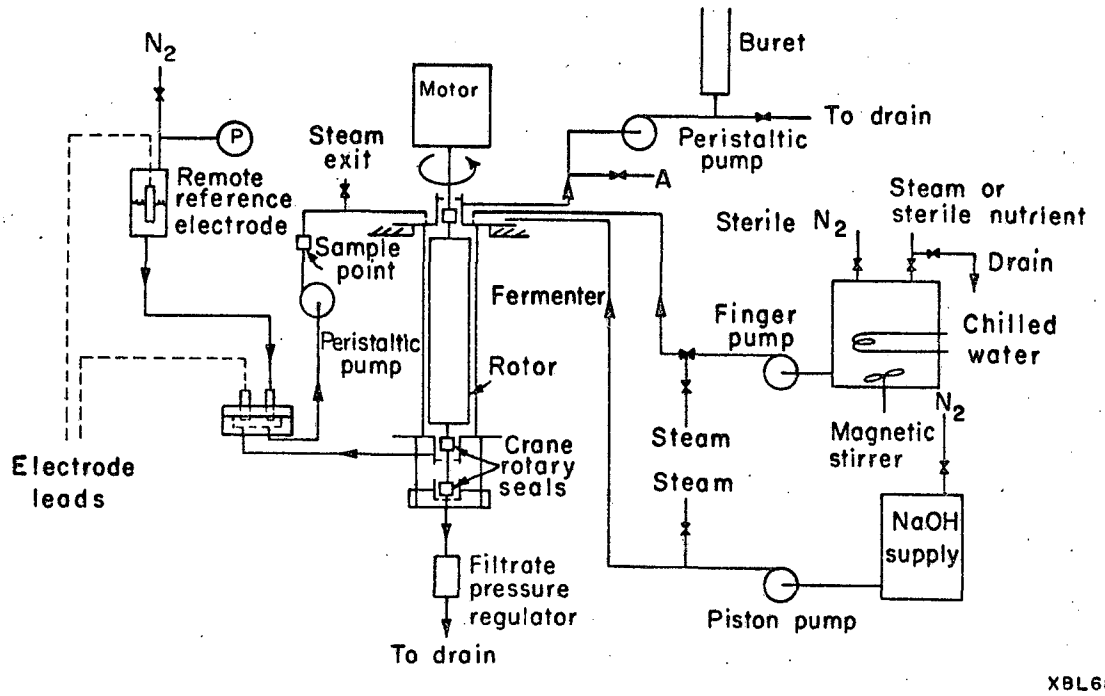

Fig. 1. A schematic diagram of the fermentation system.

A. The Fermenter

Figure 2 shows a photograph of the fermenter with the rotor in place. The fermenter consisted of a 3" i.d. pyrex pipe, one foot in length. The heads were constructed of stainless steel with the glass pipe fastened to the heads with compression rings and sealed with neoprene gaskets. Crane rotory seals with ceramic-carbon faces were used to contain the fermentation broth. The heads were machined externally to hold the stationary ceramic portion of the seal, a compression ring to exert force upon the teflon ring sealing the ceramic face to the head, and a bearing housing. The assembly was contained by a gland which screwed into threads machined into the head. On the culture side of the heads, a cavity for the carbon portion of the seal which rotated with the shaft was machined. Liquid connections to the fermenter were 1/8" stainless steel tubes welded into the heads, four in the top and one in the bottom. Two of the lines into the top head were used to feed nutrient medium and NaOH into the system; a third was the return line for the recycle. The fourth line, which exited at the extreme top of the seal cavity, was used to remove broth from the system during continuous operation. The line in the bottom head led to the pH electrode holder before returning to the fermenter via the top head.

B. Filtration Rotor

The rotor was designed to fulfil several purposes: (1) to support the membrane which would separate the micro-organisms from the broth, (2) to remove the filtrate from the fermenter, (3) to serve as an agitator to completely mix the culture, and (4) to achieve as high a filter area to volume ratio as possible. The ultimate density of a bacterial culture which can be grown in this type of system is directly proportional to the ratio of filter area to culture volume since the limiting step is the filtration rate obtainable under conditions of moderate pressure drop through the membrane. For this reason, care was taken to limit the volume of the fermenter in the end areas without

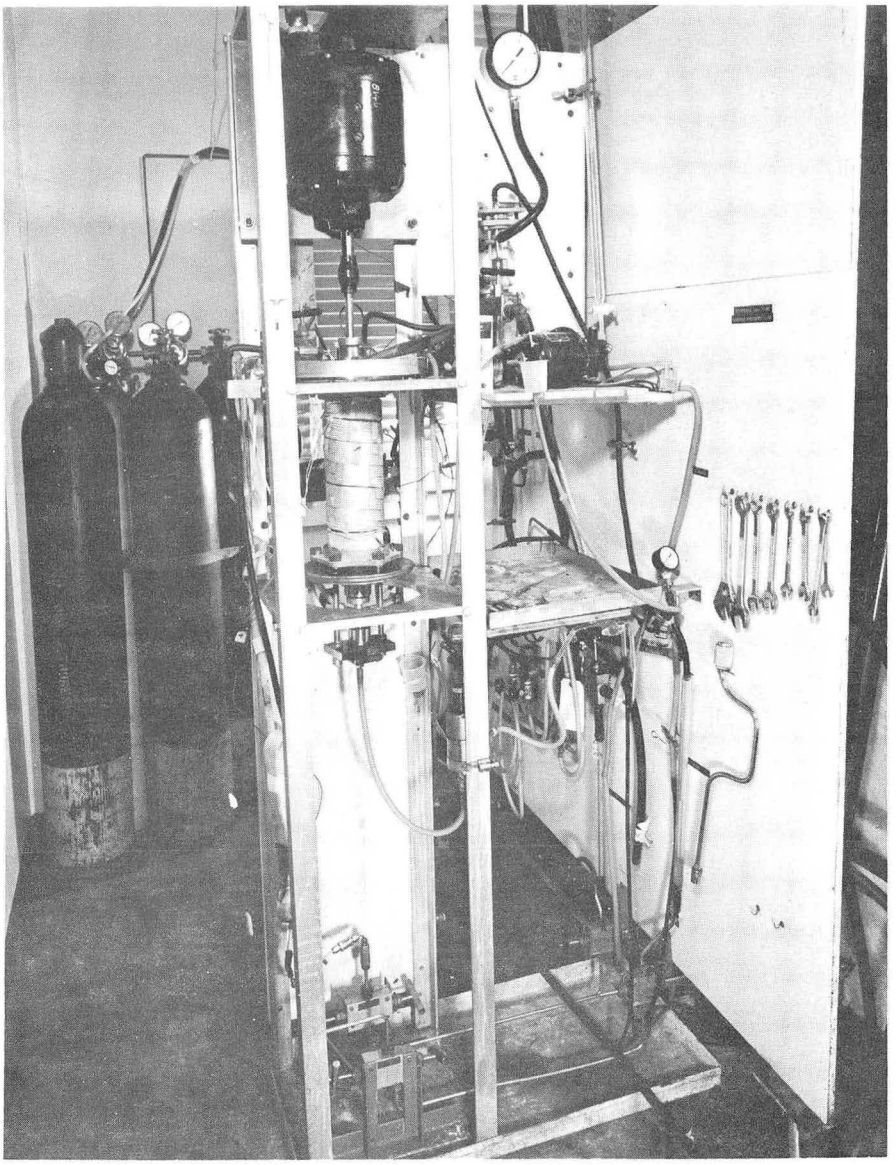

XBB 683-1028

Fig. 2. A photograph of the fermenter.

making assembly of the fermenter too difficult. Clearance at the top and bottom was restricted to 1/8" each. To accommodate the rotory seals, wells were machined into the heads so that as little culture volume as possible was added to the system. Another major fermenter volume was located in the annulus between the stationary outer cylinder and the rotating filter. There is a lower limit to the gap which can be tolerated because mixing of the broth becomes more difficult the smaller the gap becomes. In fact, special means had to be devised to assure that adequate mixing was achieved in the fermenter. The diameter of the filter rotor was chosen to be 2-1/2" which left a 1/4" annulus.

A Taylor Number of 5,600 was computed for this system using the fluid properties of water and a rotational speed of 600 RPM. Turbulent conditions normally prevail beyond Taylor Numbers of 400. Experiments using dye tracers showed that little or no axial mixing occurred. To improve the mixing characteristics of the system, an internal pumping arrangement was devised.

A schematic diagram of the rotor is shown in Fig. 3 and a photograph with the membrane attached in Fig. 4. The rotor was composed essentially of a series of concentric cylinders with a central cylinder, a 1/2" o.d. heavy walled stainless steel tube, forming the power shaft connecting the motor to the rotor. On this shaft were attached the rotating portions of the Crane seals. The remaining two cylinders with their end plates formed the filtrate unit which was connected to the central shaft by two shear pins. The bottom shear pin was hollow and connected the interior of the filtrate unit to the hollow shaft and served as the exit line for the filtrate. The filtrate flowed down the shaft, through an external seal and then exited from the system.

The external surface of the filtration unit was a perforated plate support for the filter membrane. The filter membrane was a rectangular sheet of type WH Millipore filter material which was wrapped around the support surface and glued along the seam with Silastic RTV 891 silicon rubber cement. After the cement had set, the ends were given a light coat of glue and sealed at the ends with "O" rings as shown in the diagram.

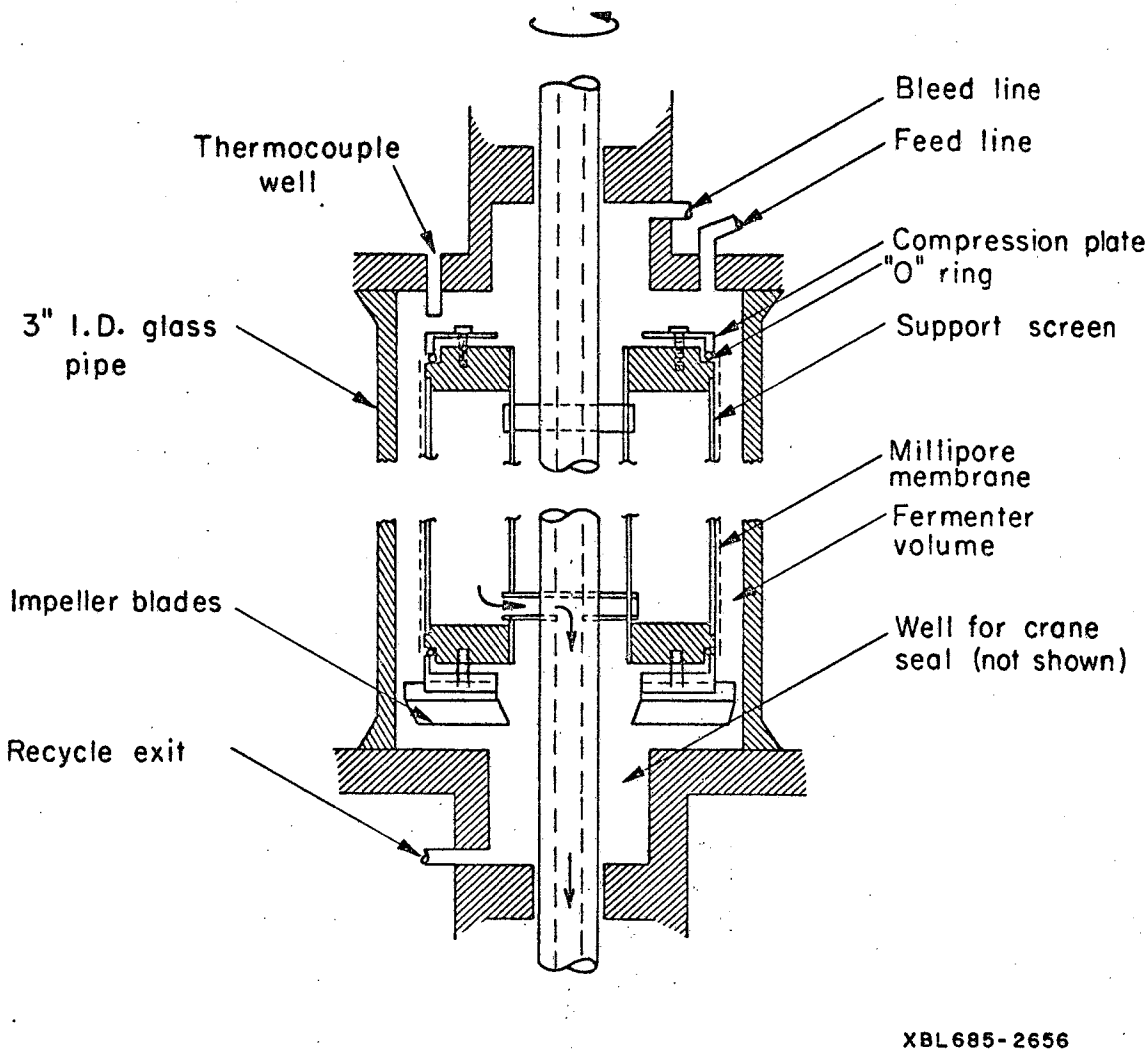

Fig. 3. A schematic diagram of the filtration rotor.

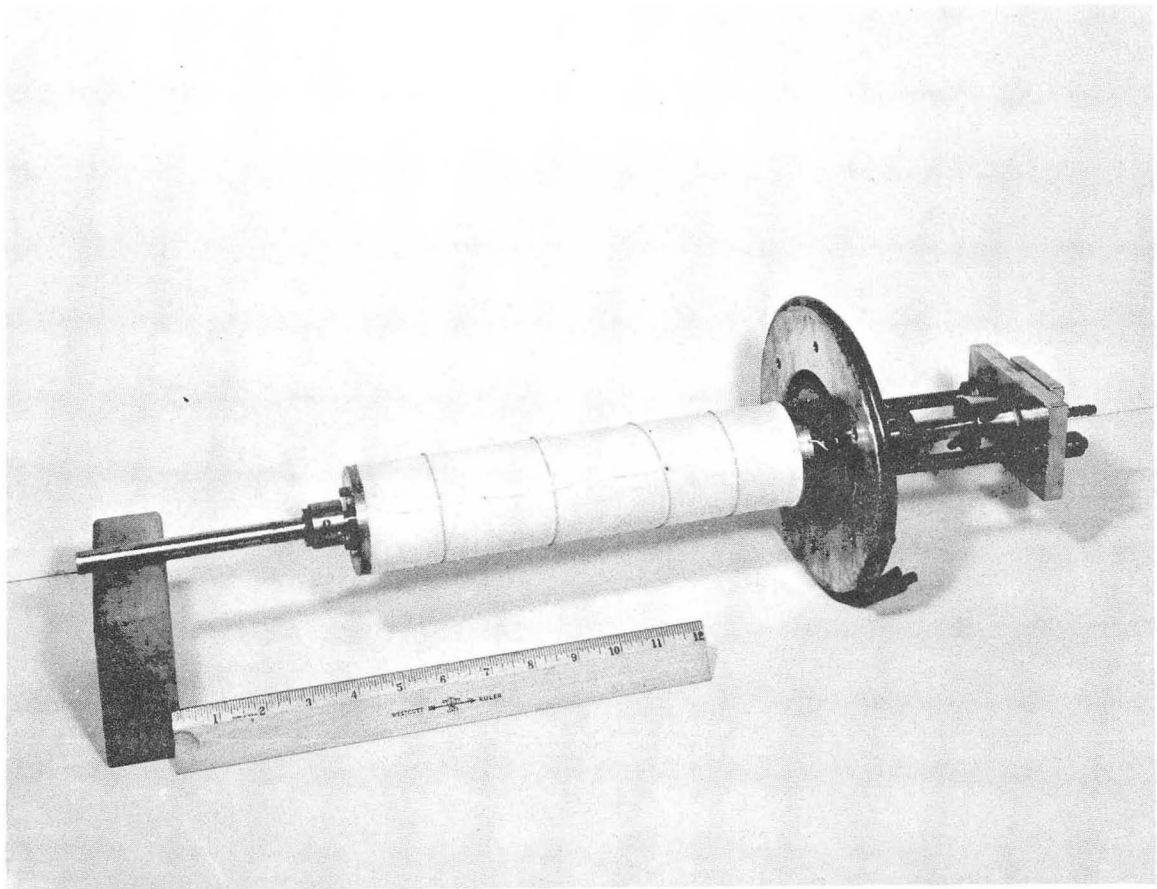

XBB 683-1030

Fig. 4. A photograph of the filtration rotor.

Attached to the bottom of the filtrate unit was a set of impeller blades which rotated with the filter. These impellers pumped the broth up the outside annulus and down through the inner annulus between the filtrate unit and the central shaft. This internal pumping action gave rise to excellent mixing. Dye tracer experiments showed that complete dispersion occurred within three to five seconds, while residence time distribution experiments demonstrated that the fermenter was uniformly mixed.

The area of the filter which was available for filtration was about 450 $cm.^2$ The area would have been larger except for the glued areas at the ends and along the seam which took up about 10% of the filter membrane. The fermenter volume including recycle lines was 620 ml. When the system was used for batch and continuous operation, the rotor was removed and the volume was 1360 ml.

C. Media Supply

Sterile nutrient was pumped into the fermenter by a Sigmamotor peristaltic pump from a 110 liter stainless steel supply tank. Approximate flow rates were set using the speed control box on the pump, and the actual rate was calculated from a knowledge of the effluent rates from the fermenter. Fresh supplies of sterile nutrient were prepared in smaller stainless tanks and asceptically transferred via steam sterilized high pressure hose to the large storage tank. Nitrogen pressure was used to effect the transfer. The smaller preparation tanks were 40 liter in volume and were designed to fit into standard vertical autoclaves for steam sterilization of the media. These tanks contained coils for rapid cooling after sterilization was completed.

Sodium hydroxide was added to the fermentation broth by means of a small piston pump with a variable stroke adjustment supplied by the Jaeco Pump Company. The pump was powered by a dc electric motor which was used to control the pumping rate to attain pH control. The NaOH was supplied from a 60 liter stainless tank. A photograph of the nutrient supply system is shown in Fig. 5.

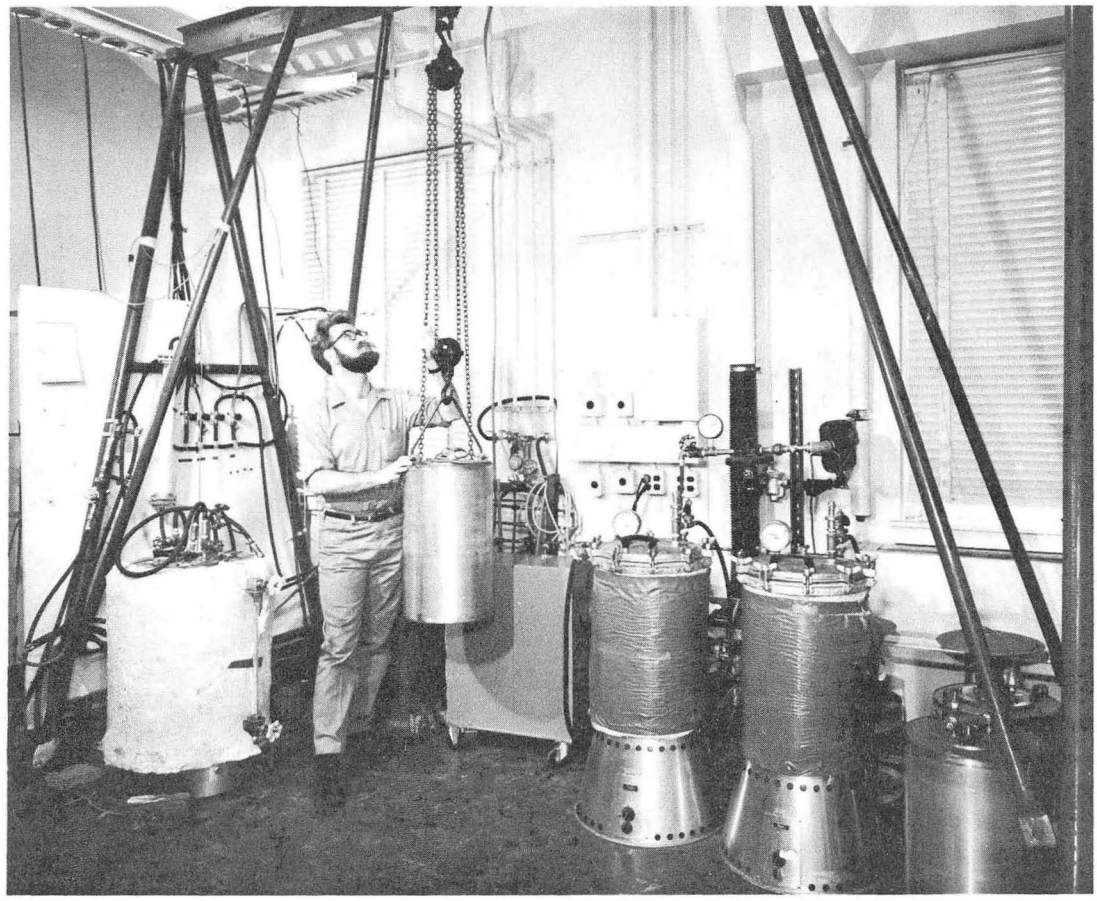

XBB 683-1027

Fig. 5. A photograph of the storage tanks and the nutrient make-up area.

D. Instrumentation Systems

Figure 6 shows a schematic diagram of the control systems used with the fermentation unit. The systems consisted of three motor control units, a closed loop temperature control unit for the fermenter and a closed loop pH control system. A multipoint recorder measured the temperature at various points in the fermenter with thermocouples.

The motor control units were simple variac controlled, full wave rectifying units designed to control the speed of dc motors. One of these units controlled the rotational speed of the filter while the others controlled the recycle pumping rate and the bleed effluent rate.

Temperature was measured by a copper-constantan thermocouple located in a well in the top head of the fermenter. The signal was recorded on a L and N Speedomax G recorder equipped with front set switches which were used for ON-OFF control of a heating tape wrapped around the fermenter. Two heating tapes equipped with variacs were used in parallel; one was operated continuously to carry the basic heating load while the other was controlled by the recorder to supply the fine control. Power input to the fermenter by the stirring action of the rotor and the friction in the seals necessitated the addition of a small cooling coil to the bottom head of the fermenter. This coil consisted of a copper tube wrapped around the edge of the head and soldered to it to increase the heat transfer. Circulation of tap water through the coil gave adequate cooling and resulted in good temperature control. By adjusting the voltage applied to the heating tapes, temperature control of $\pm$ 1/4 ^{o}C was obtained. The cycle time for the temperature fluctuations due to the ON-OFF mode of control was approximately ten minutes.

Since lactic acid was produced continuously by the metabolism of the organism studied, continuous pH control on a closed loop basis became necessary. Furthermore, an accurate record of the amount and rate of base addition was required.

The pH measuring electrodes were located in the recycle line in the fermenter. The signal from the electrodes was measured and

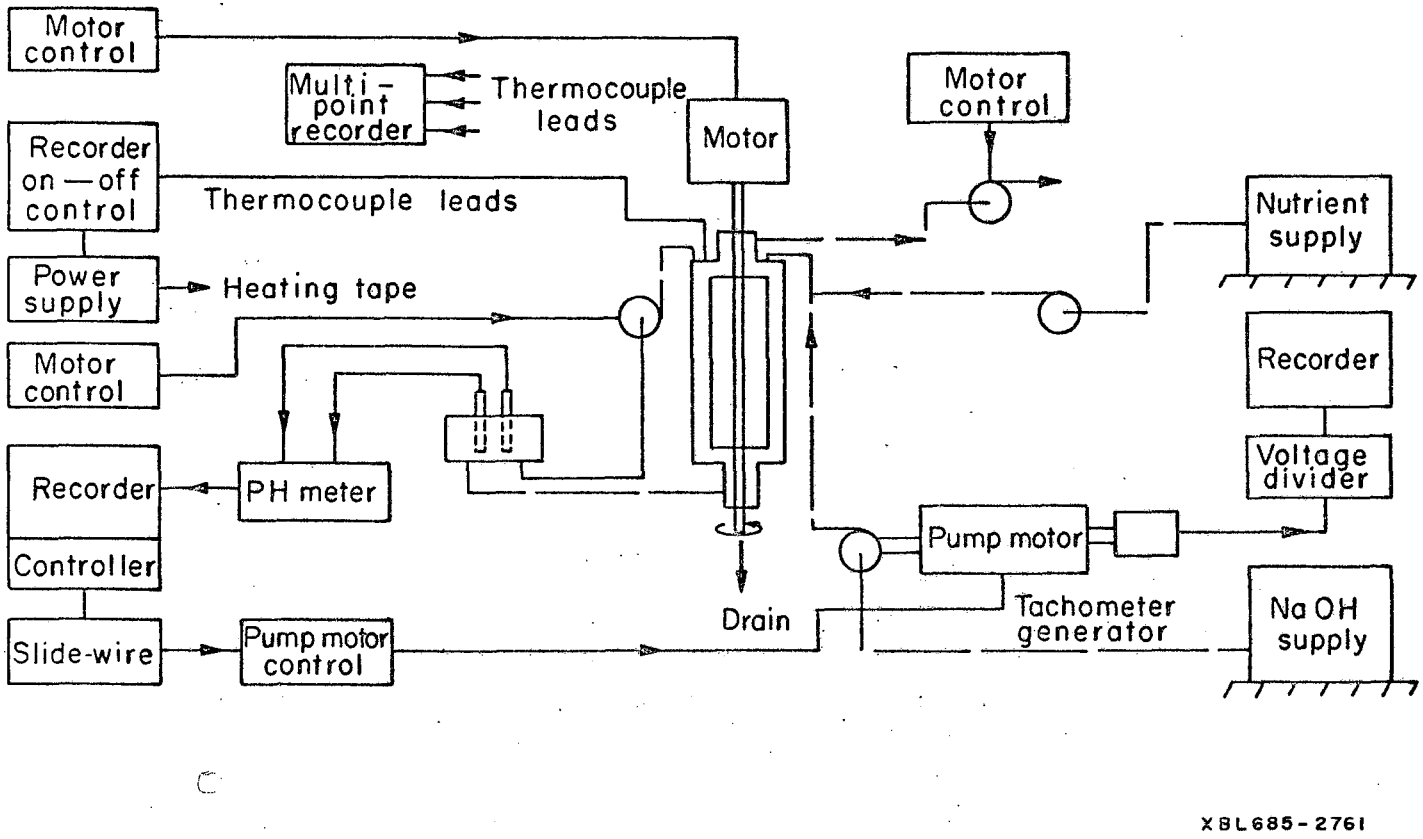

Fig. 6. A schematic diagram of the instrumentation systems.

displayed on a Beckman Model J Industrial pH Analyser. The Model J produced a millivolt signal proportional to the pH and it was recorded on a L and N Electronik 18 Recorder Controller. The final control element in the system was the NaOH addition pump. The speed of this pump was controlled by a General Electric Statatrol Drive and dc motor. The Statatrol unit was a silicon controlled rectifier with a variable potentiometer slidewire for adjusting the motor speed. The interconnection between the controller and the Statatrol unit was accomplished using a L and N re-transmitting slidewire unit equipped with an auxiliary slidewire. This auxilliary slidewire was used to control the Statatrol Drive. The position of slidewire was mechanically linked to the output signal of the Controller by the positioning motor in the re-transmitting slidewire unit. Using this type of control, the addition of sodium hydroxide could be varied from zero to the maximum in a continuous fashion.

One of the major problems which arose with the pH system involved the electrodes and their position. Insertion of the electrodes directly into the fermenter was not possible due to the lack of space. Even if sufficient space was made, the proximity of the rotor and its high rate of rotation would probably cause signal problems with the glass electrode. Placing the electrodes in either of the exit lines would not work due to the time lag between a pH change in the fermenter and the time that the electrodes picked up the upset. The only remaining possibility was to remove a recycle stream from the fermenter, pump it through an external electrode holder and return it to the main fermenter volume. Since the fermenter volume was designed to be fairly small, a large fluid volume in the recycle had to be avoided. A peristaltic pump which had a low working volume and could withstand 40 psi pressure could not be found and one had to be designed and built. The pump worked by compressing thick walled rubber tubing between a rotating arm and a fixed semicircular bearing surface. The arm was pivoted about the center of the circle and was driven by a dc motor whose speed could be varied to control the pumping rate. Using 1/8" i.d. tubing, pumping rates between zero and 75 ml per minute could be attained.

The electrode chamber was machined from stainless steel and was designed to hold two small electrodes. The fluid volume was as small as possible and contained approximately 5 ml of broth. The electrodes were sealed into the holders with "O" rings and glands. A major problem occurred in the operation of the control system which forced the premature termination of many of the continuous runs. Erroneous signals were generated by the electrodes which caused the control system to adjust the pH to the wrong value, thus ruining the experiment. The problem appeared to be in the electrodes which, before the run began, were giving accurate pH readings. The symptoms varied from one aborted run to the next but in all cases, the culprit appeared to be a malfunctioning reference electrode.

Checking the reference electrode showed that the fiber tip was slightly plugged. The electrode operated satisfactorily while measuring the pH of a buffer solution in a beaker. However, when that electrode was inserted into the holder with the recycle pump running, periodic fluctuations occurred in the signal which were in phase with the pumping rate of the peristaltic pump. Apparently the liquid junction of the reference electrode was not allowing an adequate flow of KCl to enter the system. Replacing the electrode would solve the problem for a short time but would not allow extended operation of the control system.

To circumvent the plugging problem, a remote reference electrode was constructed. The electrode was submerged in a KCl solution contained in a pressure tight vessel. An aqueous KCl salt bridge connected the electrode to the fermentation system. The orfice of the salt bridge was constructed from a piece of glass tubing with the end covered with type GS Millipore membrane. The membrane was glued to the glass with Silastic RTV 891 silicon rubber cement. To reduce the flow of electrolyte, the surface of the membrane was covered with glue with the exception of a very small area. This orifice had sufficient mechanical strength to withstand 10 to 15 psi pressure drop; it permitted only a few mls per day of electrolyte to flow and it did not get plugged.

The pressure in the fermenter fluctuated depending upon the filtration rate. In order that electrolyte flowed into the system, the

reference electrode was pressured with N_2 to a value above that in the fermenter. The pressure had no effect upon the measured pH.

A record of the rate of addition of NaOH into the fermentation system was accomplished by measuring and recording the rotational speed of the dc motor driving the pump. The motor had a double-ended shaft; one end drove the pump while the other was attached to a dc tachometer-generator manufactured by Servo-Tek Products Company, Inc. The tachometer-generator produced 2.2 volts per 1000 rpm with a linearity of 0.1%. The signal from the generator, after passing through a voltage divider, was recorded on a L and N Speedomax G Recorder. The system was designed so that full scale on the recorder represented 500 rpm and provision was made so that the range could be changed automatically. When the rpm exceeded 500, the electronics would cause the recorder to return to zero and the scale would represent a rpm range of 500 to 1000. Similarly, when the rpm became to low, the range would automatically be dropped down. The use of the scale expansion devise was required because of the wide range of NaOH addition rates anticipated. It would be impossible to achieve good accuracy at speeds of 0 to 200 rpm if full scale on the recorder corresponded to 2000 rpm.

To achieve a linear relationship between rpm and pumping rate, the original ball check valves which came with the pump had to be replaced by "O"-ring sealed check valves manufactured by the Nupro Co. The piston stroke length had to be set at 45% or greater to obtain linear rates with speed. Periodic checks of the calibration showed no change with time. The calibration showed that a speed of 1000 rpm corresponded to a flow rate of 3.04 ml/min.

E. Sterilization

A variety of methods were used to sterilize the experimental apparatus. Where possible, 15 psi steam was used. For the sterile nitrogen line and bacterial filters, a mixture of 10% ethylene oxide in carbon dioxide was used. The Millipore membrane could not withstand steam temperatures and still maintain its mechanical strength. The

preparation of the fermenter was done in two stages. First, the equipment was steam sterilized for several hours with the rotor in place but without the membrane being attached. The system was allowed to cool before the rotor was removed for installation of the membrane. After the glue had set, the rotor was replaced and a solution of 2% formaldehyde was circulated throughout the fermenter and the exit lines. The sterilant remained in the system for an hour at 50°C before it was removed and the equipment thoroughly flushed with sterile water. Sterility checks demonstrated that sterile conditions could be achieved and maintained for several days.

Steam has a deleterious effect on pH electrodes. During steam sterilization the electrodes were removed from their holder and replaced during the formaldehyde flushing step. Since steam only was used in the equipment sterilization for CST runs, the electrode holder was bypassed during steaming and sterilized separately with formaldehyde with the electrodes in place. After a sterile water flush, the holder was aseptically connected to the recycle lines. No problems with contamination were experienced using the above technique.

For steam sterilization to be effective, care must be taken to have live steam flow through every line and valve. Any dead end must be considered not sterile.

Prior to the installation of high pressure steam supply to the apparatus, the ethylene oxide-carbon dioxide mixture was used together with low pressure steam supplied by the verticle autoclaves, to sterilize the fermenter. This technique was used only for the batch runs. Steam was passed through the fermenter for several hours and then cooled. A vacuum pump was used to remove the air from the system before the gas was admitted. The pressure was adjusted to 10 psi, the temperature to 50°C and the system left to sterilize for at least four hours. The sterilant was removed and the system flushed thoroughly with sterile dry nitrogen. This technique was adequate but the straight steam sterilization was much preferable.

F. Sampling and Analyses

Samples of the fermentation broth were removed through a serum cap in the recycle line using a sterile syringe and were immediately immersed in an ice bath to stop the cells from growing. The cell mass was determined indirectly by measuring the optical density (OD) of the culture. Preliminary experiments showed that OD was linear with cell mass as long as the OD did not exceed 0.35. The OD was measured on a Beckman model DBG spectrophotometer at a wave length of 720 mu where the medium background absorption was minimal. The DBG is a double beam instrument and water was used in the reference beam. The OD of the cell free media was subtracted from the measurements of cell density to give a corrected OD. Since most of the samples had an OD much higher than 0.35, dilutions using a buffer-formalin solution were made. Samples from the continuous stirred tank runs were directly analysed for dry weight as well as OD. Dry weights were measured by filtering samples through pre-weighted Millipore filter discs and drying the membrane and collected cells overnight at 95°C before weighing. From the results for continuous runs CG and CJ, one unit of OD corresponded to a dry weight of 0.347 mg/ml.

The amount of NaOH added to the fermentation broth was determined from the record of the addition rate. The trace on the chart paper was cut out at 30 minute intervals and weighed. The amount of base added in this 30 minute interval was determined from the calibration of flow rate versus rpm.

Glucose was measured by two methods. Initially, the improved reducing sugar analysis developed by Kusmierek[29] was used. This technique reacted a known volume of boiling Fehling's solution with glucose which reduced cupric ion to cuprous. The remaining cupric ion was treated with an iodide solution with the formation of free iodine. The iodine was titrated with standard potassium thiosulfate to a starch endpoint. The thiosulfate titer was maximum when a water blank was used and decreased with increasing glucose concentration. The glucose present was determined from the difference between the blank and sample titers.

Difficulties were encountered in achieving reproducibility and considerable scatter occurred in the data. This method was used for all the batch runs and some of the CST runs. For the rest of the experiments, an enzymatic preparation for glucose analysis marketed by Worthington Biochemical Corp. under the trade name of Glucostat was used. Glucostat is a coupled enzyme system suitable for the quantitative and specific determination of glucose based on the following simplified scheme of reaction:

$$\text{glucose} + O_2 + H_2O \xrightarrow{\text{glucose oxidase}} H_2O_2 + \text{gluconic acid}$$

$$H_2O_2 + \text{reduced chromogen} \xrightarrow{\text{peroxidase}} \text{oxidized chromogen.}$$

Oxidized chromogen absorbs very strongly at 400 mμ and the amount of absorption is a measure of the glucose present.

Lactic acid was determined using the lactate dehydrogenase enzyme preparation produced by the Worthington Biochemical Corp. This enzyme, in conjunction with a hydrogen acceptor, oxidizes L-lactate to pyruvic acid. The acceptor used was potassium ferricyanide and the rate of reduction was followed spectrophotometrically at 420 mμ. The absorption of ferricyanide was a maximum at this wavelength while the absorption of ferrocyanide was negligible. The decrease in absorption of the sample following complete reaction was a direct measure of the lactate originally present.

III. EXPERIMENTAL RESULTS

The results from the experimental program are presented in the following sections, mainly in graphical form. The numerical data from the experimental runs are tabulated in the Appendix. The experiments are presented in order of increasing operating complexity, beginning with batch culture, then continuous culture and finally the continuous operation with filtration. The mathematical framework describing each mode of operation is included at the most convenient position.

The operating temperature and pH conditions were restricted to a single value each and they remained constant throughout the experimental program. The temperature was set at 37°C and the pH at 7.0.

A. Batch Fermentation

1. Experimental Results

Batch experiments were conducted to determine preliminary growth characteristics of S. faecalus and to develop a suitable nutrient medium for the continuous cultures. To simplify the interpretation of experimental results, the medium should be sufficient in all components except for one which is chosen to limit growth. Since the pathway of glucose metabolism was fairly well known, it was desired to use glucose as the limiting substrate.

The choice of a nutrient medium was made on the basis of cost, ease of preparation and future reproducibility of results. A completely defined medium for S. faecalus has been published by Toennies and Shockman.[28] This recipe contains some 44 components and an estimate of the cost for chemicals at the estimated flow rates in continuous culture with filtration showed that media costs would be in the thousands of dollars for the amount of experimental work envisioned. A semi-defined medium recipe published by Bauchop and Elsden[26] contained fewer components and replaced pure amino acids with a casein hydrolysate. This medium has the advantage of lower cost while maintaining fairly secure control of the nutrient composition since amino acid analyses of casein

are available.[30] Use of a well defined medium for microbial growth gives more control to the experimenter in studying the characteristics of cells from one lot of chemicals to the next. Results using a complex nutrient such as yeast extract can and do vary when different batches of yeast extract are used.

Preliminary batch experiments were conducted on the Bauchop and Elsden semi-defined medium to check the growth characteristics with our strain of S. faecalus. The first runs gave poor results with the log phase ending at an OD between 0.5 and 0.6, a point where very little of the glucose was consumed. Addition of sodium acetate to the medium improved the growth but still some component other than the energy source limited the growth rate. A series of experiments in which the various components of the medium were increased failed to give a clue to the source of the nutrient limitation. The possibility of product inhibition was investigated. The broth from Run S was centrifuged and the nutrient recipe was made up using the supernatent instead of water. The medium was heated briefly at 100°C to kill vegatative organisms before innoculating a fresh starter culture to begin the batch run. The growth curve was very similar to Run S with the only appreciable difference being a slight decrease in the maximum rate of growth. Run S had a doubling time of 24 minutes, while Run T doubled every 29 minutes. This experiment does not completely rule out product inhibition for a heat labile component may have been destroyed in the brief heating step. However, the inhibition of growth by low concentrations of lactate, less than 10 to 15 grams per liter, can be ruled out.

The experimental results for Run S are presented to illustrate the growth of S. faecalus on the semi-defined medium. The composition of the medium used is included in the Appendix. The mineral solution and glucose were sterilized separately from the remaining nutrients and asceptically added later. Approximately one liter of nutrient was prepared and asceptically transferred to the sterile fermenter. The pH was adjusted from its initial value of 6.6 to 7.0 by the addition of NaOH from the caustic storage tank. The temperature was adjusted to

37°C before the starter culture was innoculated. The innoculum used was 20 mls of an early stationary phase culture grown in a medium similar in composition to that used in the batch experiment. The initial OD in the fermenter after innoculation was between 0.04 and 0.05.

The experimental data for Run S is contained in Fig. 7 to 12 while the actual numbers are tabulated in the Appendix. Corrections to the raw data were made for the volume of base added and samples withdrawn using the scheme outlined by Luedeking.[1] The data presented are on the basis of one liter of nutrient.

Figure 7 shows the growth of the culture as a function of time. Growth is depicted by two variables, OD which is a measure of the dry weight and viable cell count. The log phase of growth is quite short and the greater fraction of growth occurs during the slow decrease in growth rate. Growth stops after five hours when the glucose is exhausted in the medium. Based on the OD curve, the maximum specific growth rate, μ, for this run is 1.79 hr^{-1} which corresponds to a doubling time of 24 min. The doubling time based on the viable counts in the log phase is smaller than that for OD but increases much faster as the culture growth rate slows. The size of a discrete cellular particle measured by the plating technique is obviously changing as time progresses. This observation will be discussed further when the size distribution for Run S as a function of time is presented a little later.

Figures 8, 9, and 10 represent the material balances for the batch experiment. According to the matabolic pathway, glucose should be converted to lactate almost stoichiometrically in the presence of excess glucose as is the case for this run. In Fig. 8 the lactate produced is plotted against the glucose remaining in the broth and the slope of the line drawn through the data gives the yield of lactate from glucose. The yield for Run S is approximately 97% and demonstrates that only very small amounts of other metabolic end products are produced.

The lactic acid produced by the cell was neutralized by the addition of NaOH. Since lactic acid is a relatively strong acid, all of the acid produced will be converted to sodium lactate at a pH of 7.0.

Therefore, the amount of base added should represent the amount of acid produced. Figure 9 shows the relation between NaOH addition and glucose consumption. For this run, the amount of NaOH added would indicate that conversion of glucose to lactate was only 88%. In Fig. 10, the base consumed is plotted versus the lactate concentration in the broth and shows that the amount of base added is approximately 9% less than the amount of lactate produced. The value for base consumption is lower than Run S than for other runs and may be due to experimental error.

The growth of S. faecalus on this medium appeared to be limited not by glucose as desired, but by some other nutrient. The effect of glucose consumption and its utilization to support new growth is demonstrated in Fig. 11 where the OD of the culture is plotted versus the lactate produced. Since the conversion of glucose to lactate is nearly stoichiometric, the use of lactate concentration as a measure of the amount of glucose consumed was preferred because the glucose analyses tended to have considerable experimental scatter. Figure 11 demonstrates an interesting phenomenon which was observed in all of the batch runs; namely that for a period of time in the initial stages, the production of energy represented by lactate formation was directly proportional to cell growth and then was followed by a changing relationship which suggests partial dissociation of cell growth and energy production. It is apparent that there is a shift in the utilization of energy by the cell. The very large rate of glucose consumption also suggests the possibility of dissociation of cell energy production and cell multiplication. The data beyond the dissociation point again appears to be linear with cell concentration. Other experiments did not show linearity in the later growth period and no systematic relationship could be determined. In fact, for some runs a stationary phase was reached before glucose exhaustion and the curve became almost vertical.

The rate of base addition is shown in Fig. 12 and is proportional to the rate of glucose consumption. This rate demonstrates that during the log period of growth, the consumption of NaOH is also exponential. However, during the phase of declining rate of cell multiplication, a corresponding decline in consumption rate did not occur. The exhaustion of glucose was very abrupt.

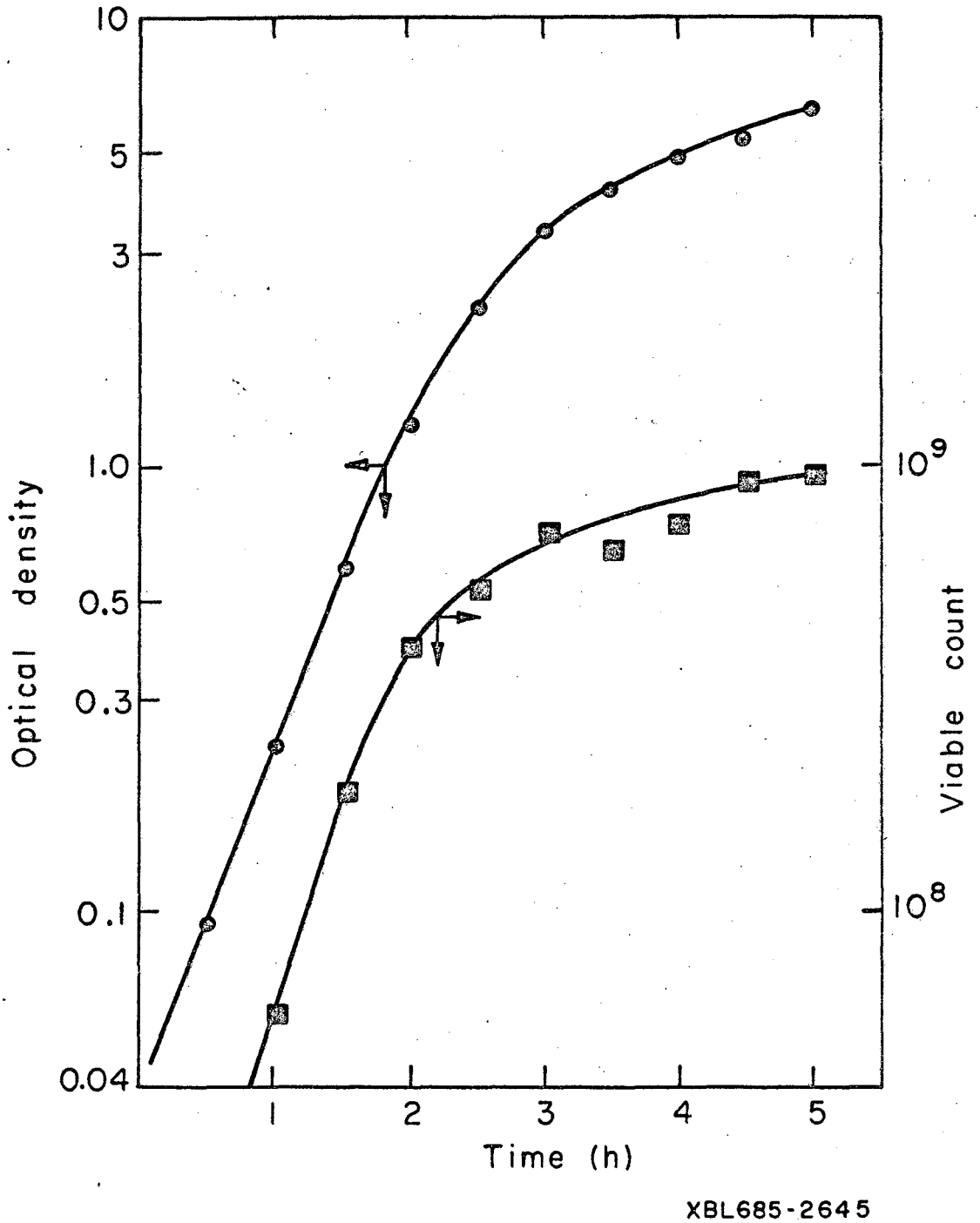

Fig. 7. The growth curve for batch Run S using the semi-defined medium. Cell concentration measured by optical density and viable count.

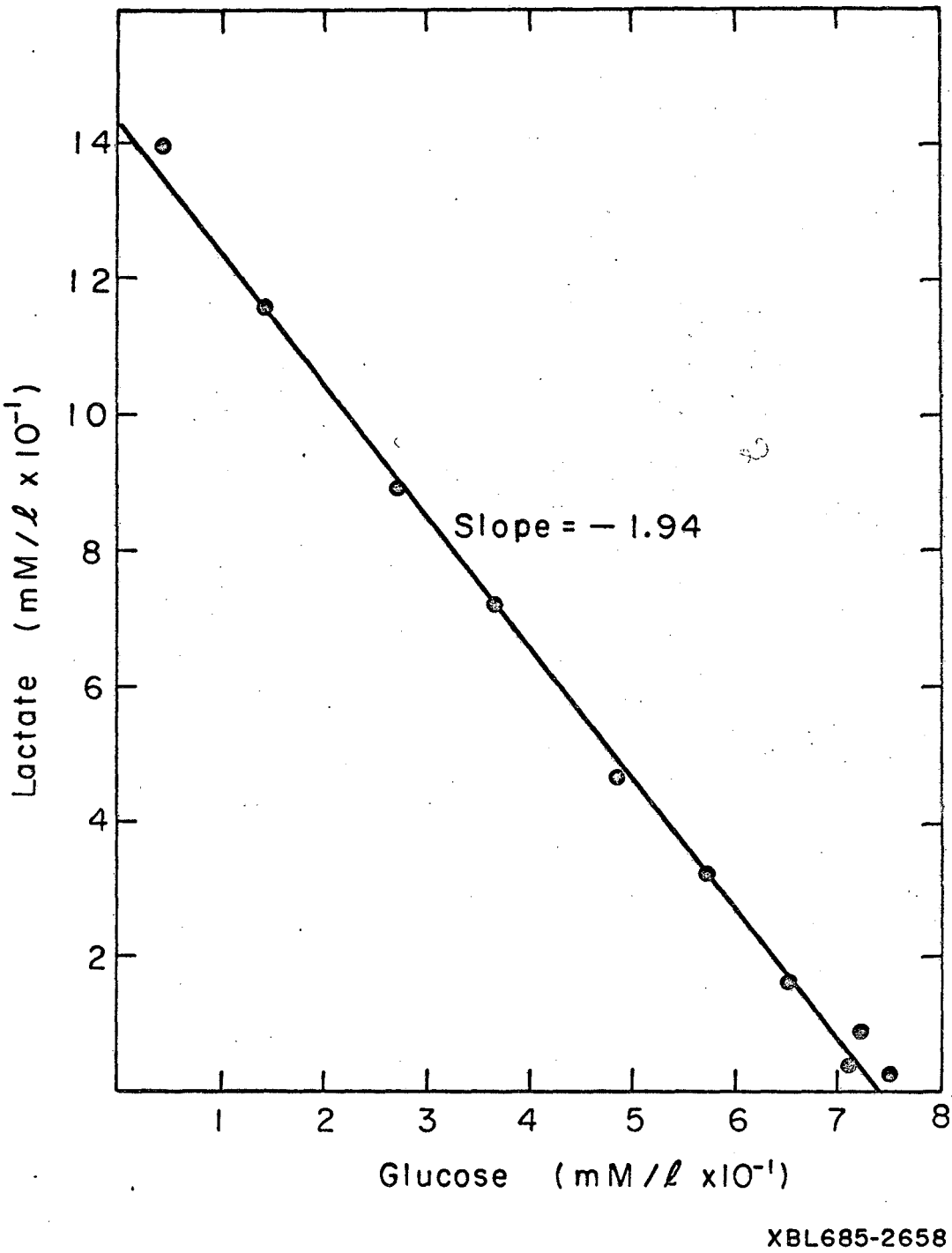

Fig. 8. The material balance on the glucose consumed in batch Run S; lactate produced versus glucose remaining in solution.

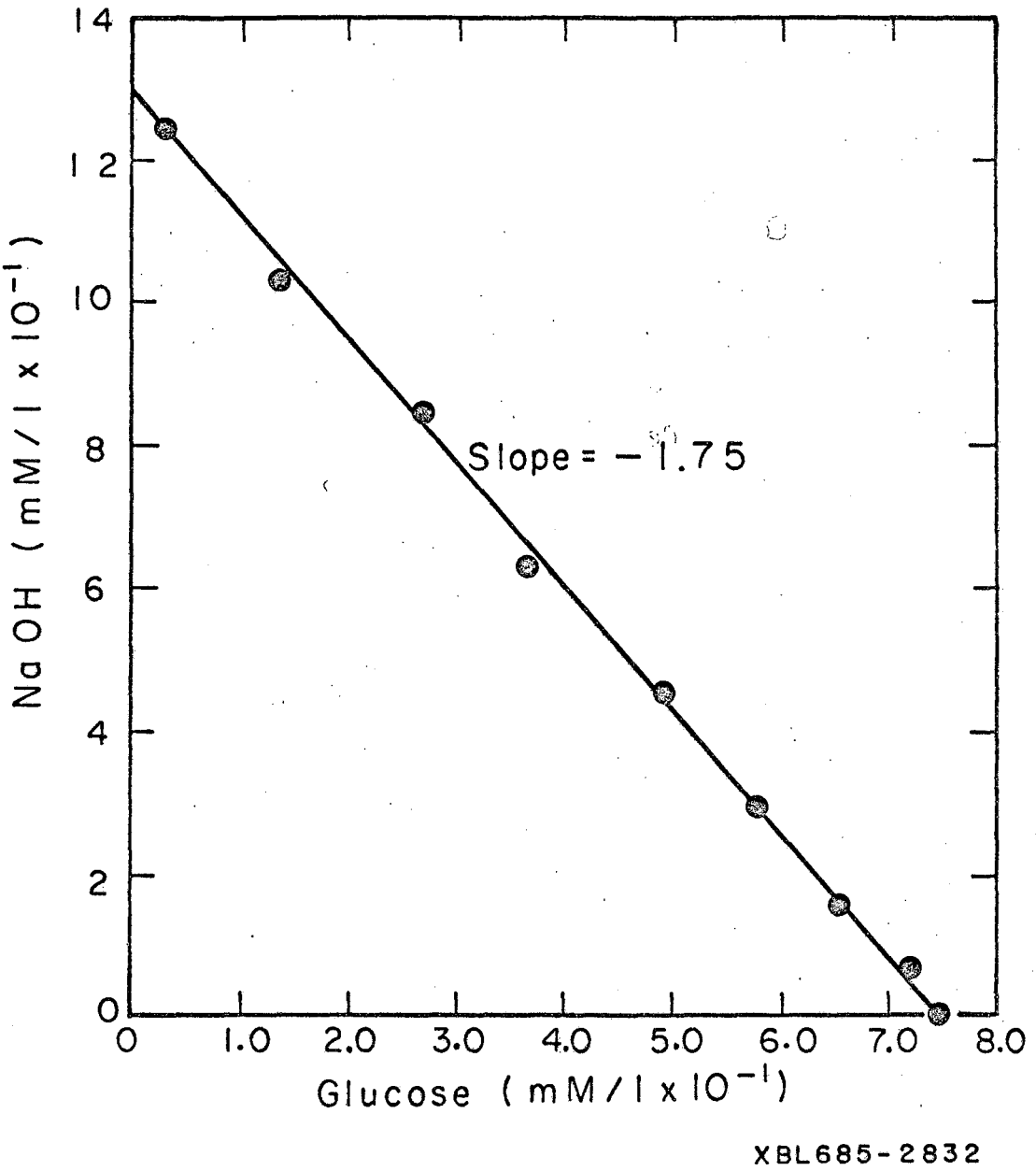

Fig. 9. The material balance on the glucose consumed in batch Run S; NaOH consumed versus glucose remaining in solution.

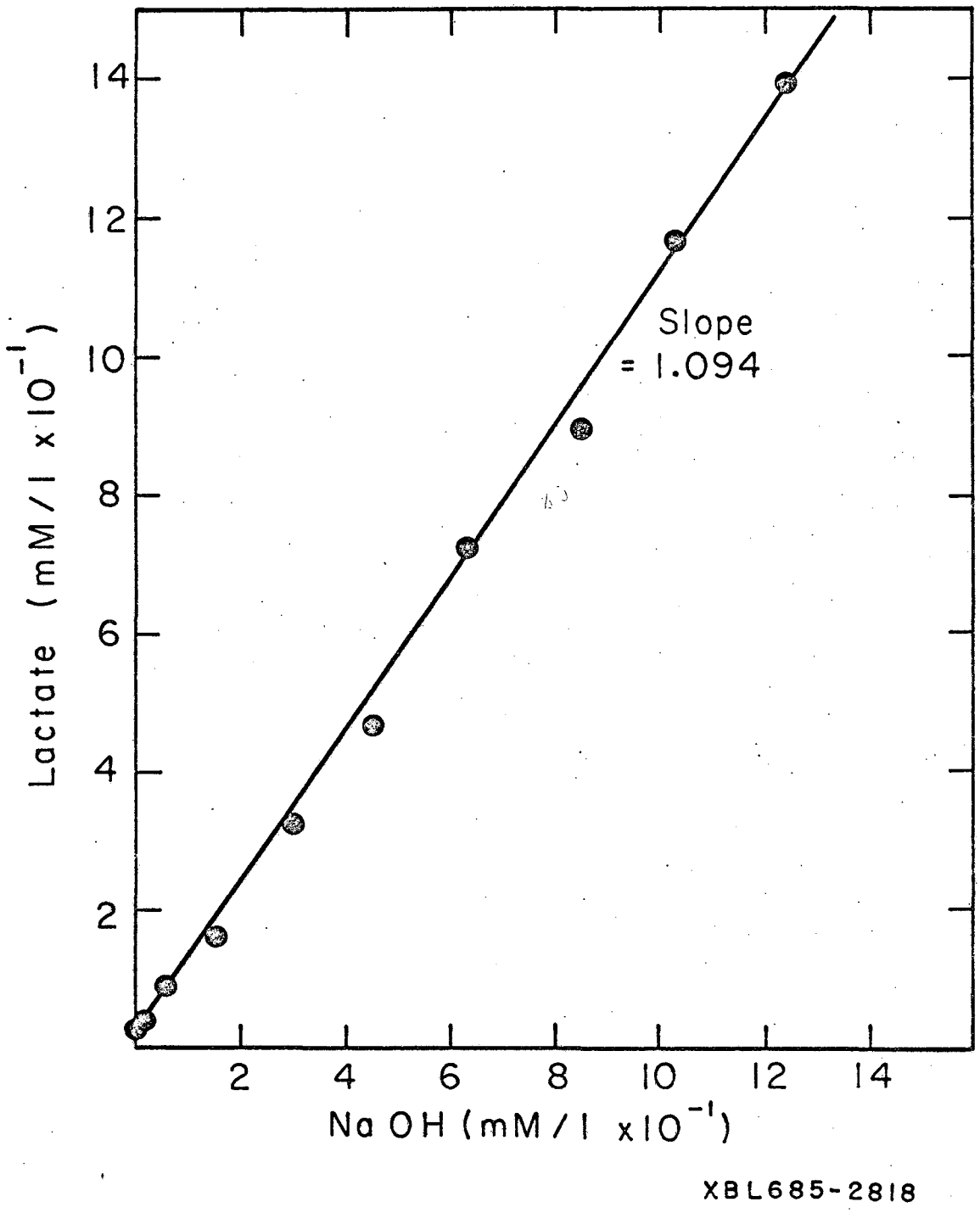

Fig. 10. The lactate produced versus the NaOH consumed during batch Run S.

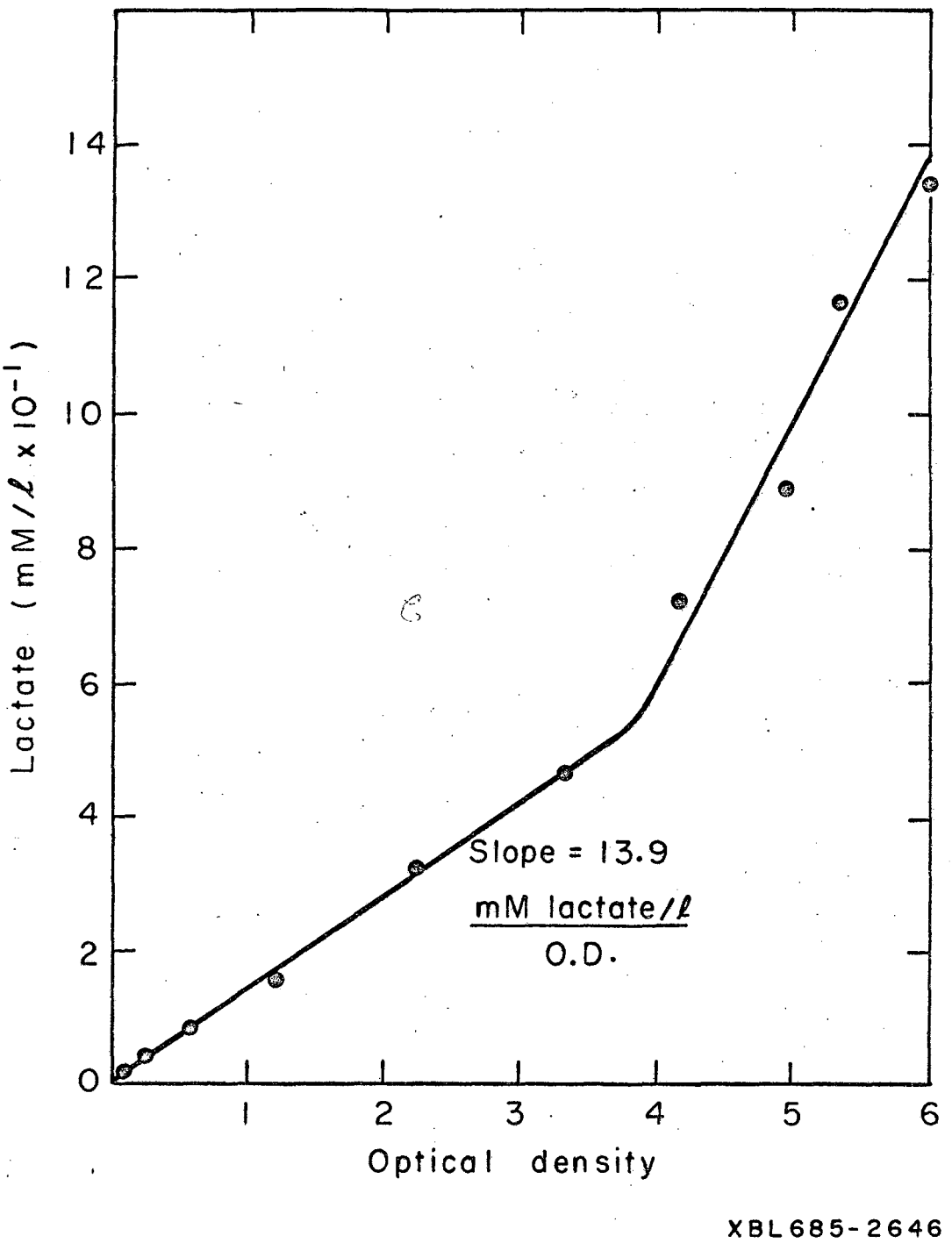

Fig. 11. Glucose consumption (as measured by lactate production) versus the bacterial cell concentration during batch Run S.

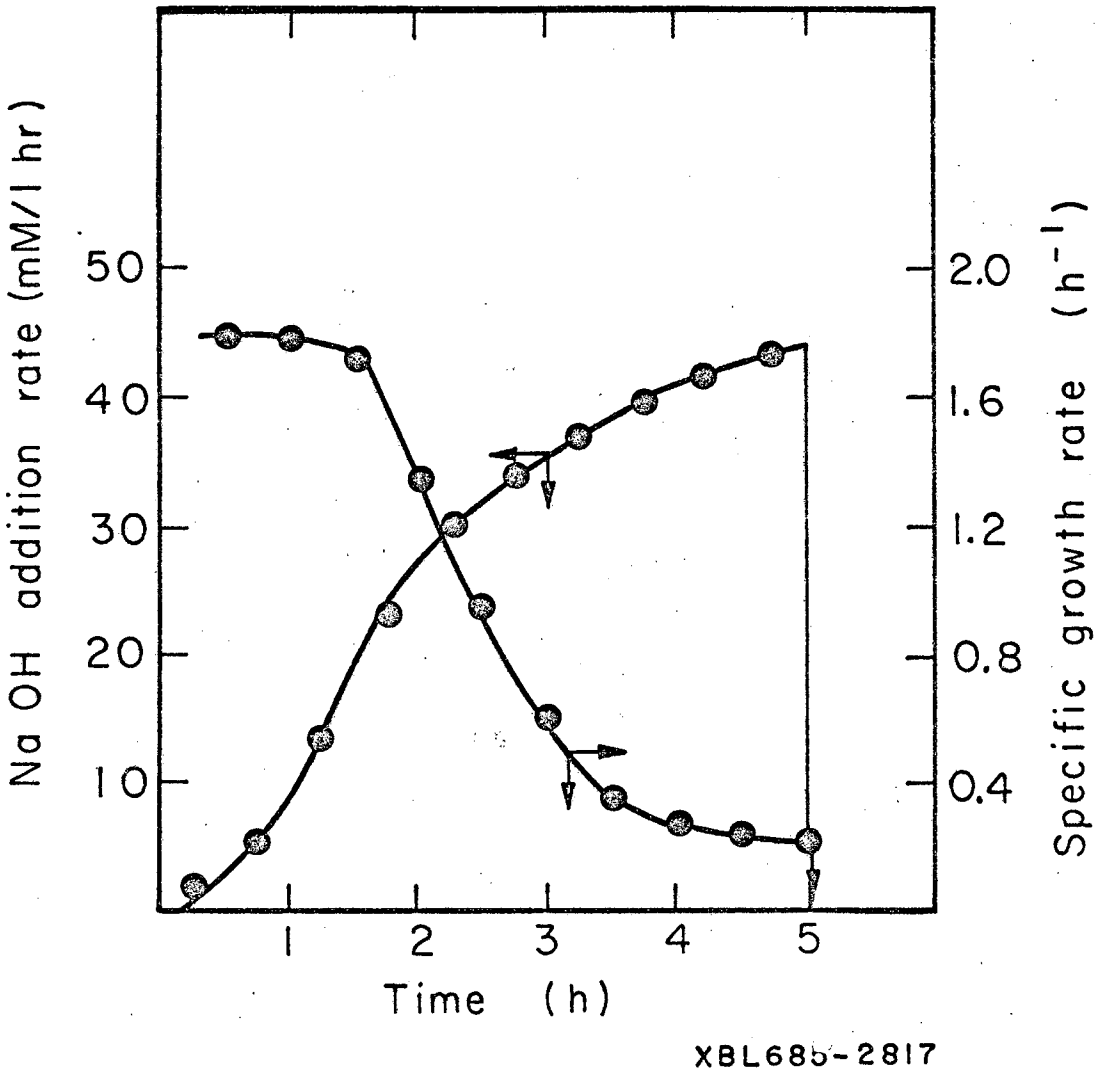

Fig. 12. The NaOH addition rate and the specific growth rate as a function of time for batch Run S.

The data for Run S is shown to demonstrate the growth characteristics observed on the semi-defined medium. Attempts at determining the limiting substrate were unsuccessful. Furthermore, in runs following S, growth rates on identical nutrient medium became very poor and erratic. After a number of experiments, it was suspected that trace components in the casein were responsible for the erratic results. The concentration of these traces constituents appeared to vary from lot to lot. Since the advantage of a semi-defined medium is in reproducibility of experimental results then if slight changes in composition of nutrients do result in widely varying results, the use of such a medium is no longer justified.

Preliminary experiments with a complex medium containing yeast extract showed much better growth than was possible on the semi-defined recipe. The medium used is tabulated in the Appendix and the results of several experiments designed to establish growth characteristics are presented in Fig. 13 to 20. The incorporation of vitamins in addition to those present in the yeast extract appeared to be necessary. During a continuous run, the vitamins were left out and poor growth occurred. Injection of these vitamins immediately improved growth.

Figures 13, 14, 15 and 16 show the growth curves for four runs at different glucose and yeast extract concentrations. The medium for Run AB contained 20 gm/l yeast extract and 10 gm/l glucose. Since the rate of glucose consumption was so much larger than during growth on the previous medium, an additional 6 gm/l was added just after the original 10 gm/l was exhausted. The general characteristics which were observed in Run S were present in Run AB. The complex medium was a better nutrient for the micro-organisms since the log phase was extended considerably. Furthermore, dissociation of energy production and cell multiplication occurred at higher cell concentrations as is shown in Fig. 20 where the base consumed is plotted against cell concentration. This extension of the linear relation between energy and cell production results in a larger cell density in the final sample.

The material balances for Run AB are shown in Figs. 17, 18, and 19. In Fig. 17 the lactate concentration is plotted against the glucose

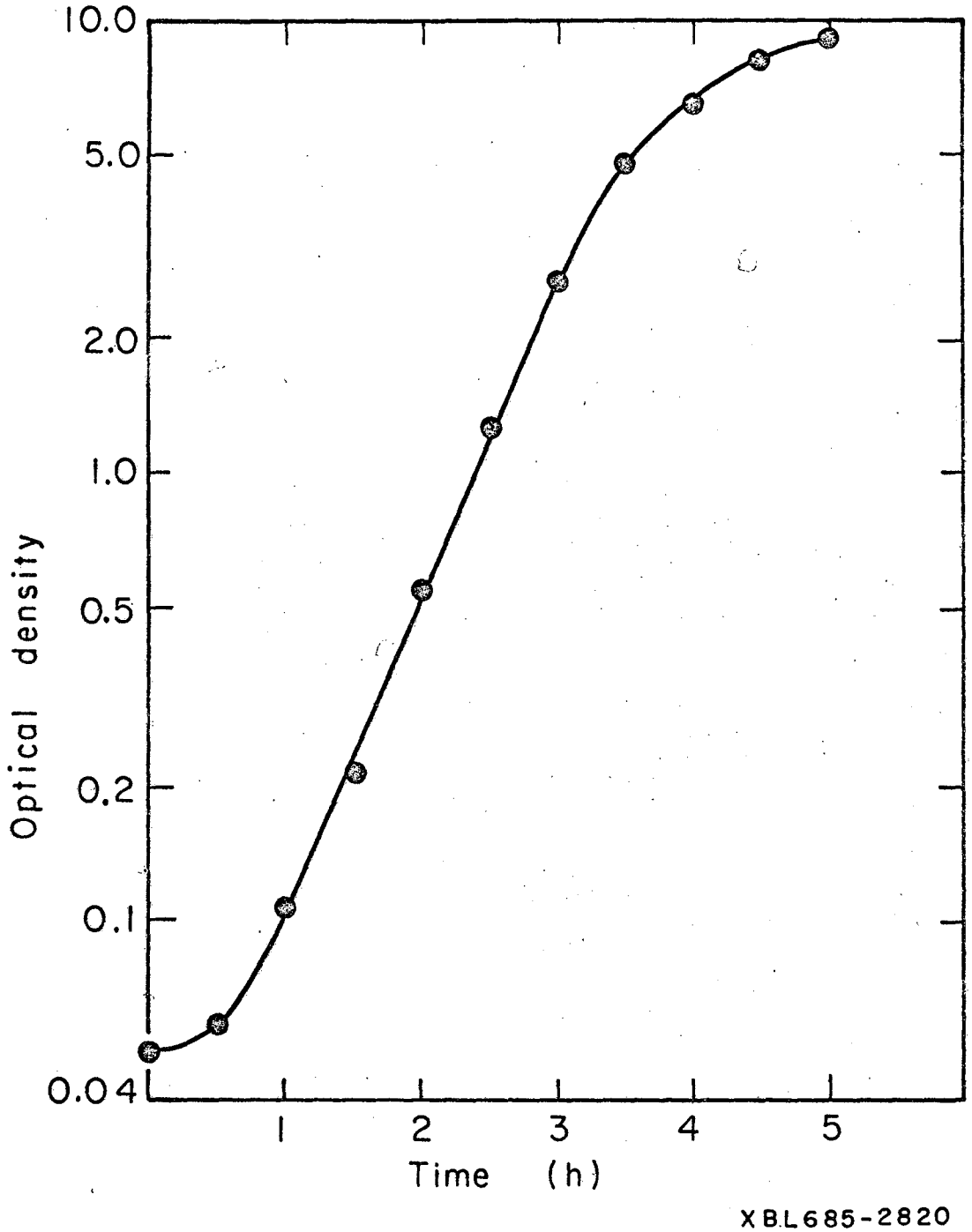

Fig. 13. The growth curve for batch Run AB using the complex medium and 10 gm/l glucose.

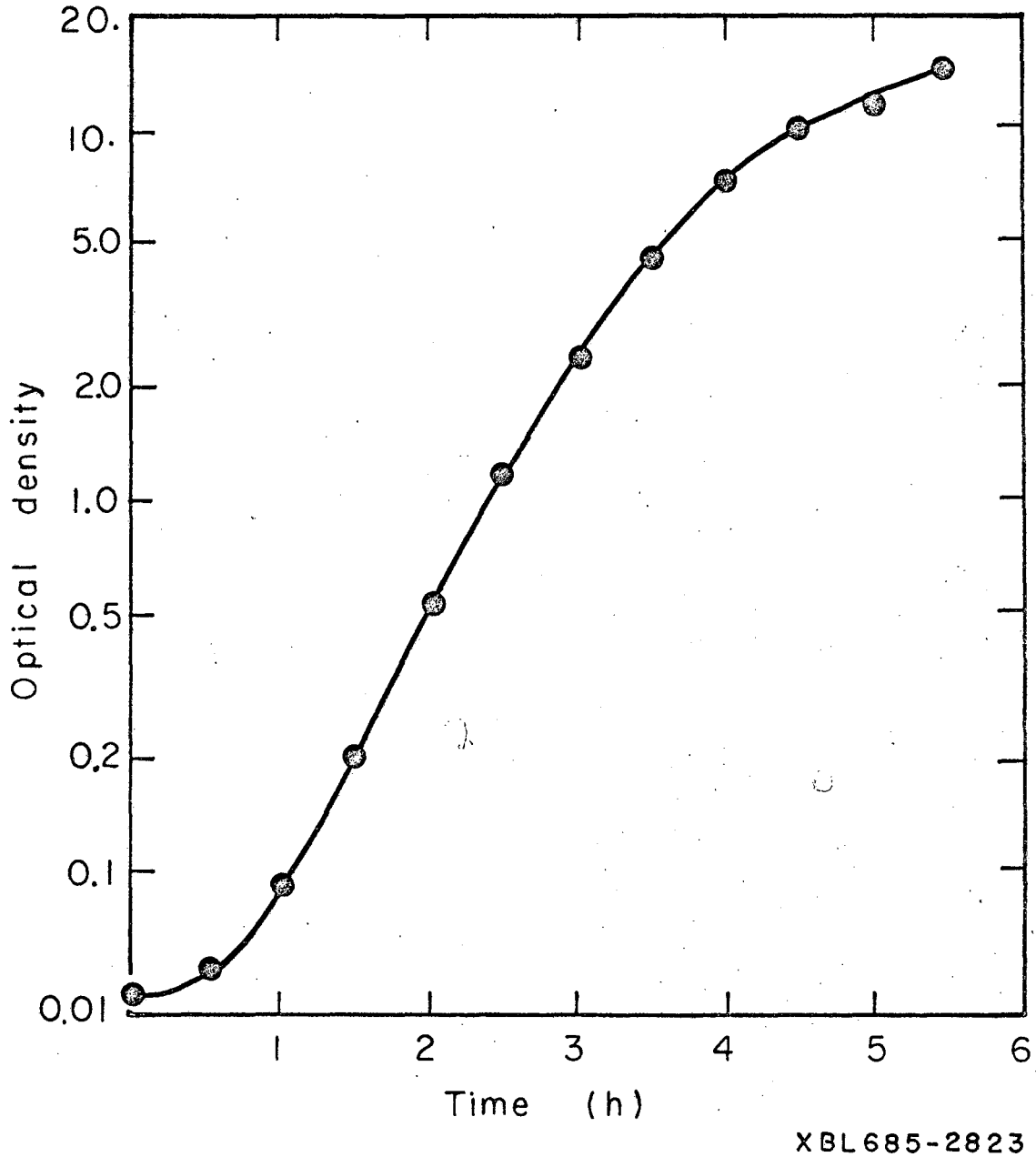

Fig. 14. The growth curve for batch Run AC using the complex medium with 30 gm/l glucose.

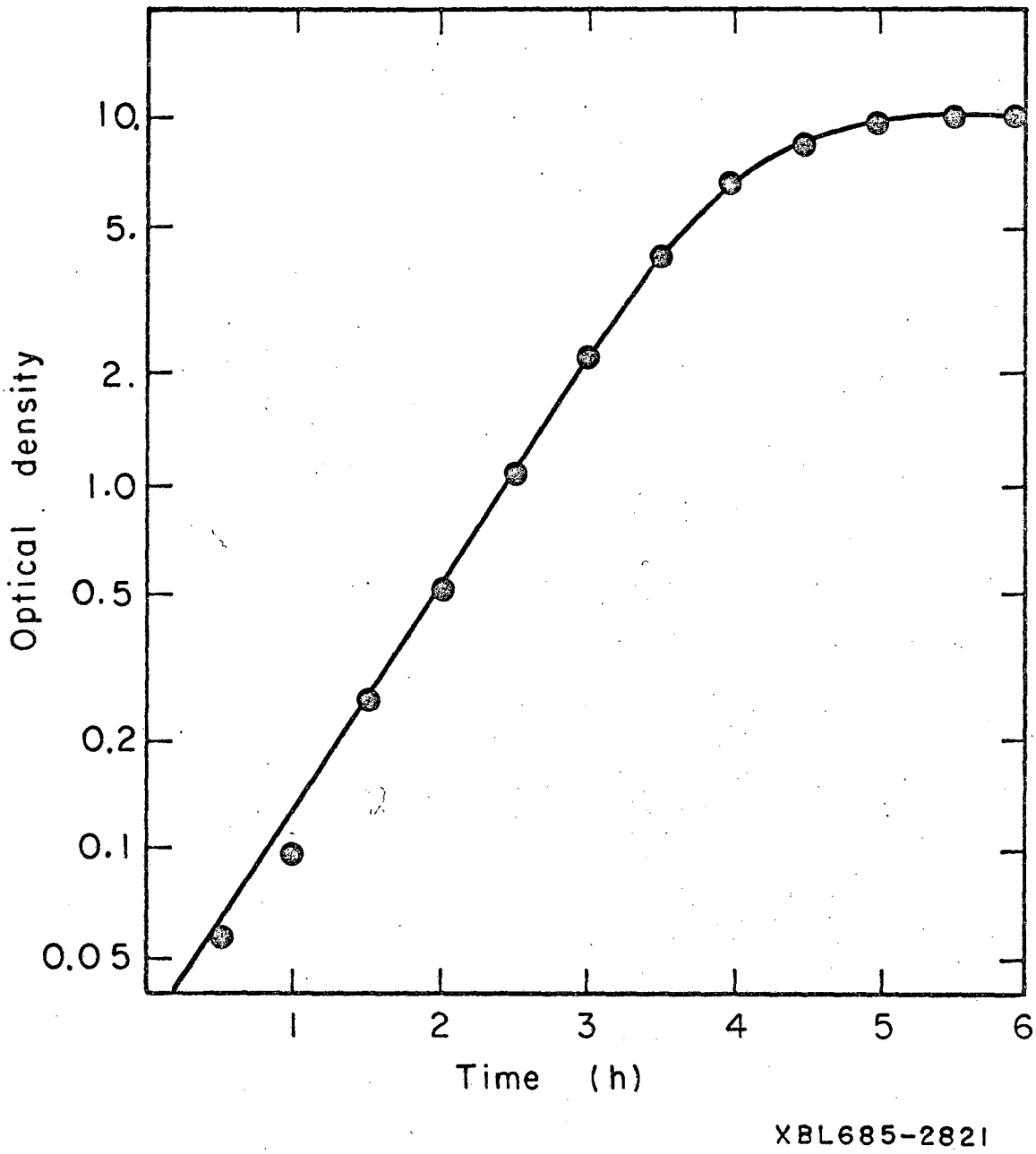

Fig. 15. The growth curve for batch Run AE using the complex medium with 30 gm/l yeast extract and 30 gm/l glucose.

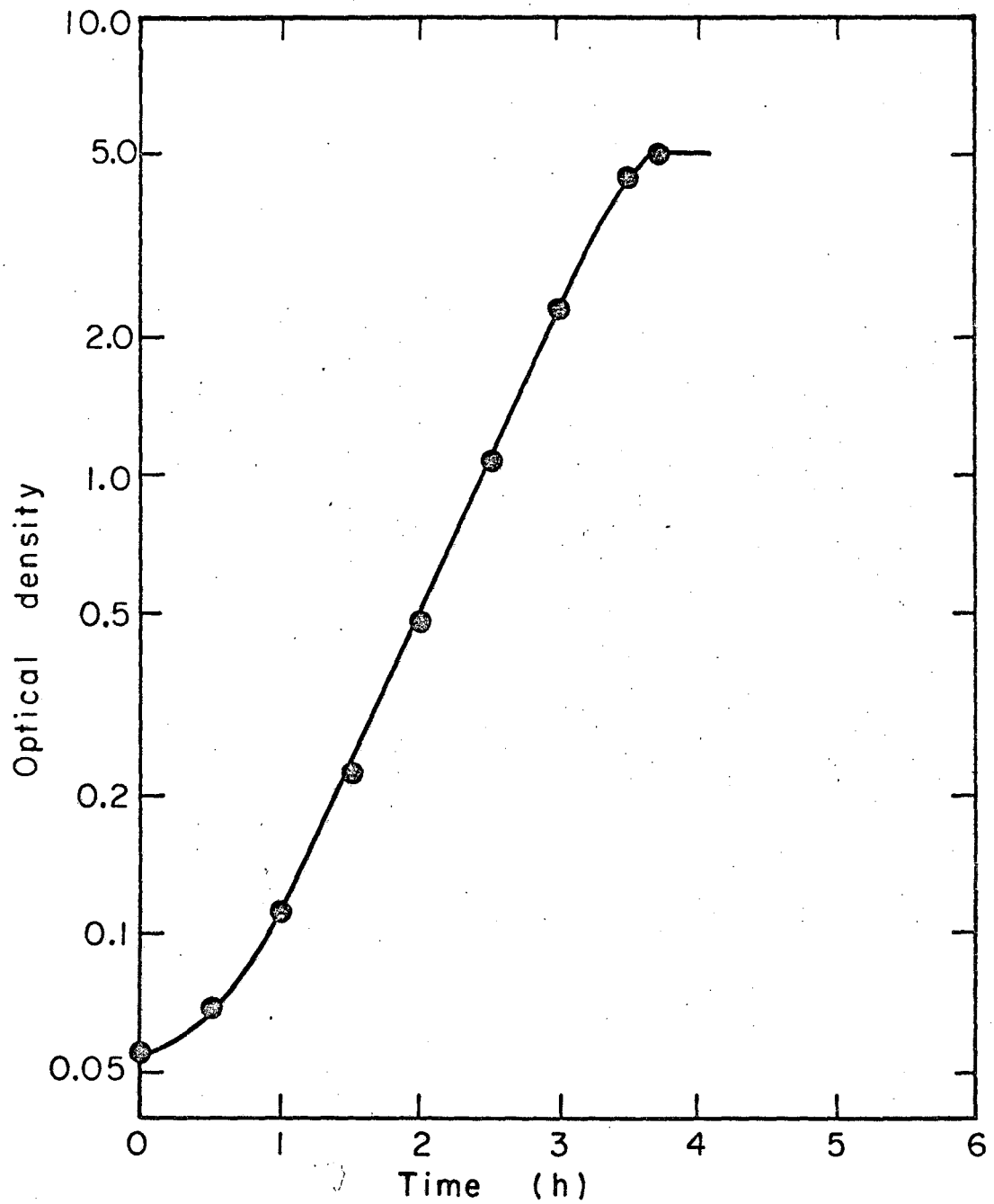

Fig. 16. The growth curve for batch Run AI using the complex medium and 7 gm/l glucose.

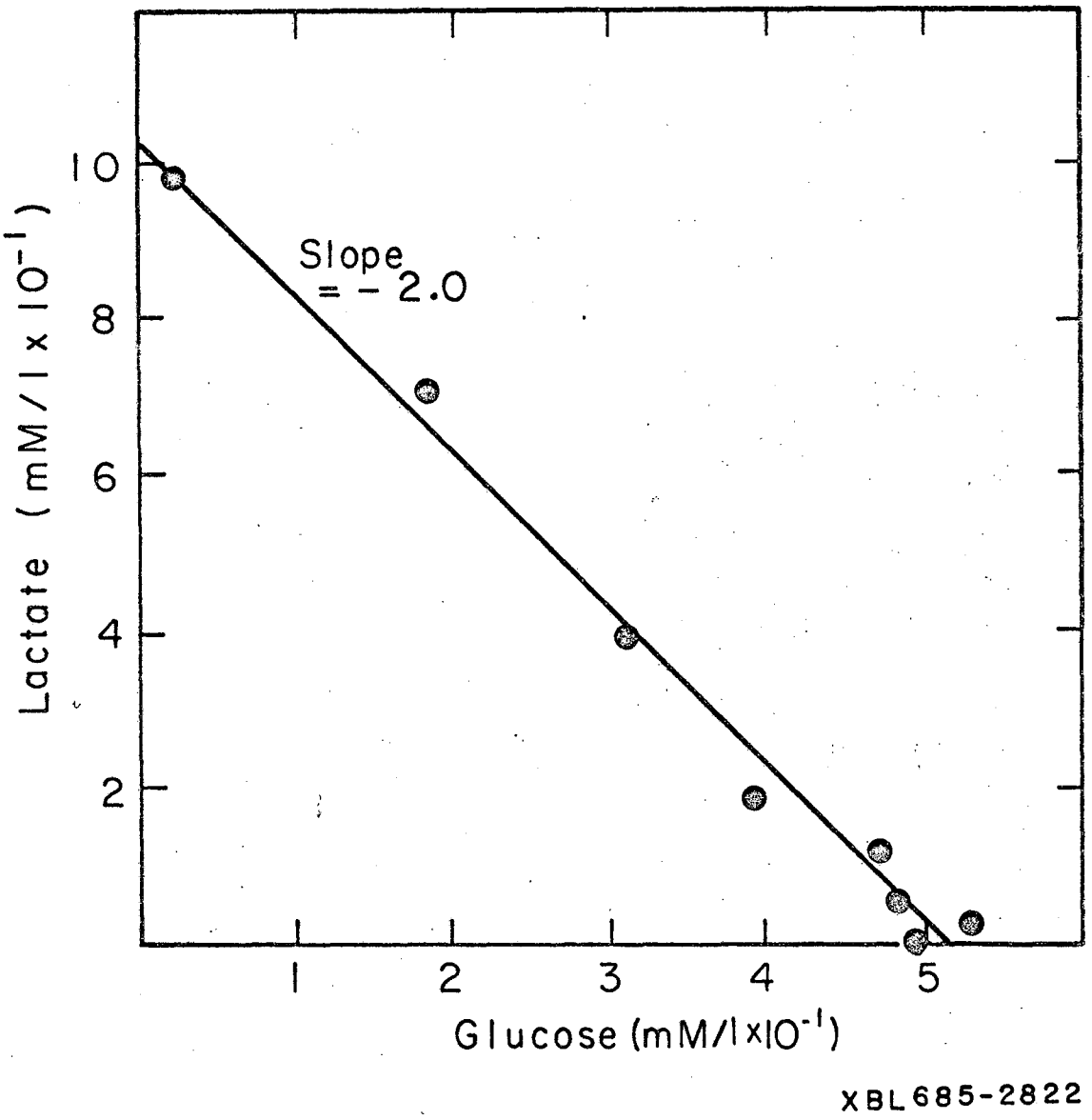

Fig. 17. The material balance on the glucose consumed in batch Run AB; lactate produced versus the glucose remaining in solution.

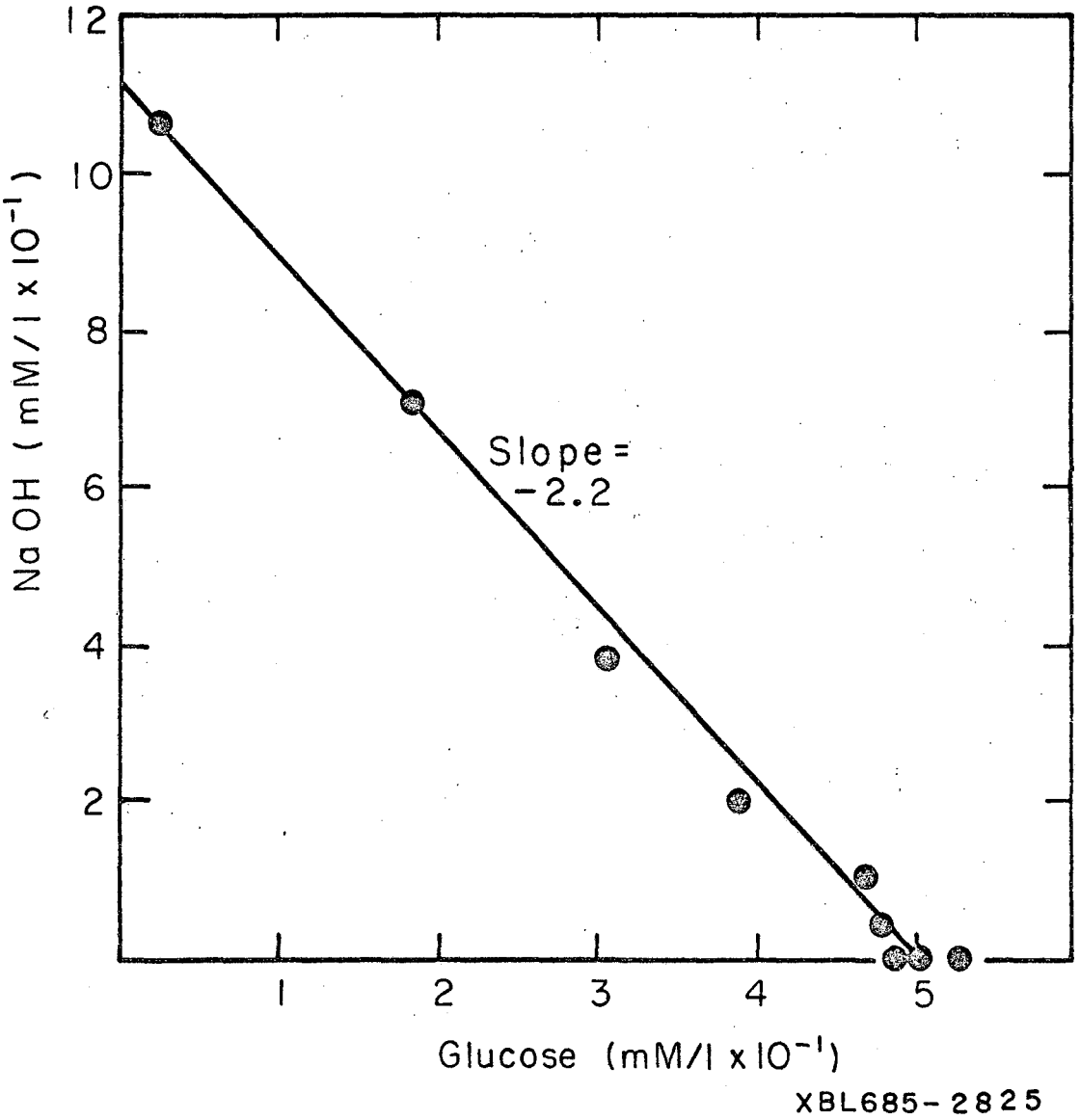

Fig. 18. The material balance on the glucose consumed in batch Run AB; NaOH consumed versus glucose remaining in solution.

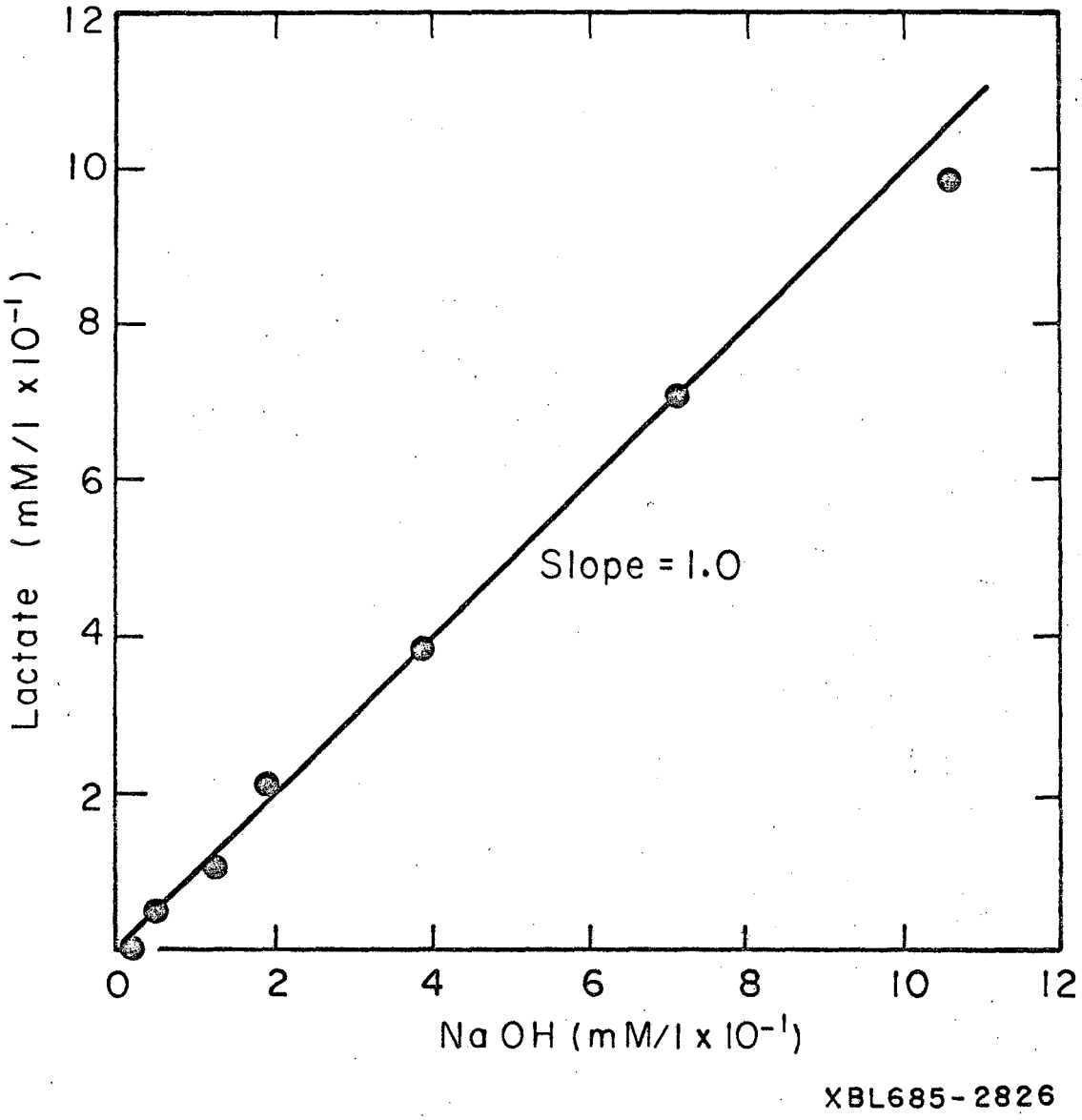

Fig. 19. The lactate produced versus the NaOH consumed during batch Run AB.

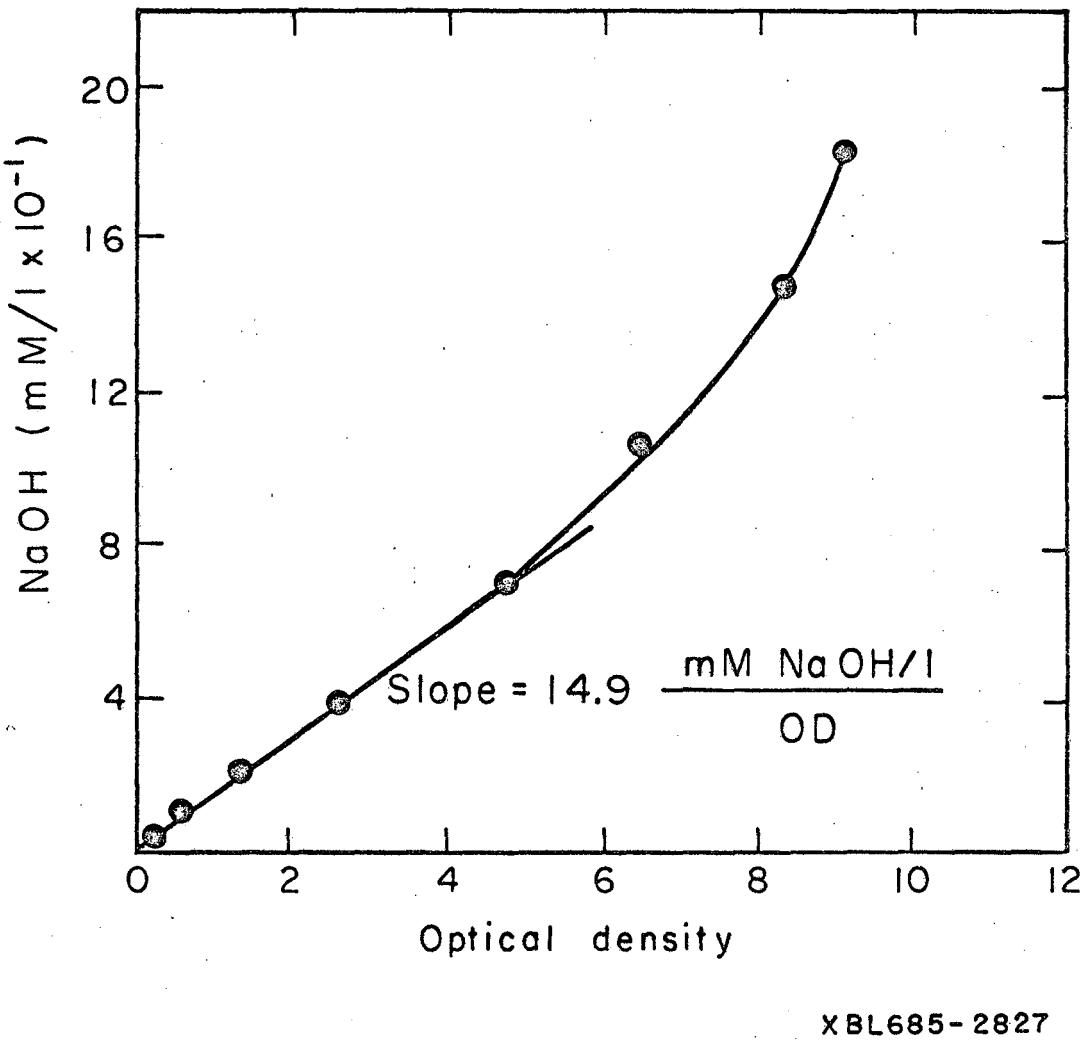

Fig. 20. Glucose consumption (as measured by NaOH consumption) versus the bacterial cell concentration during batch Run AB.

concentration. A linear curve with slope of -2.0 fits the data fairly well demonstrating that near stoichiometric conversion of glucose to lactate occurs. Figure 18 shows the relation between base consumption and glucose concentration. The amount of base added appears to be higher than the glucose consumed by approximately 10%. This deviation from stoichiometry may be due to giving too much weight to the last two data points, for when the lactate concentration is plotted versus the base consumed in Fig. 19, a linear curve with slope equal to 1.0 represents the data well.

The medium for Run AC contained 20 gm/l yeast extract and 30 gm/l glucose. The growth curve is presented in Fig. 14. A comparison of this curve with that for AB in Fig. 13 shows little difference except that the growth period is extended due to the additional glucose present.

Another run, which is not presented, with 10 gm/l yeast extract and 10 gm/l glucose showed that the cell concentration at which dissociation occurred was dependent upon yeast extract concentration. Run AE was grown on medium containing 30 gr/l yeast extract and 30 gm/l glucose in order to see if an increased yeast extract concentration would extend the linearity between glucose consumption and cell concentration. There was little enhancement over 20 gm/l yeast extract. The growth curve for Run AE was terminated much earlier than any of the other batch experiments as is shown by the data presented in Fig. 15. In fact, a stationary phase occurred while one third of the glucose remained. This glucose was metabolized at a high rate with little or no increase in cell concentration. The only difference in medium composition was a reduced phosphate level for Run AE, although the amount present was considerably more than usually needed to supply phosphate ion for microbial metabolism. The presence of high phosphate levels is usually for buffering purposes.

From Runs AB, AC and AE, it appeared that a concentration of yeast extract of 20 gm/l would support the consumption of 7 gm/l glucose before dissociation of energy production and growth began. To test this, a run was made using these concentrations and the result is shown in Fig. 16. The specific growth rate remained constant until just before the glucose was exhausted while a plot of base consumption versus OD showed that only a small amount of dissociation occurred.

2. Cell Size Distribution

The size distribution of samples of cells was determined using a modified Coulter Particle Counter constructed and described by Edwards and Wilke.[10] The device worked by drawing a suspension of particles through a small orfice 39 μ in diameter. A small constant electrical current was imposed across the orfice and as a particle passed through, a voltage signal proportional to its volume was generated. The signal was sorted by a pulse height analyser and stored in a multichannel memory. The channel number was proportional to particle volume. To calibrate the device, a sample of particles of known size was measured. The calibration using 1.304 μ polystyrene spheres is shown in Fig. 21.

The size distribution for samples taken during Run S are shown in Figs. 22, 23 and 24 in chronological order. The distributions have been normalized in order that comparisons between the samples can be made. Each figure contains several curves which are designated by different sample numbers. The time interval between samples is 30 min. with the first sample, S1, coming 30 minutes after innoculation. The distributions display a consistent trend as the fermentation progresses. Initially a broad distribution occurs showing a continuous range in particle size. The next sample, S2, shows the beginning of two dominant cell sizes, the smaller one near channel number 35 and the larger at channel number 50. As growth continues, the fraction of the cells which have these two sizes increases as shown by the increased maxima of the peaks. Furthermore, the smaller particles begin to dominate the larger so that by sample S4 one peak remains with a shoulder representing the larger size. This type of distribution continues for the remainder of the batch run with the shoulder being more or less pronounced. The primary peak tends to become narrower with time and the maximum begins to shift position to higher channel number. The distribution in Fig. 24 for the last samples show the initial stages of broadening. The peak maximum changes only slightly to higher channel number and the height of the peaks begins to decrease. After S10, the glucose was exhausted and growth stopped.

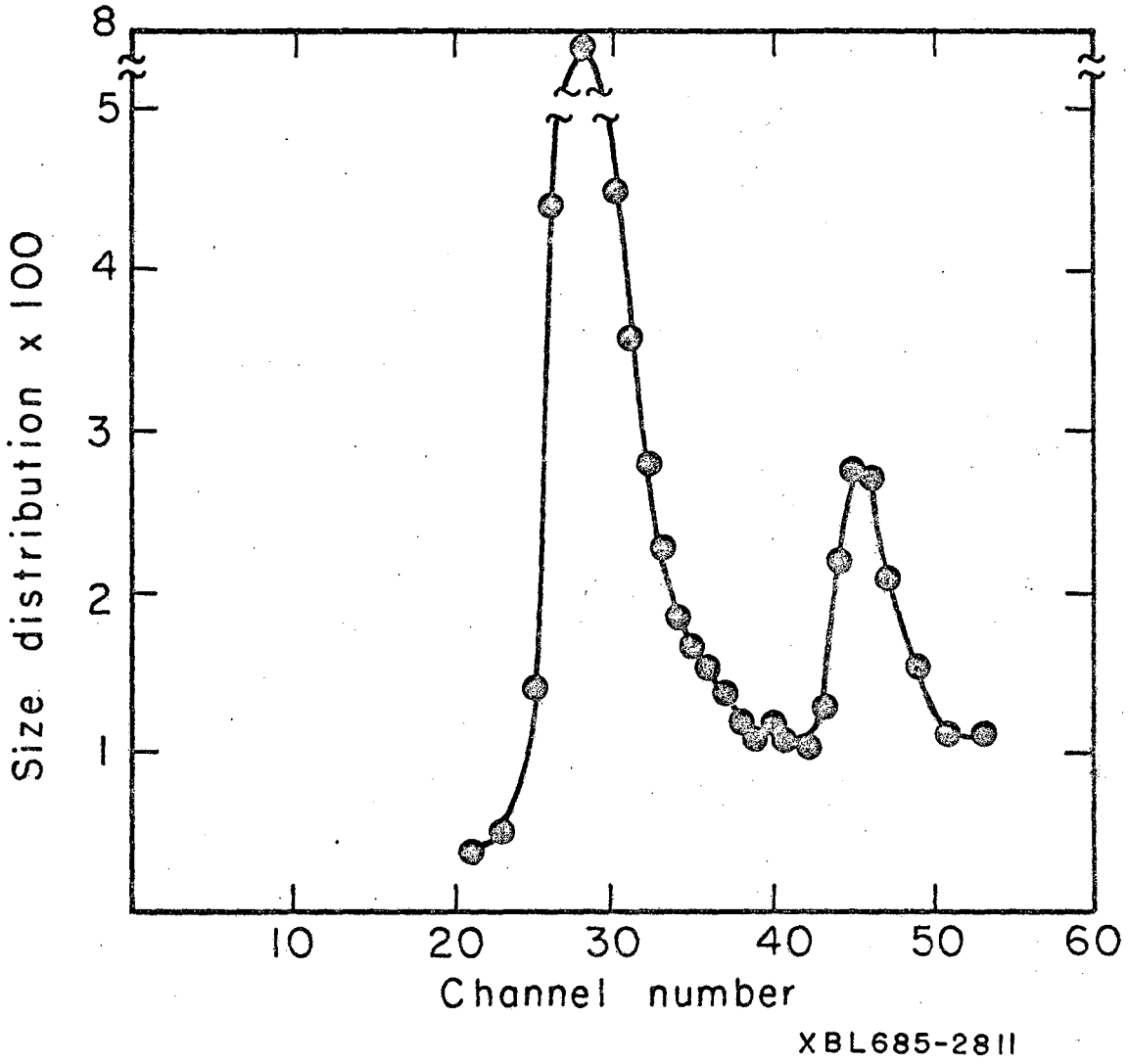

Fig. 21. The normalized size distribution for the standard 1.304 micron polystyrene spheres. The channel number is proportional to particle volume.

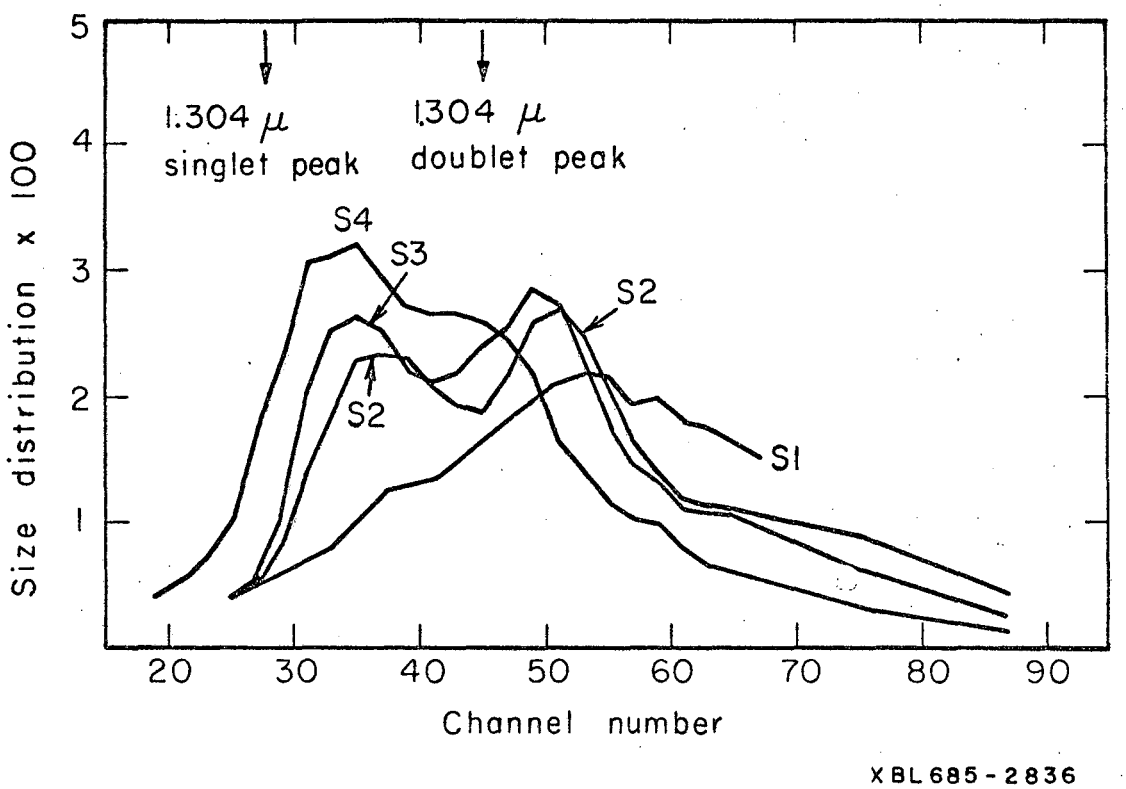

Fig. 22. The normalized size distribution for samples 1 to 4 of batch Run S. The sample time interval was 30 minutes. Channel number is proportional to particle volume.

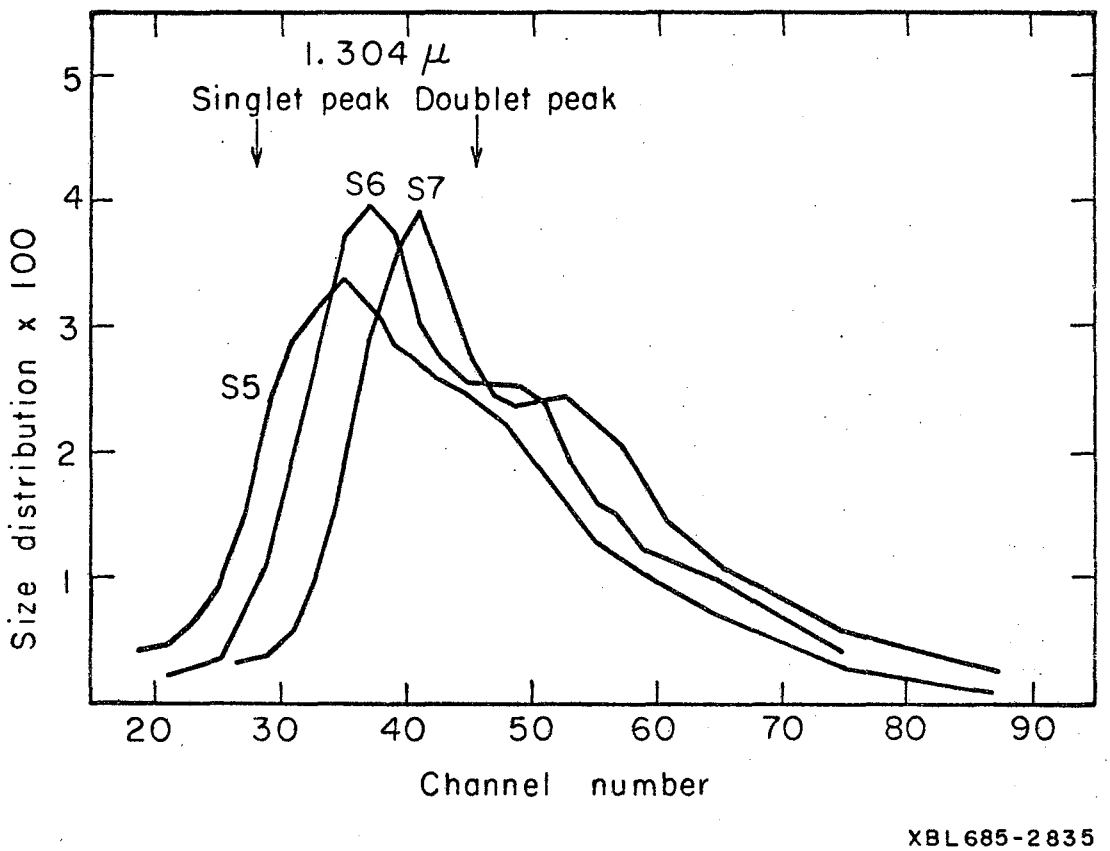

Fig. 23. The normalized size distribution for samples 5 to 7 of batch Run S. The sample time interval was 30 minutes. Channel number is proportional to particle volume.

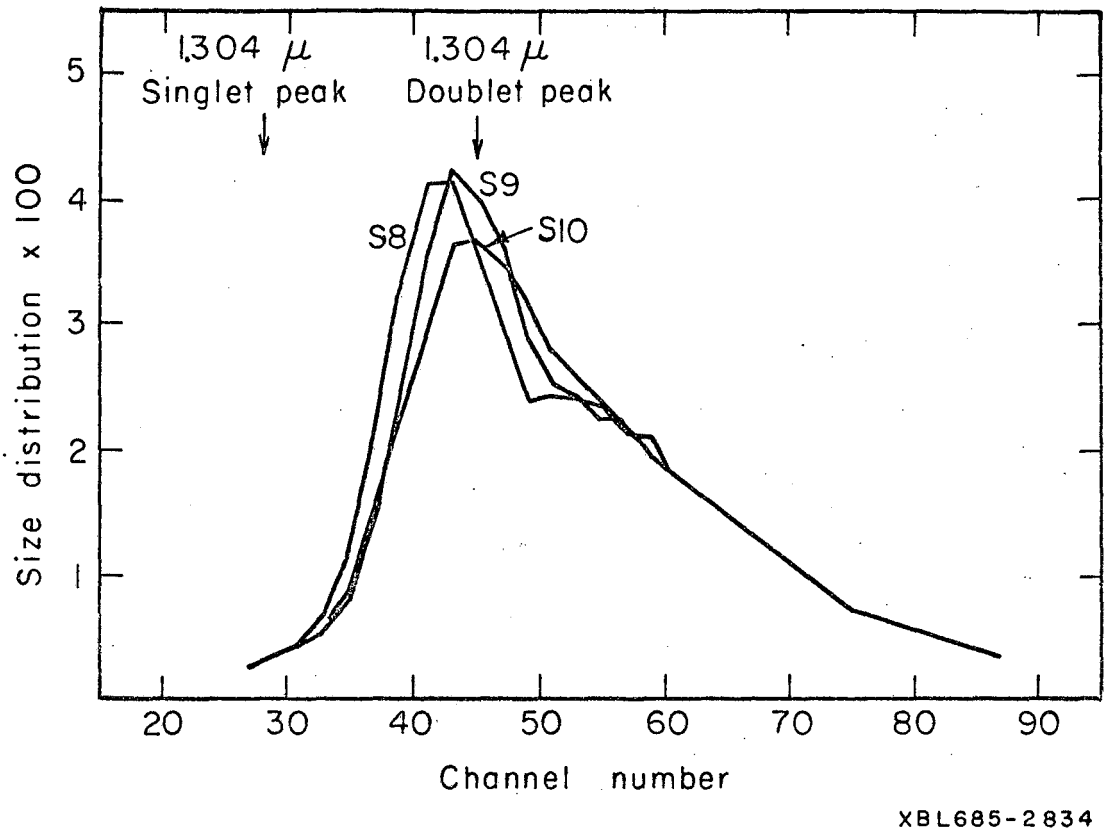

Fig. 24. The normalized size distribution for samples 8 to 10 of batch Run S. The sample time interval was 30 minutes. Channel number is proportional to particle volume.

During the course of the batch run, the average size of a discrete cellular particle decreases initially, reaches a minimum and then begins to increase as the run approaches termination. S. faecalus, during reproduction, passes from the spherical cocci to a dumb bell shape before splitting into two cocci. The splitting of the cocci does not always occur after duplication and short chains of cocci arise. During periods of rapid growth, short chains of dumb bells occur. From microscopic observation, the predominance of singlets and doublets was not obvious although they appeared in large numbers. The diminishing of chains both in number and length was noticable.

These results for Run S were typical of those obtained for all of the batch experiments. Some variation in the prominence of the peak for the larger particle size occurred but the general profile and its change with time during the growth cycle was similar for all of the runs.

3. Mathematics of Batch Growth

Bacteria reproduce by binary fission, a process similar to autocatalytic chemical reaction. The differential equation describing this mechanism is:

$$\left(\frac{dN}{dt}\right)_G = \mu N \qquad (1)$$

where: N = cell concentration
t = time
μ = specific growth rate.

During the growth of a culture, glucose is catabolized to produce energy with the formation of lactate.

$$\frac{dP}{dt} = - Y_{P/S} \frac{dS}{dt} \qquad (4)$$

where: P = product concentration-lactate
S = substrate concentration-glucose.

In this equation, $Y_{P/S}$ is the yield constant for this process. This yield constant, which has been shown as the slope of the lines in Figs. 8 and 17, approaches the stoichiometric value of 2.0 in the batch runs. The energy produced during the conversion of glucose to lactate is used by the cell for reproduction and possibly for cell maintenance. The presence of a maintenance energy requirement in bacteria has been shown by Marr et al.[31] and Dawes and Robbins[32] for Escherichia coli, Herbert[6] for S. marsescens and by Pirt[33] for several other organisms. A discussion of the energy of maintenance concept for micro-organisms has been published by Dawes and Robbins.[34] Luedeking and Piret[36] have shown that for L. delbruckii, a homofermentive lactic acid bacteria, the rate of lactate production (or glucose consumption) was proportional to the rate of growth plus a maintenance term. However, Rosenberger and Elsden[3] have shown that for S. faecalus, dissipation of energy may occur in the presence of an excess of glucose. The dissociation of energy production which was observed in the batch runs may be explained by either of these two mechanisms. The shape of the curve for lactate production versus cell concentration is similar for S. faecalus and for L. delbruckii, although the amount of lactate produced after the dissociation occurs is much larger for S. faecalus.

The experimental data derived from the batch runs were examined by these two mechanisms to see whether a distinction could be made between them.

Luedeking's model expressing the relation between substrate consumption (or lactate production) and its utilization for growth and maintenance is expressed in Eq. (5).

$$-\frac{dS}{dt} = \alpha \left(\frac{dN}{dt}\right)_G + \beta N \qquad (5)$$

where α is a constant expressing the amount of glucose required to produce new cells and β is the maintenance term. Substituting Eq. (1) into 5 yields:

$$-\frac{dS}{dt} = \alpha\mu N + \beta N \, . \qquad (6)$$

Rearranging (6) results in:

$$-\frac{1}{N}\frac{dS}{dt} = \alpha\mu + \beta \quad . \tag{7}$$

The left hand side of Eq. (7) is the specific rate of glucose consumption which plotted versus μ , the specific growth rate, should yield a linear curve with slope equal to α and the intercept equal to β .

It has been shown in the figures pertaining to the material balances that stoichiometric conversion of glucose to lactate is approached and that stoichiometric neutralization of lactic acid by NaOH is attained. Since, the rate of base consumption was more precisely known that either glucose or lactate, Eq. (6) was expressed in terms of NaOH.

$$\frac{1}{N}\frac{d(NaOH)}{dt} = Y_{P/S}(\alpha\mu + \beta) \quad . \tag{8}$$

The rate of base addition to the fermenter was measured experimentally as described previously. The data was plotted on semi-log paper as a function of time and a smooth curve drawn through the points. This curve was used to determine the base consumption rate at selected times. The specific growth rate was evaluated by graphical differentiation of the semi-log plot of OD versus time. Near the end of the growth period, where the exponential character of the growth cycle ended, slopes were taken from a linear plot of OD versus time. Agreement between the values of μ derived from these two plots was good. The use of semi-log rather than linear plots for the determination of rates was due to the exponential growth characteristics of batch cultures. Experimental errors were more readily smoothed.

A computer program developed and described by Edwards and Wilke[10] which curve fits a logistic equation to batch data was used to check the results of the graphical technique and good agreement was found. Unfortunately, the computer program tended to "blow up" during the fitting routine so that the time spent for debugging became excessive. Since the two techniques gave equally good results, use of the computer was discontinued.

Equation (8) is expressed in graphical form for Runs S, AB, AC and AE in the lower portion of Figs. 25, 26, 27 and 28, respectively. While the data are somewhat scattered, the linear relation between specific base consumption and specific growth rate is apparent leading one to believe that Eq. (8) is an accurate representation of the fate of the energy produced during glucose catabolism. The values of α and β for these runs are tabulated in Table I. The values of α and β for Runs S and AB are quite close but those for Runs AC and AE are much different with the maintenance energy term, β, being twice as large and the value of α being approximately half. The last two data points for Run AC do not lie on the curve but are much lower so that the differences between the first two runs and AC may be due to errors in determining the specific rates although such large deviations are unlikely. In any event, the maintenance term for these runs is quite large compared to the amount of glucose required to produce new cells. Luedeking and Piret's data[36] for a similar organism, L. delbruckii, yields a ratio of β to α of 0.25, a value much smaller than those determined from the present experiments. In fact, for Runs AC and AE, the specific consumption of glucose is almost independent of specific growth rate.

Table I. The constants for the Luedeking Model.

Run	α-mM Glucose/l/OD	β-mM Glucose/l/OD hr.
S	5.0	2.6
AB	5.3	3.0
AC	3.3	6.
AE	2.5	5.4

If the dissociation of energy production from growth is not due to the maintenance term but due to dissipation of energy, then the rate of glucose consumption would be related to the specific growth rate by the following equation:

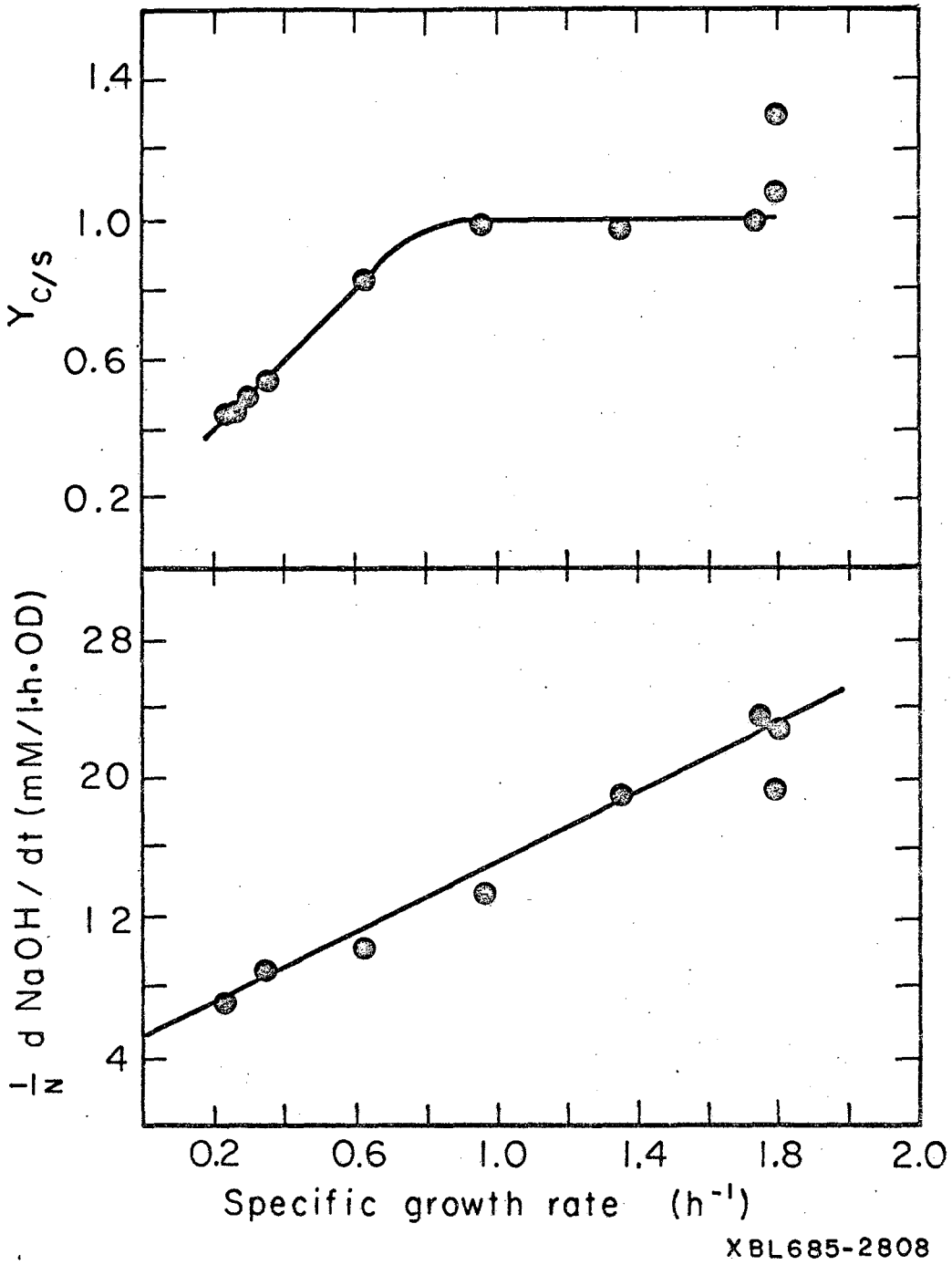

Fig. 25. Testing of the batch Run S data by two different models. Upper graph: the energy dissipation model. The fraction of glucose consumed which supplies the energy for the production of new cells is plotted as a function of specific growth rate. Lower graph: the Luedeking et al. maintenance energy model. The specific NaOH consumption is plotted as a function of specific growth rate.

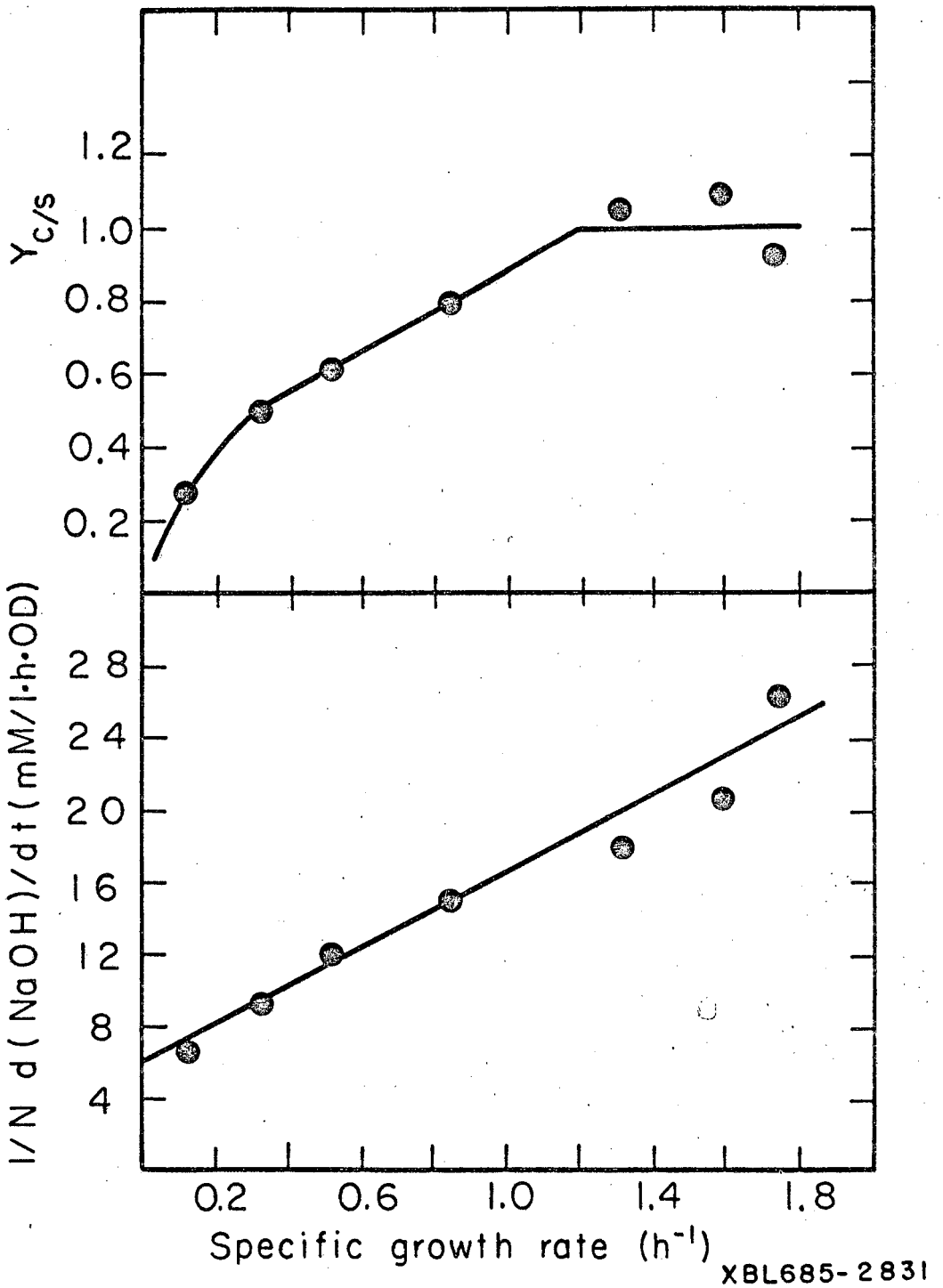

Fig. 26. Testing of the batch Run AB data by two different models. Upper graph: the energy dissipation model. The fraction of glucose consumed which supplies the energy for the production of new cells is plotted as a function of specific growth rate. Lower graph: the Luedeking et al. maintenance energy model. The specific NaOH consumption is plotted as a function of specific growth rate.

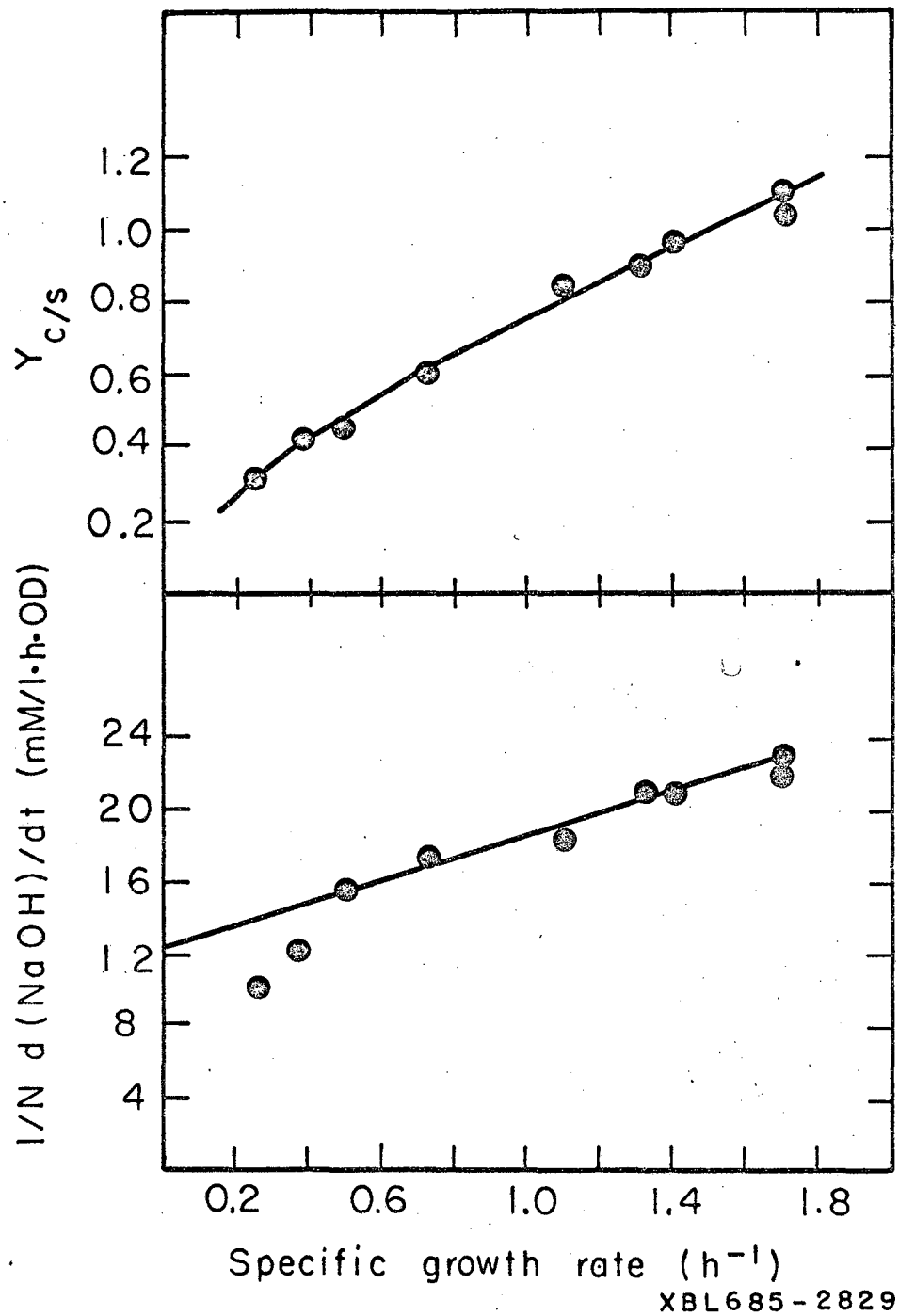

Fig. 27. Testing of the batch Run AC data by two different models. Upper graph: the energy dissipation model. The fraction of glucose consumed which supplies the energy for the production of new cells is plotted as a function of specific growth rate. Lower graph: the Luedeking et al. maintenance energy model. The specific NaOH consumption is plotted as a function of specific growth rate.

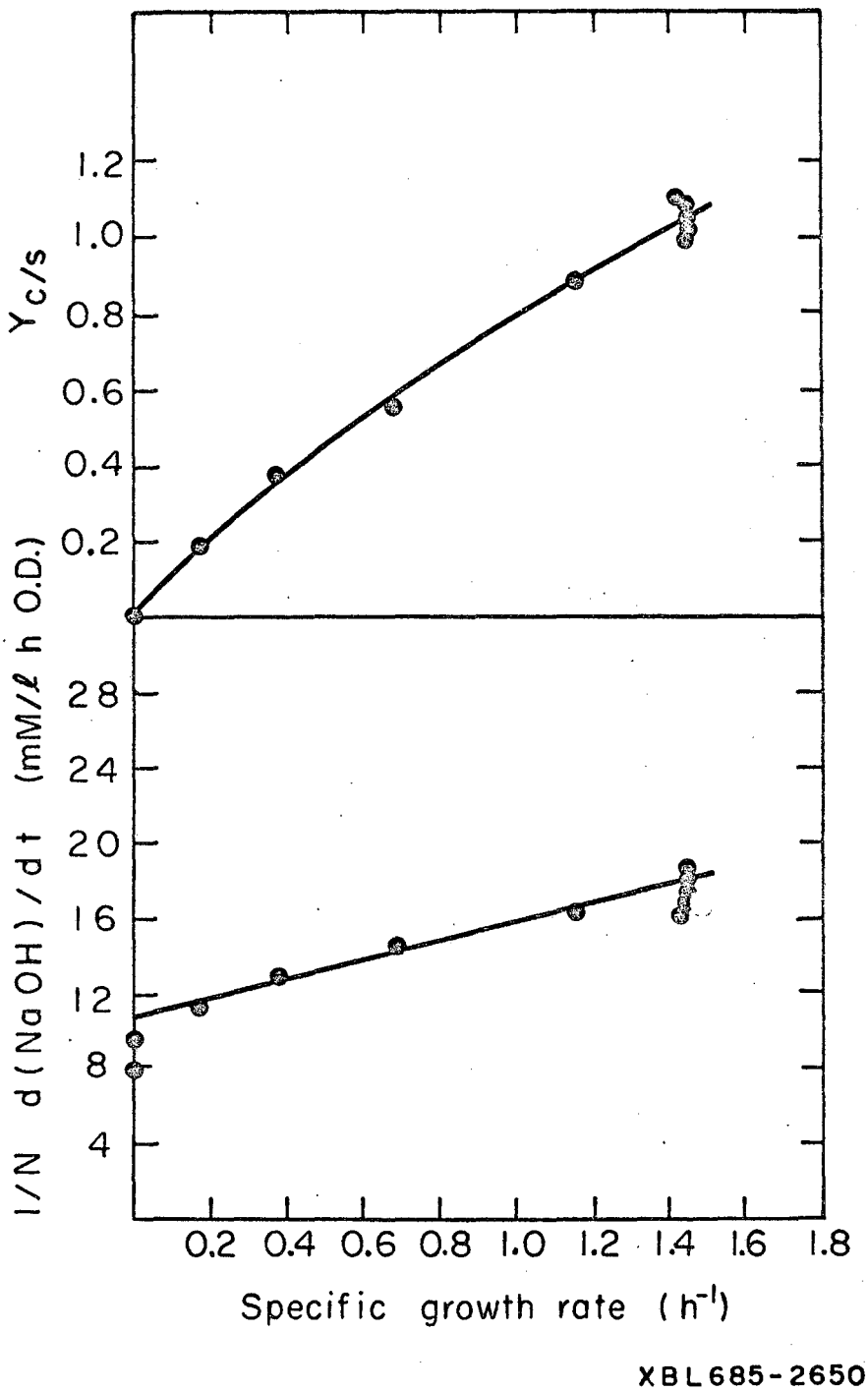

Fig. 28. Testing of the batch Run AE data by two different models. Upper graph: the energy dissipation model. The fraction of glucose consumed which supplies the energy for the production of new cells is plotted as a function of specific growth rate. Lower graph: the Luedeking et al. maintenance energy model. The specific NaOH consumption is plotted as a function of specific growth rate.

$$-\frac{dS}{dt} = \frac{\alpha \mu N}{Y_{C/S}} \qquad (9)$$

where $Y_{C/S}$ is the fraction of the glucose consumed which is used to promote growth. The constant, α, has the dimensions mM glucose/OD as in Eq. (5). During the initial stages of batch growth, the rate of substrate consumption as measured by lactate production or base consumption, was directly proportional to the rate of growth. If the value of $Y_{C/S}$ is taken to be 1.0 during this period, then α is equal to the initial slope of the curve in Figs. 11 and 20 divided by the stoichiometric constant 2.0. The values of α for Runs S, AB, AC and AE are summarized in Table 2.

Table II. Constant for the energy dissipation model.

Run		α-mM Glucose/l/OD
S		6.95
AB		7.45
AC		7.15
AE		6.35
AI		6.80
	Average	6.94
	Standard deviation	5.9%

The values of α for these runs are nearly equal and if Eq. (9) represents the true state of affairs, then the amount of energy required to produce new cells is fairly independent of the media, for Run S used the semi-defined medium while the rest used the yeast extract medium.

Using Eq. (9) and the values for α from Table II, $Y_{C/S}$ values were calculated for the four batch runs and plotted in the upper portion of Figs. 25, 26, 27 and 28. For Eq. (9) to be valid, $Y_{C/S}$ should approach zero as μ goes to zero. For Run AE, $Y_{C/S}$ does become zero

but for Runs AB and AC, the approach to the origin is less well indicated. An extrapolation of the data for Runs S would indicate that $Y_{C/S}$ does not go to zero but information at sufficiently low μ was not available due to the exhaustion of glucose.

The values of $Y_{C/S}$ should be equal to 1.0 up to the point where dissociation occurs. Fair agreement results during the log phases of growth and, for Runs S and AB, even well into the declining growth period. In all of the runs, the point of dissociation deduced from Eq. (9) was at higher growth rates than was indicated from the product concentration versus OD plots. This difference may be due to errors introduced by the graphical differentiation necessary for the use of Eq. (9).

A comparison of the two models relating growth and glucose consumption shows that either model could be used. Inconsistencies occur in the data when analysed using either model and it is not possible to conclusively demonstrate which one is correct. Further information taken from continuous fermentation experiments where glucose-limited growth occurred showed that little or no glucose was utilized for maintenance purposes and that the energy dissipation model appears to be more nearly correct.

B. Continuous Stirred Tank Fermentation

Following the development of a satisfactory growth medium, continuous fermentation experiments were undertaken to determine if the growth characteristics observed in batch culture remained unchanged during continuous growth. The nutrient composition was the same as used for batch Run AI which contained 7 gm/l glucose and 20 gm/l yeast extract. The amount of vitamins was reduced 40% with no effect on growth. Complete elimination of vitamins markedly reduced growth. At high nutrient feed rates, precipitation of magnesium ammonium phosphate occurred. A reduction of 60% in the amount of mineral solution containing the magnesium reduced the precipitation with no effect on growth.

The procedures used to prepare large quantities of medium and to sterilize the apparatus have been described previously. The pH of the

sterile medium was slightly below 7.0 and adding NaOH at a constant rate resulted in a linear change of pH with time. The rate of change of pH per milliliter of NaOH was calculated and used to correct the base addition rates during continuous fermentation in order that the amount of acid produced during the fermentation could be determined from the titration.

1. Experimental Results

Figure 29 presents the optical density developed in the fermenter and the broth glucose concentration as a function of dilution rate. The data have been converted to a unit nutrient feed basis by correcting for the volume of base added. The curves have the typical form for continuous fermentation with OD being nearly constant at low dilution rates and then decreasing as the rate approaches cell washout. As the cell concentration began to decrease sharply, glucose appeared in the effluent broth. All of the glucose concentration data at high dilution rates fell on the same curve. Only one glucose concentration at the maximum dilution rate is presented although there was a slight variation in feed concentration from run to run, e.g., 36.5 mM/l for Run CG and 38.9 mM/l for Run CJ.

The runs were conducted at the same conditions so that the OD curves for the different runs should have fallen on top of each other. At the lower dilution rates where glucose concentration was zero, the data does not coincide while at the higher rates, good agreement was found.

Run CG was completed using one tank of medium and the results are quite consistent. During Run CJ, the nutrient supply became exhausted after sample CJ11 and had to be replenished. Whether some error in medium preparation caused the change in OD versus dilution rate curve is not known. The growth was glucose limited but the small differences in glucose concentration in the feed could not explain the change in the maximum cell concentration which occurred when the nutrient was replenished.

The yield of lactic acid produced during the continuous fermentation differs from that produced during batch culture. Figure 30 presents

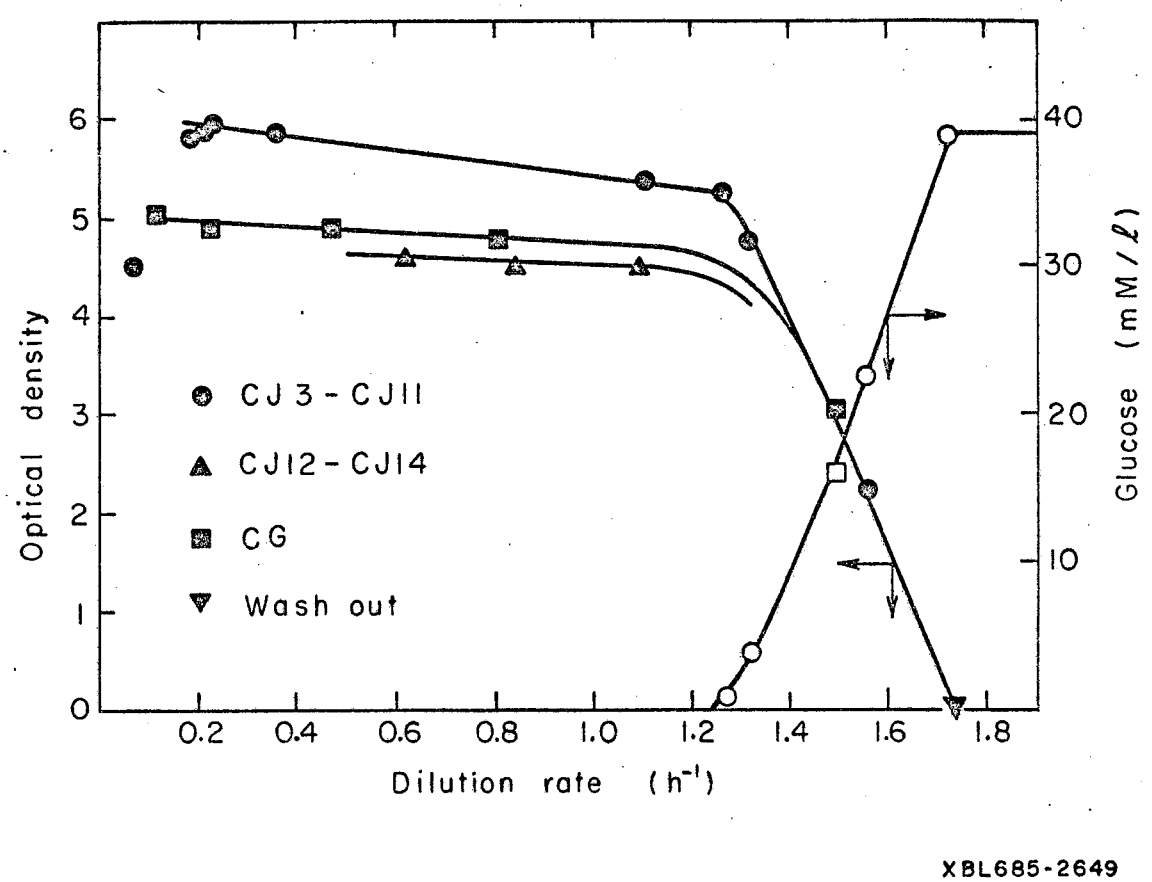

Fig. 29. The cell concentration and the glucose concentration as a function of dilution rate for the continuous stirred tank experimental Runs CG and CJ. The data are presented on the basis of one liter of nutrient medium with corrections made for the volume of NaOH added.

the lactate concentration per liter of nutrient medium as a function of dilution rate. At high dilution rates, the decrease in lactate concentration is due to washout of the culture and the presence of unconverted amounts of glucose. However, at dilution rates below 1.2 hr^{-1}, glucose concentration is essentially zero so that the decreasing lactate concentration is due to the partial diversion of the glucose to products other than lactate. Further evidence that such a diversion is occurring is illustrated in Fig. 31 which shows the rate of NaOH consumption per liter of nutrient medium as a function of dilution rate. At high flow rates, the decrease in base addition is due to washout. At lower flow rates, the rate of NaOH consumption does not follow the rate of lactate production but appears to be a mirror image. The conversion of the pyruvate to formate and acetate has been shown by Rosenberger and Elsden,[3] suggesting that the increased quantities of NaOH required by the continuous culture was due to these acids being produced. The matabolic pathway can be summarized by the following equations.

$$\text{1 mole glucose} \rightarrow \text{2 moles pyruvate}$$
$$\text{x moles pyruvate} \rightarrow \text{x moles lactate}$$
$$\text{(2 - x) mole pyruvate} \rightarrow \text{(2 - x) formate + (2 - x) moles acetate.}$$

Since the base neutralizes all of the acid produced, the amount of formate plus acetate is equal to the difference between the total base added and the lactate produced. Therefore, the fraction F of the initial glucose fed which can be accounted for is given by:

$$F = \frac{0.5P + 0.5\left[\frac{NaOH-P}{2}\right] + S}{S_0} \qquad (10)$$

where P and S refer to the concentration of lactate and glucose in the broth and S_0 is the initial glucose concentration. The approximate validity of this material balance is shown in Fig. 32 over a range of specific growth rates. Three sets of data are presented; two are the

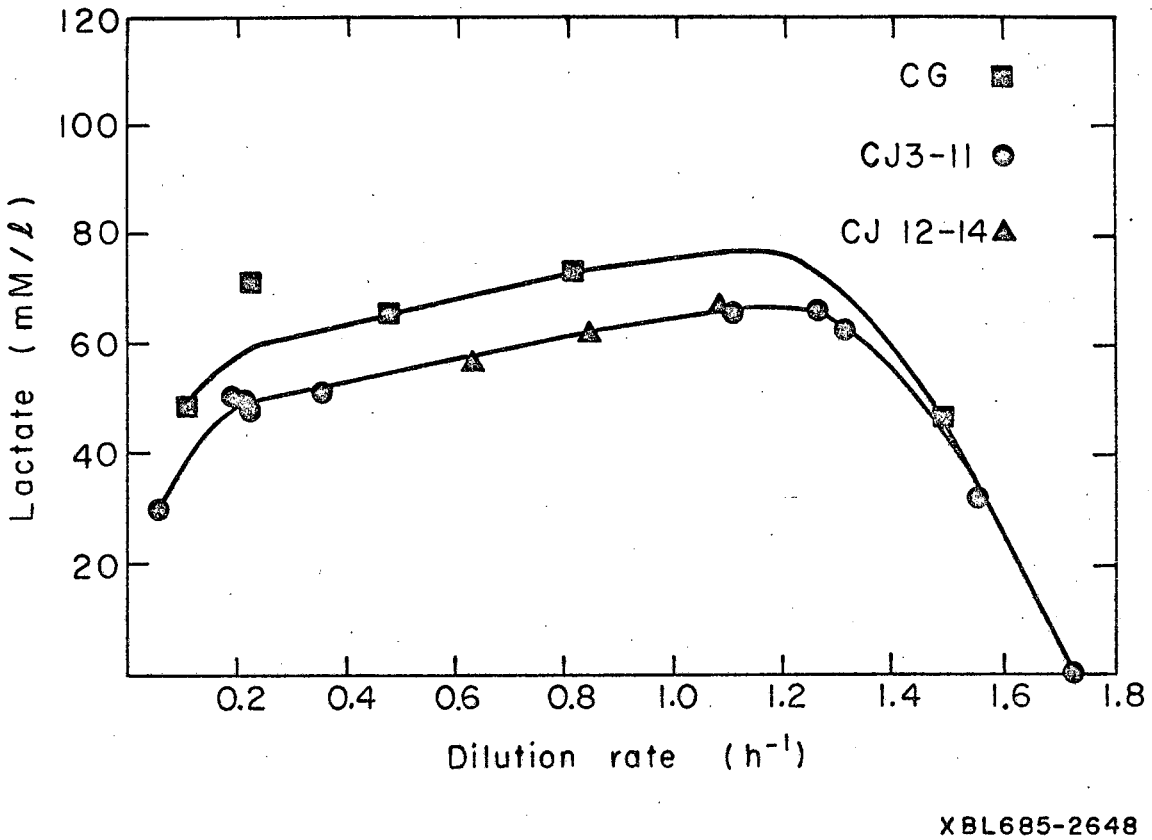

Fig. 30. The lactate concentration as a function of dilution rate for the continuous stirred tank experimental Runs CG and CJ. The data are presented on the basis of one liter of nutrient medium with corrections made for the volume of NaOH added.

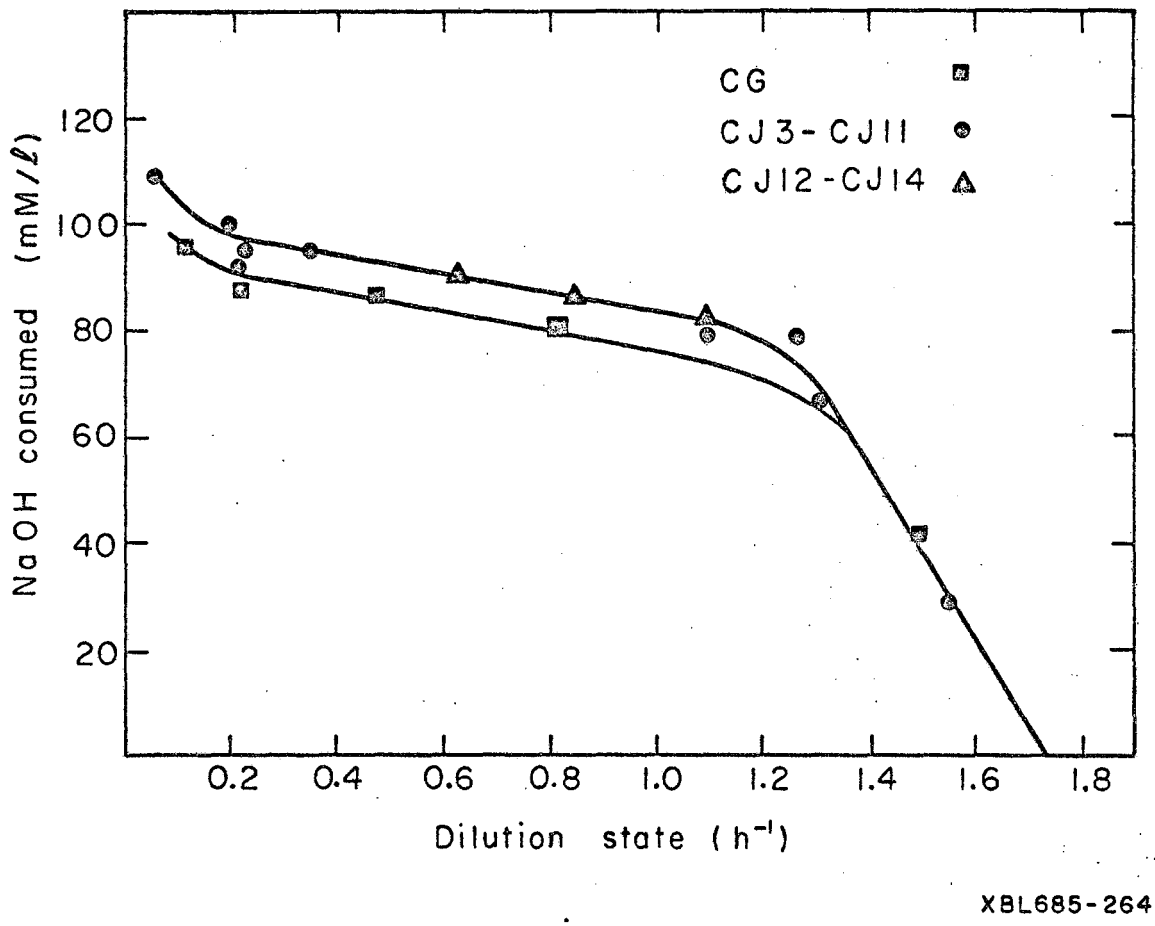

Fig. 31. The NaOH consumption per liter of nutrient medium for the continuous stirred tank experimental Runs CG and CJ.

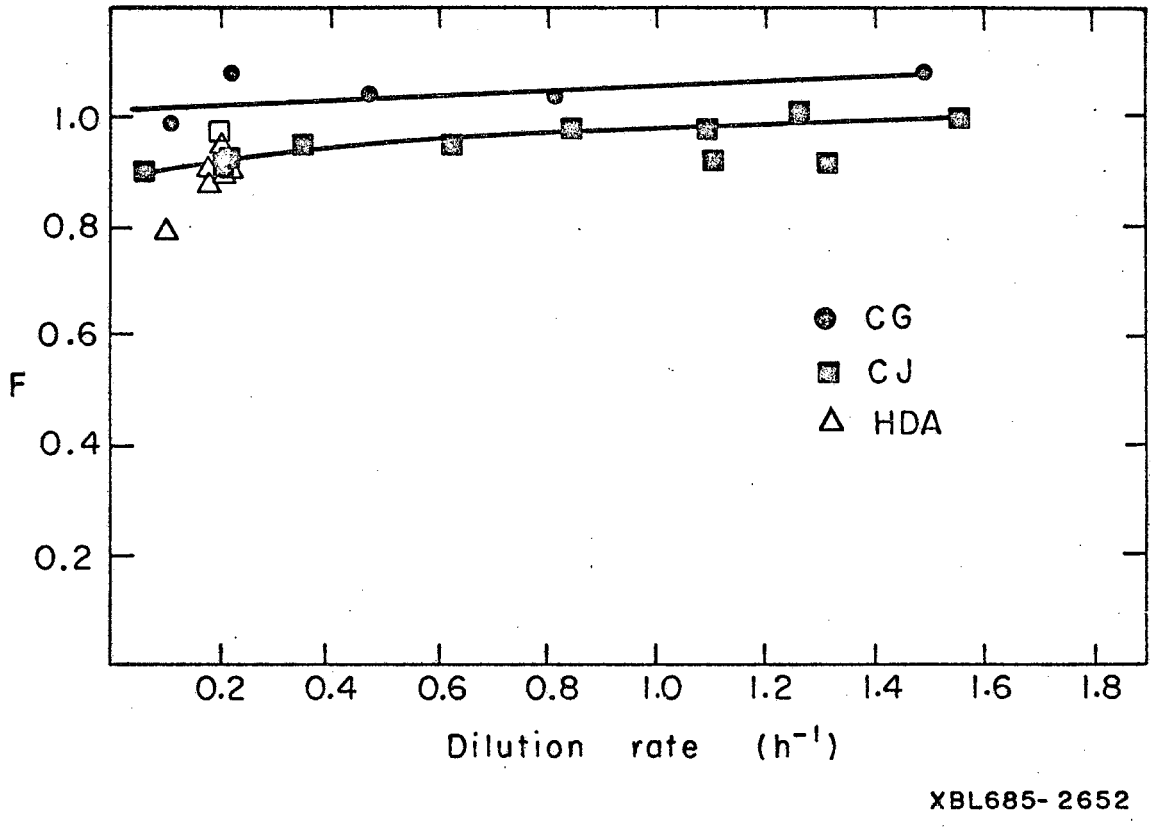

Fig. 32. The fraction of the glucose fed to the fermenter which can be accounted for in the effluent (using Eq. 10) for stirred tank experimental Runs CG and CJ, and for the steady state high density experimental Run HDA.

steady state, low density data for Runs CG and CJ while the third set is for the high density, steady state Run HDA. The other experimental results for HDA are presented and discussed in a following section.

The value of F was a slight function of specific growth rate. The shape of the curves for Run CG and CJ are similar but the data for CG was consistantly about 7% higher. The lactate analysis for Run CG may have been in error, for sample CG9 gave 47.1 mM lactate/l of feed while only 40.8 mM NaOH/l of feed were added. If the base added to sample CG9 is assumed to give the correct glucose to lactate conversion, then the value of F is 1.0.

At high growth rates, all the glucose fed to the system could be accounted for and almost all of it was converted to lactate. The lactate yield constants as defined by Eq. (4) were computed for these runs and they are shown on Fig. 46. Discussion of these data is presented in a later section dealing specifically with lactate yield constants.

The fraction of glucose which can be accounted for by the proposed material balance, decreases to 0.9 as the specific growth rate approaches zero. The data for Runs CJ and HDA agree well except for one sample, HDA5, which was about 12% low. The continuous culture data of Rosenberger and Elsden[3] for S. faecalus agree well with the results obtained here. At low growth rates, 90% of the glucose consumed was converted to lactate, formate and acetate, while at higher growth rates, nearly 100% of the glucose was converted to these products.

2. Mathematics of Continuous Fermentation

For a continuous fermenter operated with no cells entering with the feed, Eq. (11) represents the material balance for the cells contained in the system.

$$\frac{dN}{dt} = \left(\frac{dN}{dt}\right)_G - \frac{v}{V} N \qquad (11)$$

$$= 0 \quad \text{at steady state}$$

where:

v = rate of overflow

V = fermenter volume.

From Eq. (1)

$$\left(\frac{dN}{dt}\right)_G = \mu N . \tag{1}$$

Therefore, during the steady state operation of a continuous fermenter, the specific growth rate is uniquely defined by the dilution rate.

$$\mu = \frac{v}{V} . \tag{12}$$

The substrate material balance is expressed in Eq. (13).

$$\begin{aligned} \frac{dS}{dt} &= \frac{v_f}{V} S_0 - \left(\frac{dS}{dt}\right)_{consumed} - \frac{v}{V} S \\ &= 0 \quad \text{at steady state} \end{aligned} \tag{13}$$

where:

v_f = feed rate

S_0 = initial substrate concentration.

During the discussion of the batch growth results, two different models for the rate of glucose were examined; the Luedeking maintenance energy model and the energy dissipation model. In the continuous fermentation experiments, the initial glucose concentration was kept low in order that growth would be glucose limited. If the Luedeking model is assumed, then

$$-\left(\frac{dS}{dt}\right)_{consumed} = \alpha \mu N + \beta N . \tag{6}$$

Substituting Eq. (6) into Eq. (13) and re-arranging:

$$\alpha \frac{v}{V} + \beta = \left(\frac{v_f}{V} S_0 - \frac{v}{V} S\right) \frac{1}{N} . \tag{14}$$

Equation (14) is plotted (for Runs CG and CJ) in Fig. 33 which shows that the intercept is equal to zero. Therefore, no apparent maintenance energy is required. Furthermore, the values of α calculated from the slopes of the linear curves agree quite well with those summarized in Table II for the energy dissipation model. It can be concluded, then, that Eq. (9) is the correct representation of the glucose consumption mechanism with $Y_{C/S} = 1.0$ for glucose limited growth.

The data for these continuous runs do not fall on a single curve. The differences in growth which were evident in Fig. 29 for the OD versus dilution rate data appear in Fig. 33 as changes in the yield of cells per mole of glucose consumed. S. faecalus has very fastidious nutritional requirements and the medium used in these experiments was undefined in composition due to the yeast extract. The same batch of yeast extract was used for all of the experiments but it is possible that alterations in cell metabolism may have occurred giving rise to slight changes in cell yield.

3. Washout Experiment

A continuous fermenter can be used to experimentally determine the maximum growth rate of a micro-organism by increasing the dilution rate to a point where washout occurs. Equation (11), after substitution of Eq. (1) for $(dN/dt)_G$, becomes:

$$\frac{dN}{dt} = (\mu - \frac{v}{V}) N . \qquad (15)$$

Assume that at time $t = 0$, the dilution rate is increased to a value well beyond the maximum attainable by the cells. The cell concentration falls and the growth rate, which had been nutrient limited, begins to increase and after a short transition period, attains the maximum value. For the period when μ is constant at the maximum value, Eq. (15) can be integrated to give

$$\ell n\ N/N_0 = (\mu - \frac{v}{V})t \qquad (16)$$

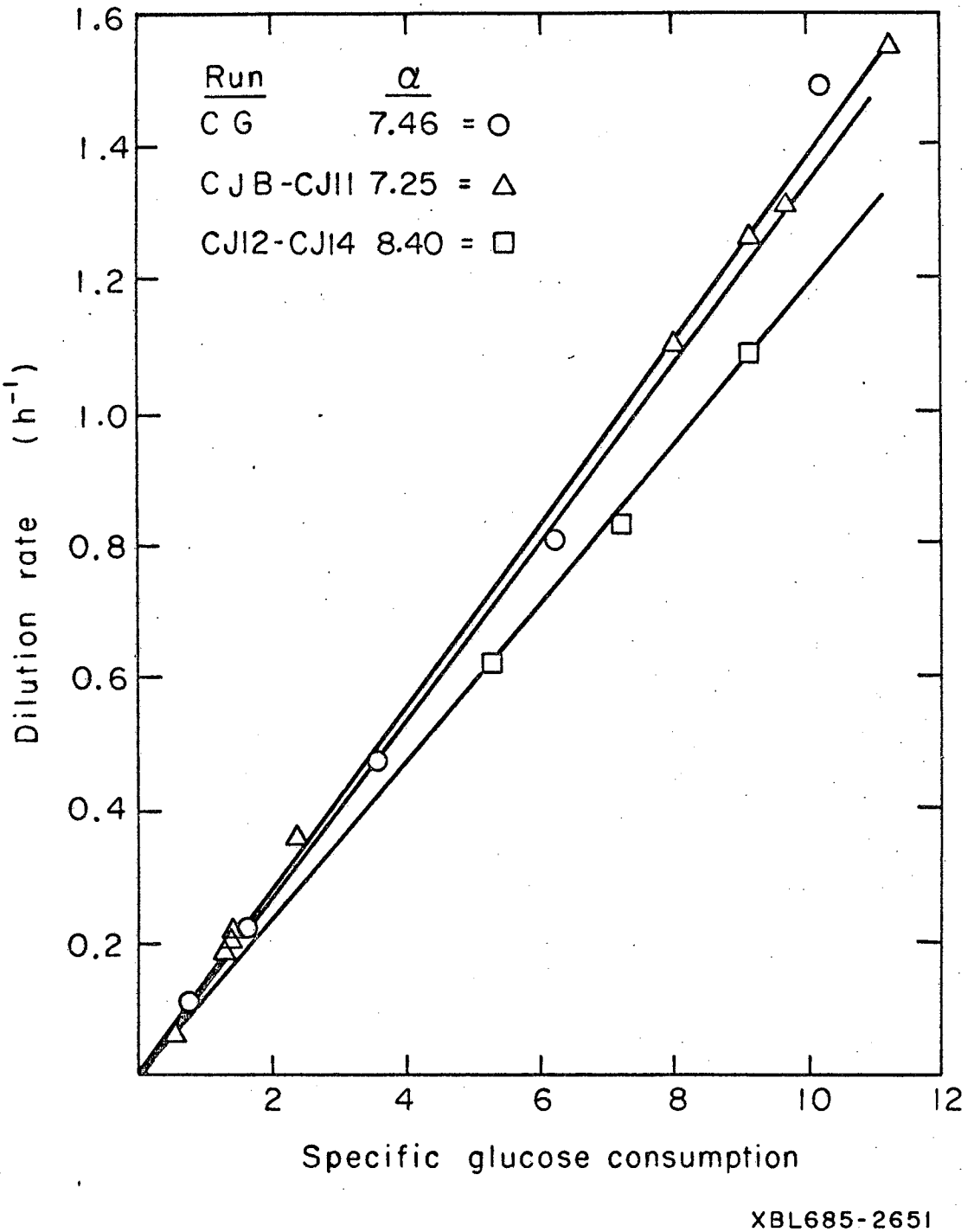

Fig. 33. The dilution rate (equal to the specific growth rate at steady state) versus the specific glucose consumption for the continuous stirred tank experimental Runs CG and CJ. The data shows that the maintenance energy term, β, in the Luedeking et al. maintenance energy model is essentially zero.

where $N = N_0$ when $t = 0$. By plotting the log of the cell concentration in optical density units versus time, the value of $(\mu - \frac{v}{V})$ can be determined directly from the slope. Figure 34 presents the data for a washout experiment. At $t = 0$, the dilution rate was increased to 2.98 hr^{-1} and cell concentration began to drop. After a short transition period of 30 minutes, maximum growth rate was attained and an exponential decrease in concentration began. From the slope of the linear portion of the semi-log plot, the maximum specific growth rate was calculated to be 1.73 hr^{-1}, a value practically identical to that obtained in batch culture.

C. Continuous Fermentation With Filtration

Preliminary experiments with the filtration rotor in place demonstrated that successful operation without an excessive pressure drop across the membrane could be maintained for a period of days. Considerable difficulties were encountered during the preliminary runs in obtaining a cell-free filtrate. A number of sterilization methods were tried but most either did not achieve complete sterility or would cause the membrane to become brittle. A successful technique using a combination of steam and formaldehyde has been presented earlier in the section dealing with equipment sterilization. Following the establishment of procedures to obtain a satisfactory membrane, it was discovered that slight leaks had developed around the shear pins which held the rotor together. These joints were sealed with epoxy glue and during repeated steam sterilizations, the glue failed. After the source of the leakage was found, another application of epoxy completely solved the problem. For example, viables counts of filtrate samples taken from Run TI gave counts of 2 times 10^3/ml during the early part of the run and 10^5/ml at the end of the run. These counts were so low that they could not be observed visually. The filtrate was perfectly clear, just like the nutrient feed.

Before the leakage problem was solved, a number of experiments were done and the amount of leakage corrected for. However, when too

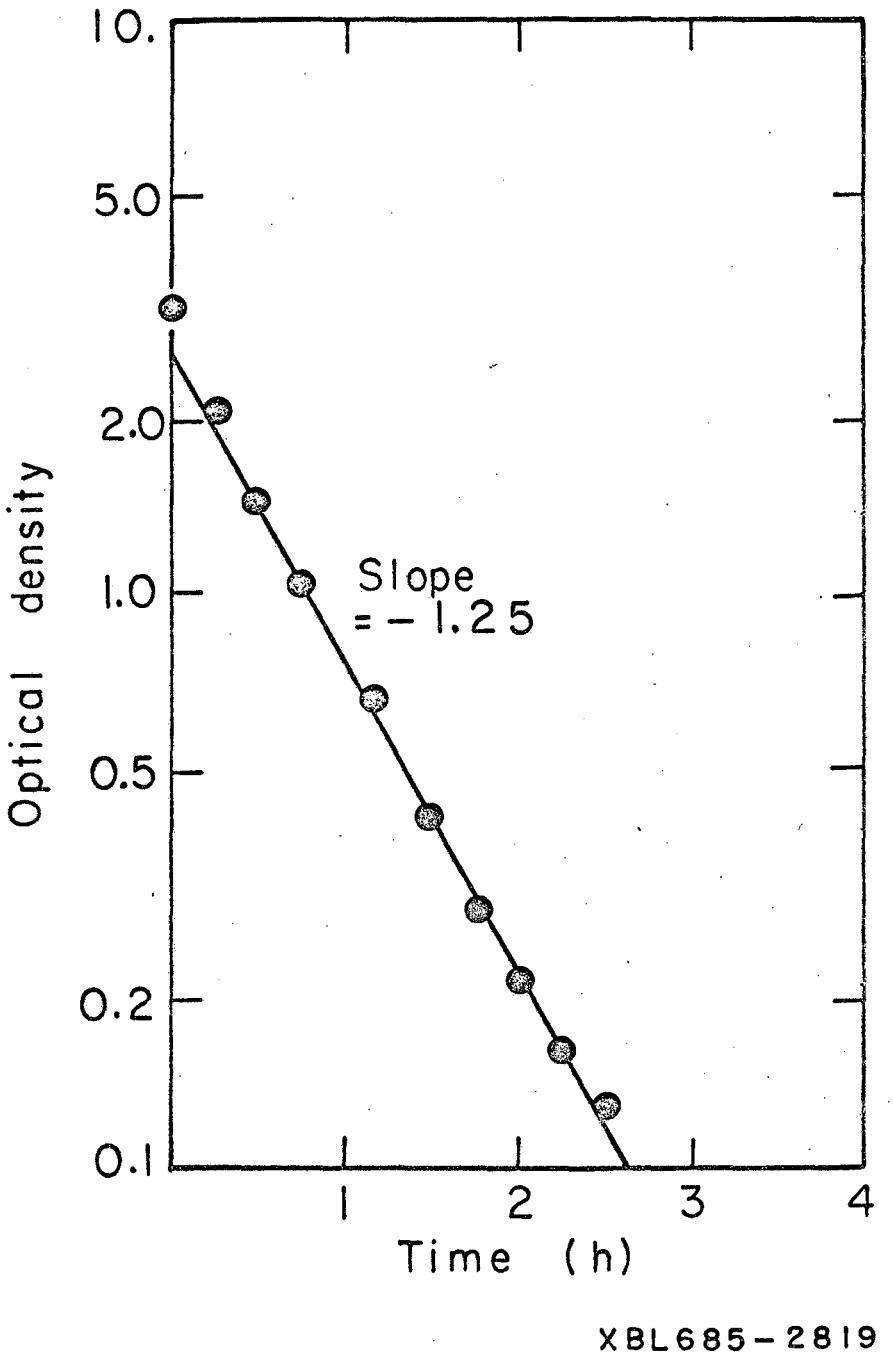

Fig. 34. Washout experiment for the determination of the maximum specific growth rate. From the slope of the semi-log plot (-1.25 hr^{-1}), the maximum specific growth rate was computed to be 1.73 hr^{-1}.

large a cell concentration developed in the filtrate, the run had to be terminated.

Originally, experiments were planned for the study of dense cultures under steady state conditions. The time required to reach steady state was quite long and flow rates, particularly the bleed rate of cells, could not be maintained accurately without constant attention. The control mechanism for the nutrient supply pump began to wear out and it was impossible to correct by fine adjustments. The control mechanism was replaced when it had deteriorated too far. The control of bleed flow rates was more critical because slight changes had a large effect upon the final cell concentration. By measuring the flow continuously in a graduated buret, the amount of effluent could be accurately controlled as a function of time but constant attention was required. The poor control of bleed rate was caused by the periodic evolution of small quantities of gas from the fermentation and, since the bleed was pumped out of the system in controlled volumes, the pumping rate had to be temporarily increased to compensate. Gas evolution was small in volume, a few ml/hr, and was present during only a small part of the run. Reduction of liquid volume in the fermenter by collection of gas was not significant due to the location of the exit line at the extreme top of the fermenter and due to the small amounts of gas involved. Evolution of large quantities of gas would have caused a severe problem.

1. Mathematics and Experimental Results

Equation (11) for the cell material balance in continuous fermentation can be expanded to account for cells lost due to leakage through the filter:

$$\frac{dN}{dt} = \mu N - \frac{V_B}{V} N - \frac{V_F}{V} N_F \qquad (17)$$

$$= 0 \quad \text{at steady state}$$

where:

v_B = bleed flow rate

v_F = filtrate flow rate

N_F = cell concentration in filtrate.

Therefore:

$$\mu = \frac{v_B}{V} + \frac{v_F}{V} \frac{N_F}{N} . \tag{18}$$

Equation (13) for the glucose material balance can also be expanded in a similar fashion to account for the filtrate.

$$\frac{dS}{dt} = \frac{v_f}{V} S_0 - \left(\frac{dS}{dt}\right)_{consumed} - \frac{v_B}{V} S - \frac{v_F}{V} S \tag{19}$$

$$= 0 \quad \text{at steady state.}$$

As has been shown by the results for continuous fermentation:

$$\left(\frac{dS}{dt}\right)_{consumed} = \alpha \mu N . \tag{9}$$

Substituting Eqs. (9) and (18) into (19) results in:

$$N = \frac{v_f S_0 - (v_B + v_F)S}{\alpha v_B} - \frac{v_F}{v_B} N_F . \tag{20}$$

The concentration of glucose was essentially zero for all samples of broth analysed. Therefore:

$$N = \frac{v_f S_0}{\alpha v_B} - \frac{v_F}{v_B} N_F . \tag{21}$$

Equation (21) can be re-arranged into a form more suitable for graphical presentation:

$$N + \frac{v_F}{v_B} N_F = \frac{v_f S_0}{v_B} \frac{1}{\alpha} . \tag{22}$$

All of the variables contained in Eq. (22) were measured with the exception of α. A plot of Eq. (22) should be linear with an intercept at zero. Figure 35 shows the data for Run HDA. A linear curve does fit the data well except for one point at the highest OD. The value of α calculated from the slope of the curve is 7.05 mM glucose/l/OD, a value very close to values determined from batch and continuous growth without filtration.

D. Transient Growth with Filtration

During the steady state runs, the concentration of glucose was negligible for growth rates below 1.2 hr^{-1}. This observation allowed the use of unsteady state experiments to investigate high density growth characteristics. The advantage of studying the transient regime lies in the greatly increased amounts of information obtained over a shorter period of time.

1. Mathematics and Experimental Results

The mathematical framework for transient behavior was developed using the equations derived for the steady state case. The material balance for the micro-organisms is given by Eq. (17) but now the time derivative of cell concentration is not equal to zero.

$$\frac{dN}{dt} = \mu N - \frac{v_B}{V} N - \frac{v_B}{V} N_F \,. \qquad (17)$$

The material balance for substrate is given by:

$$-\frac{dS}{dt} = \frac{v_f}{V} S_0 - \alpha \mu N - \frac{v_F}{V} S - \frac{v_B}{V} S \,. \qquad (19)$$

Since S is equal to zero, then $dS/dt = 0$, and Eq. (19) can be solved for the specific growth rate:

$$\mu = \frac{v_f}{V} S_0/\alpha N \,. \qquad (23)$$

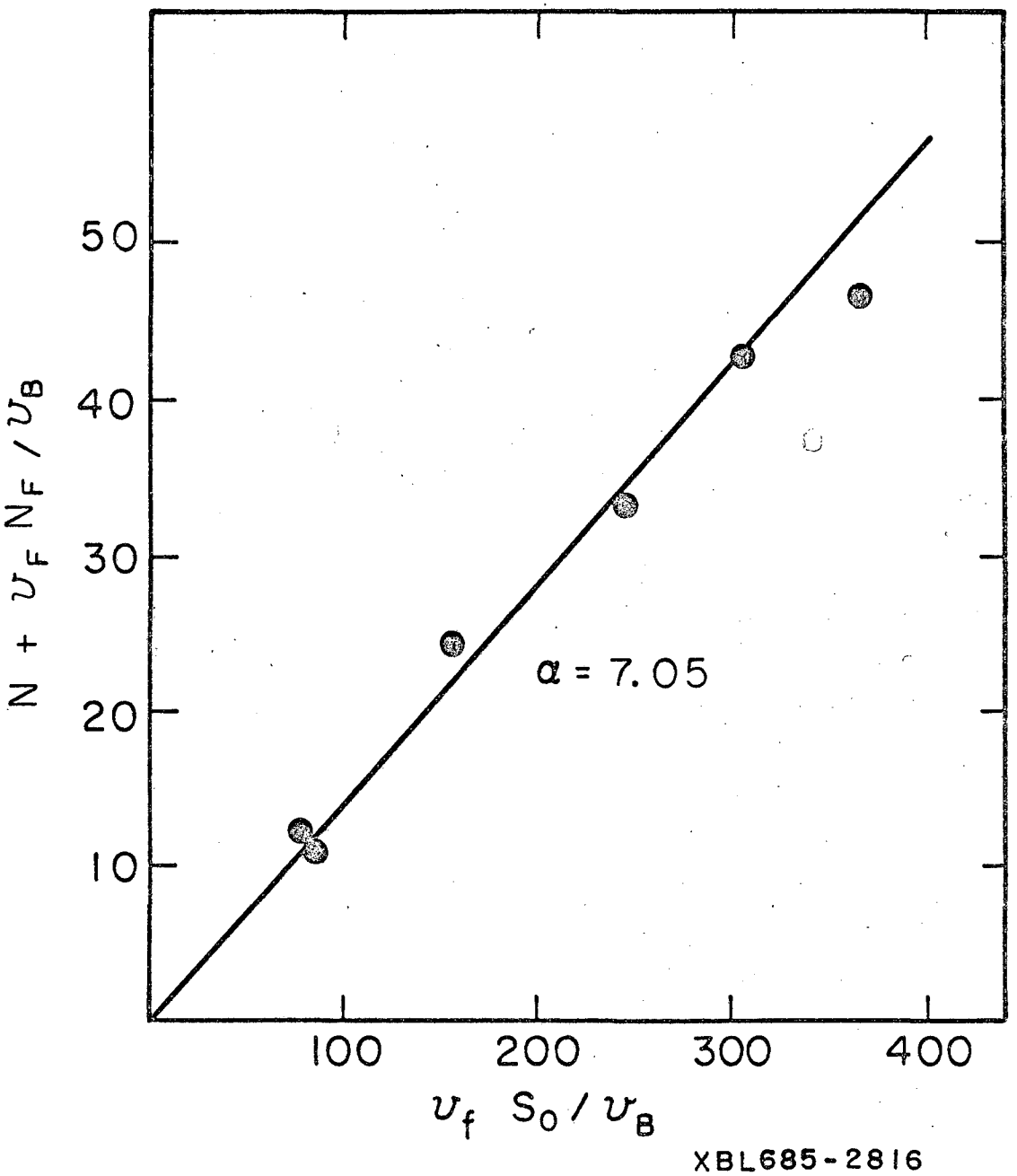

Fig. 35. The determination of the value of α for the steady state high density experimental Run HDA.

Substituting Eq. (23) into Eq. (17) results in a differential equation with N as the only dependent variable, assuming that the flow rates, feed concentrations and α remain constant.

$$\frac{dN}{dt} = \frac{v_f S_0}{\alpha V} - \frac{v_B}{V} N - \frac{v_F}{V} N_F . \qquad (24)$$

This equation can be solved with the initial condition that $N = N_0$ when $t = 0$.

$$N = A - (A - N_0) \exp\left(- \frac{v_B}{V} t\right) \qquad (25)$$

where:

$$A \equiv \frac{v_f S_0}{\alpha v_B} - \frac{v_F N_F}{v_B} .$$

A plot of N versus $\exp(- v_B t/V)$ should be linear with slope equal to $A - N_0$ and intercept equal to A as time becomes very large. The value of A defines the maximum cell concentration which can be developed.

The experimental procedure for all the transient runs was very similar. The fermenter was operated at steady state with the feed and bleed rates adjusted so that an OD around 10 was developed. At the start of the transient period, the bleed rate was adjusted to a predetermined value and the flow rate of feed increased to approximately 1 l.hr. This flow rate of nutrient was near the maximum which could be filtered for extended periods of time without excessive pressure buildup in the system. The volume of filtrate collected during the time interval between samples was measured. The bleed volume was collected and measured continuously in a graduated buret. By checking the volume collected as a function of time, very accurate bleed flow rates could be maintained. Samples of the broth were removed from the recycle line of the fermenter. The bleed flow was stopped at the sampling time and remained off until the sample volume removed from the fermenter was accounted for.

The experimental results for a series of transient runs are shown in Fig. 36 through 42 inclusive. Two curves are presented on each figure, one for the OD and the other for the lactate concentration. Before a detailed discussion of the results is presented, several general observations which were common to all of the experiments can be made. It is quite clear that the linear relationship expressed by Eq. (25) is valid. However, during most of the runs, a single straight line does not represent the data and a series of linear curves is required. Since the slope of the curves is uniquely defined by the value of A in Eq. (25), then one of the variables incorporated in A is changing. Furthermore, it appears as if an abrupt change occurs. All of the variables except α were measured and remained constant. Therefore, it must be concluded that the value of α is abruptly changing during the course of the run, indicating an alteration in the metabolic pathway scheme. Further proof that such pathway alterations (rather than measurement errors) are actually happening is given by the changes in lactate concentration at the point of change.

At the beginning of a run, the feed was increased stepwise from a low value to a much higher one. The cells had to increase their growth rate to utilize the additional substrate and their reaction was not instantaneous; a transition period was required. Adjustment to the increased feed rate was quite rapid and by the time that the first sample was taken after 30 minutes or an hour, the linear relation predicted by Eq. (25) was followed.

The yield of lactate from glucose catabolism was proportional to the specific growth rate. The growth rate prior to the initiation of the transient run was much lower than the rate after the run began. Therefore during the first part of the experiment, the lactate concentration increased due to increased yield of lactate per mole of glucose and began to decrease as the specific growth rate began to decrease. This is the reason for the maximum which appears in the lactate concentration during the initial period of the run.

The nutrient feed rate and bleed rate for Run TB were 950 ml/hr and 55 ml/hr respectively and the experimental results are shown in Fig. 36. The technique of controling bleed flow rates had not been perfected and some fluctuation occurred. The run was terminated before steady state was reached because leakage of broth through the membrane became quite large just after the data points shown were taken. The data follow Eq. (25) quite well and the value of α computed from the slope was 6.24 mM glucose/l/OD, a value close to those determined from the previous experiments. The maximum in lactate concentration is present. Since the initial OD was quite large, the specific growth rate computed using Eq. (23) for $t = 0$ was only $0.259\ hr^{-1}$ and the yield of lactate at the maximum was much smaller than the stoichiometric value. The lactate concentration appeared to approach a constant value as the run progressed.

Figures 37 and 38 show the results for Runs AC and AD respectively. These experiments were conducted at the same flow conditions with the bleed rate equal to 28 ml/hr and the feed rate equal to 850 and 1100 ml/hr respectively. Figure 37 for Run AC definitely shows that the value of α abruptly changed! The data for Run AD shows no corresponding change. The non-linearity evident in this run was due to a progressive decrease in the nutrient feed rate caused by a deterioration in the speed control mechanism of the pump. To demonstrate that the value of α remained a constant for Run AD, a general equation was developed to calculate the value of N under conditions where flow rates are changing. The course of the transient run was broken up into a series of discrete intervals corresponding to the sampling times and the average flow rate values for each interval used, together with Eq. (25), to predict the value of N at the end of each interval as a function of the initial cell concentration and the time interval. By combining the expressions for each interval, the value of N at the end of any time interval, n, could be expressed as a function of the average interval flow rates and the cell concentration at $t = 0$ by:

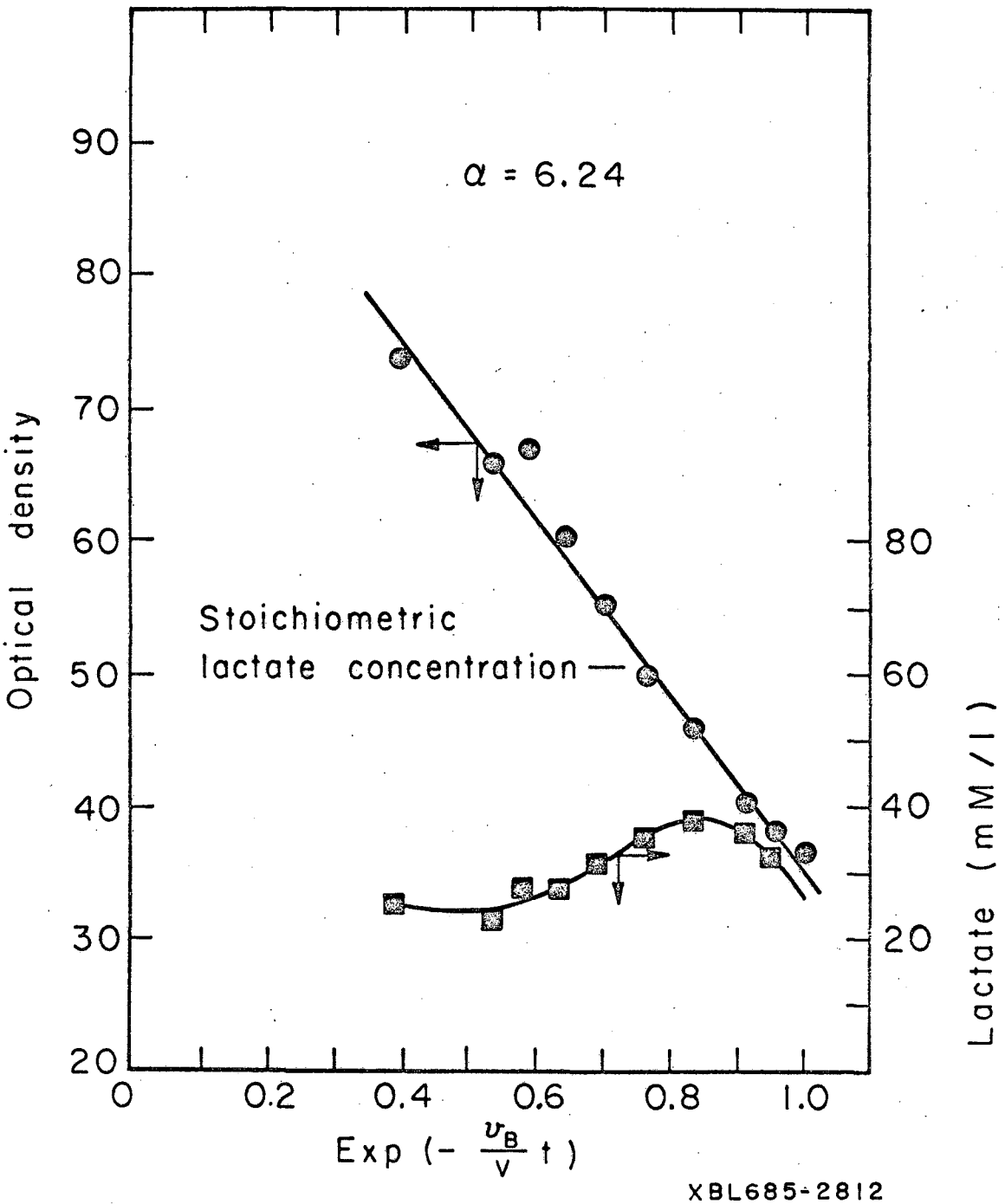

Fig. 36. The growth curve and the lactate concentration for the transient high density experimental Run TB.

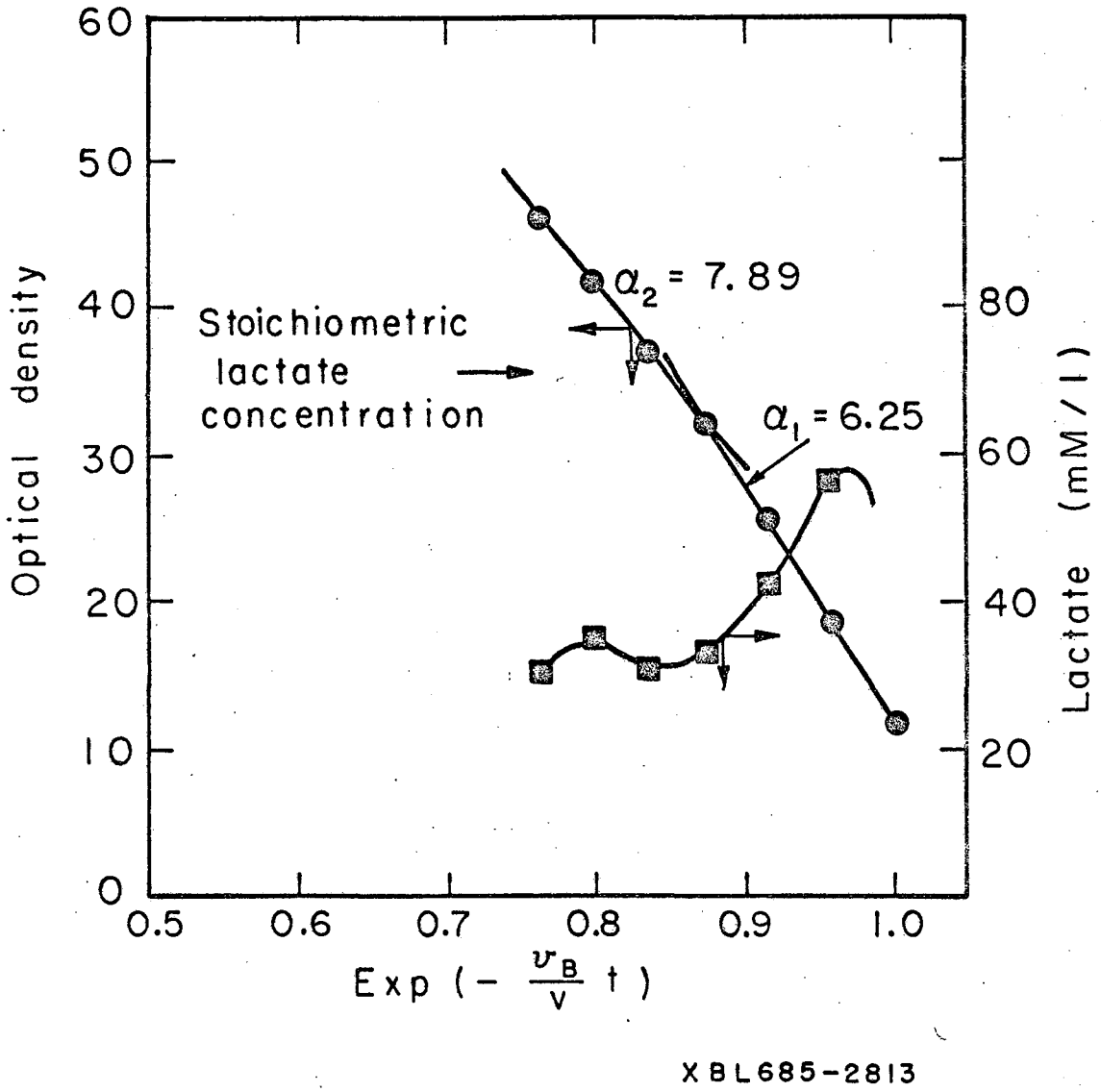

Fig. 37. The growth curve and the lactate concentration for the transient high density experimental Run TC.

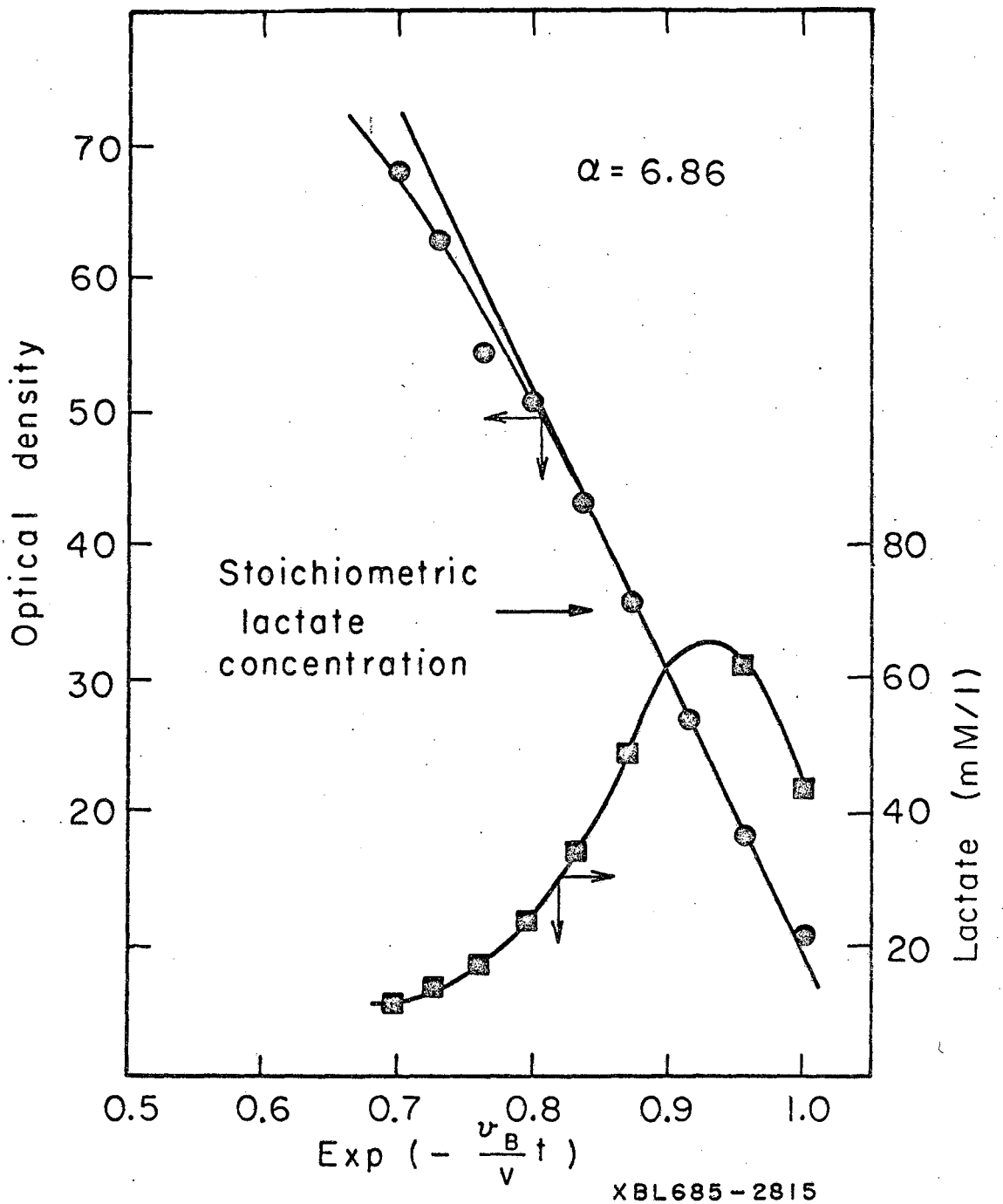

Fig. 38. The growth curve and the lactate concentration for the transient high density experimental Run TD.

$$N_n = A_n\left(1 - \exp(-D_n \Delta t_n)\right) +$$

$$\sum_{i=1}^{n-1} D_i\left(1 - \exp(-D_1 \Delta t_i)\right) \prod_{\delta=i+1}^{n} \exp(-D_j \Delta t_j) +$$

$$N_0 \prod_{n} \exp(-D_n \Delta t_n) \qquad (26)$$

where:

$$D \equiv \frac{v_B}{V}$$

$$A \equiv \left[\frac{v_f S_0}{\alpha v_B} - \frac{v_F N_F}{v_B}\right]$$

$$\Delta t_n = t_n - t_{n-1} .$$

In this expression, the variables, A_n and D_n, take on their average values during the time interval $\Delta t_n = t_n - t_{n-1}$.

The application of Eq. (26) to the data for Run AD was simplified because the time intervals and bleed rate were constant. The only variable not directly measured experimentally was α and it was evaluated from the slope of the initial portion of the curve in Fig. 38 where the feed rate was not changing very much. The initial calculated value at $t = 0$ was lower than the experimental value due to the lag which occurred in the growth process when the feed rate was abruptly increased at $t = 0$. This initial calculated value was determined from an extrapolation of the curve in Fig. 38 to zero time and was used as the starting point for the calculated OD projection. To summarize the computational procedure, Eq. (26) was used together with the initial extrapolated $OD = 8.6$ at $t = 0$, the value of $\alpha = 6.86$ computed from the initial

slope and the average flow rates between sample intervals, to calculate the cell concentration at the sampling times. A comparison between the calculated and experimental values is summarized in Table III.

The computed and experimental values agree very closely with the exception of sample TD6. The graphical presentation of the data shown in Fig. 38 indicates that the experimental value for the OD was in error. Excluding sample TD0, the standard percent deviation is 2.1% and clearly demonstrates the applicability of the mathematical formulation and that α was a constant.

Table III. Comparison of experimental and calculated cell concentrations for Run TD.

Sample Number	Experimental OD	Calculated OD
0	10.7	8.6
1	18.2	17.6
2	27.0	26.7
3	35.8	34.9
4	43.0	42.9
5	50.4	50.2
6	54.4	57.1
7	62.8	63.6
8	68.0	69.3

Standard % deviation = 2.1% (does not include sample 0)

The experimental lactate concentrations for Runs TC and TD are similar and follow the general pattern with a maximum shortly after the experiment commenced. The change in α for Run TC is accompanied by a slight increase in lactate concentration. In general, the lactate concentration decreased with specific growth rate. Since the initial cell concentration was low, the initial specific growth rate was larger than

in Run AB. Correspondingly, the fraction of glucose converted to lactate is larger. The shape of the lactate concentration curve for Run AD is different than for AC since the feed rates are different.

Both experiments had to be terminated prematurely because of mechanical problems with the filtration mechanism.

Runs TE and TF were again duplicate experiments and the results are shown in Figs. 39 and 40. The bleed rate was 90 ml/hr and the nutrient feed rates were 1050 and 770 ml/hr respectively. In both of these experiments, sudden changes in α were observed but the sequence of change was reversed. During the initial stages of Run TE, α was small and then became larger while for Run TF, the reverse was true. Run TE was started at an OD similar to Run TF but an experimental error ruined the first few data points so that the maximum in lactate concentration was missed. The first lactate value for Run TF appears to be in error since the measured amount is greater than the stoichiometric value. In neither experiment did there appear to be a change in the lactate concentration profile as a result of changes in α .

Run TF continued until steady state was almost reached. The maximum cell concentration which could be developed was slightly less than 50 OD. In order to investigate high concentrations, Run TI was done using the same bleed rate as in Runs TC and TD. The experimental results, shown in Fig. 41 and 42 exhibit a considerably more complex spectrum than any of the previous runs. No fewer than five changes in α occur during the experiment! The value of α , given in the figures, begins initially at 6.77, increases to 10.2, decreases to 5.34 and then increases to 10.47 before decreasing again. The last value of α was not calculated because too few data points were available. The changes in α were paralleled by changes in lactate concentrations and seem to be closely linked. While several changes in α were evident, the average value over the course of the run was near those obtained in the steady state experiments.

Run TI was terminated after 38 hours. The pressure in the system had increased gradually during the course of the run until 11 psi was

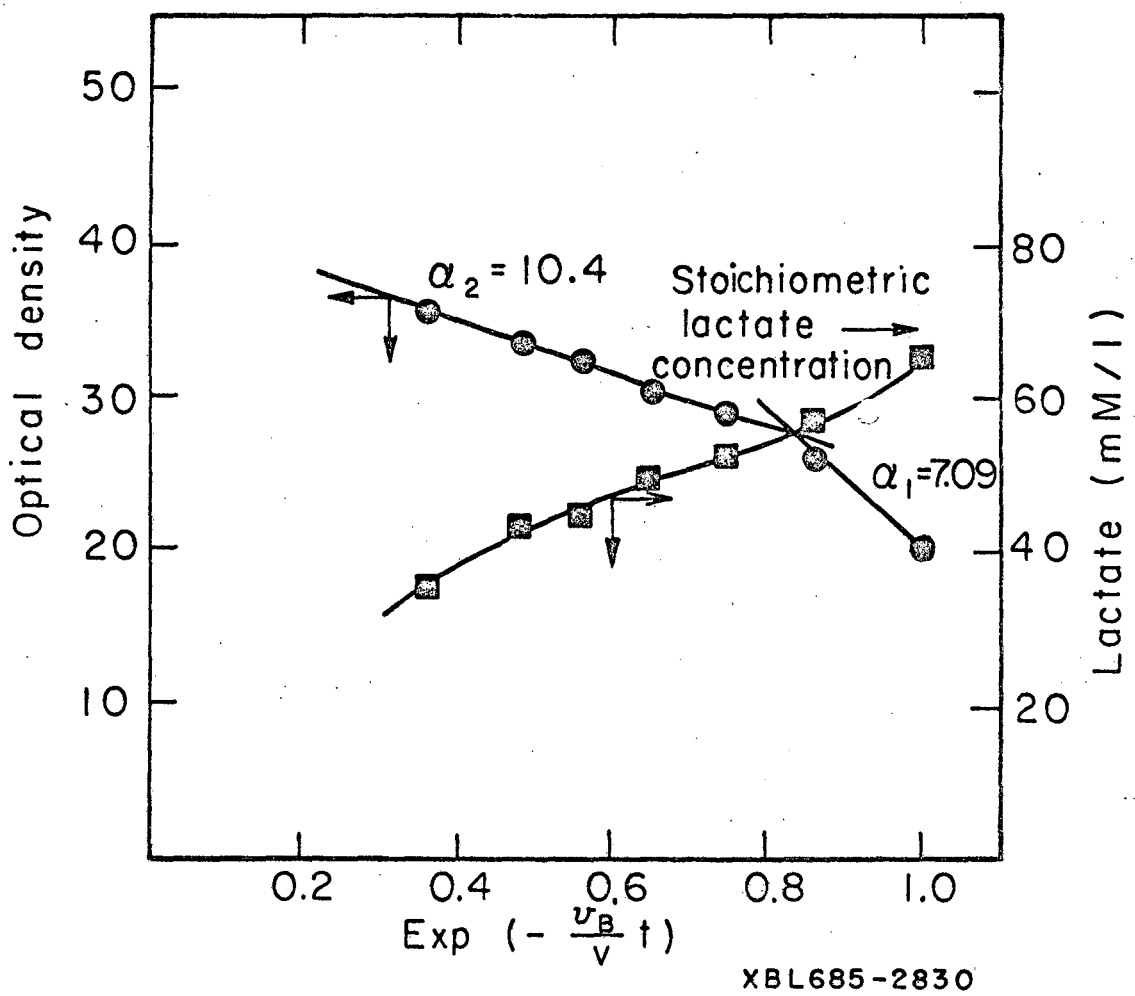

Fig. 39. The growth curve and the lactate concentration for the transient high density experimental Run TE.

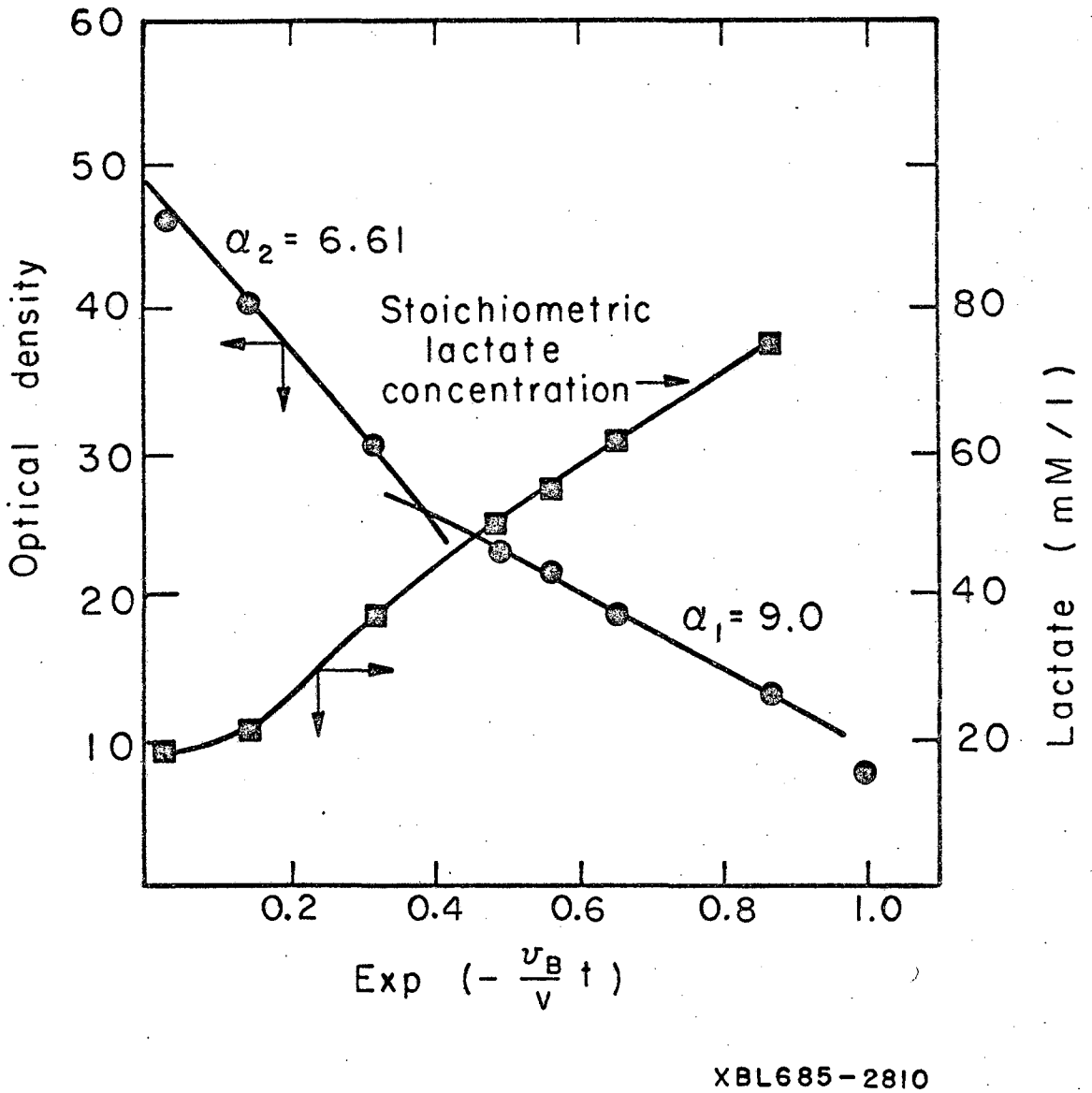

Fig. 40. The growth curve and the lactate concentration for the transient high density experimental Run TF.

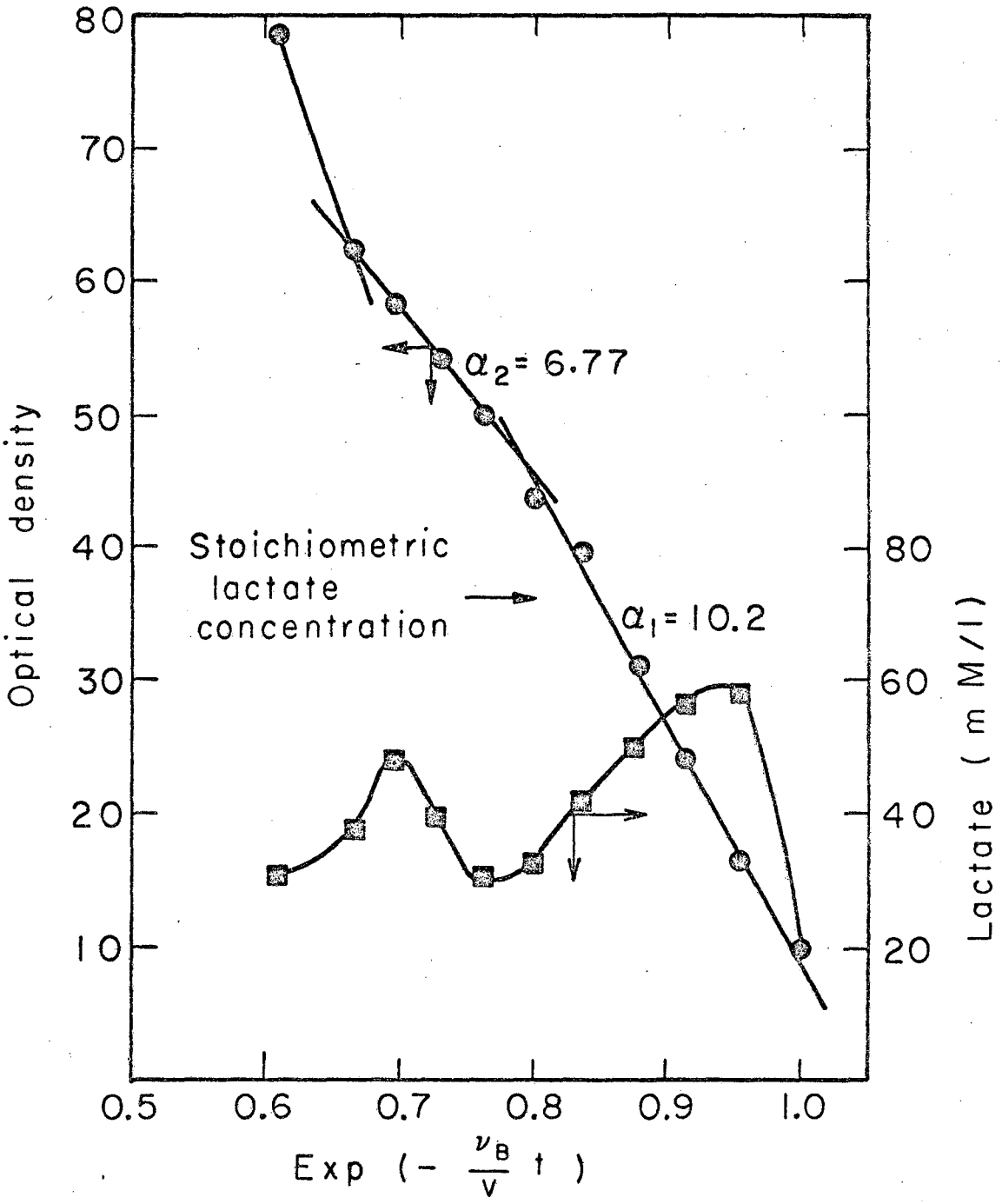

Fig. 41. The initial portion of the growth curve and the lactate concentration for the transient high density experimental Run TI.

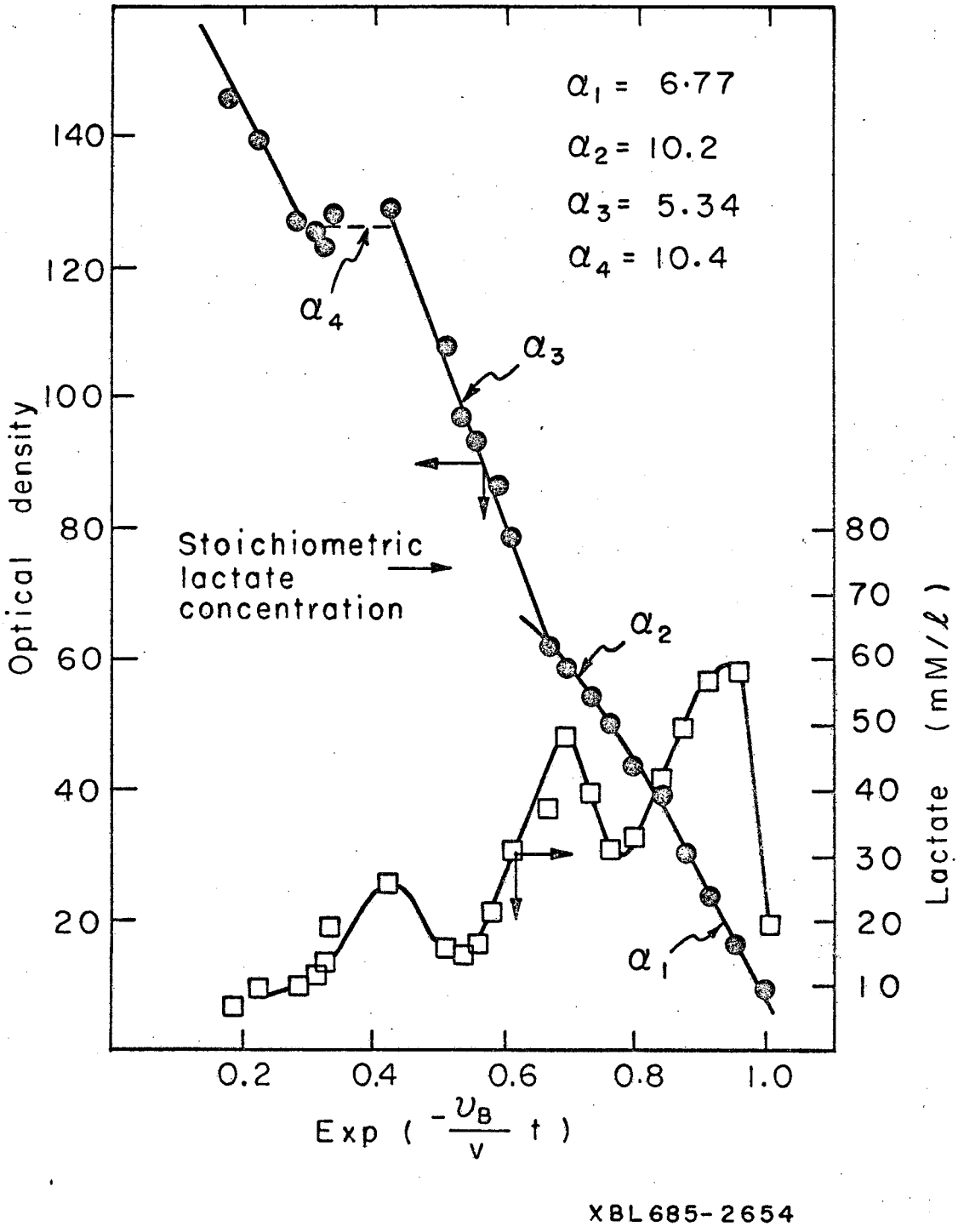

Fig. 42. The growth curve and the lactate concentration for the transient high density experimental Run TI.

reached. The run could have been continued further but little added information would have been gathered since the cellular concentration was changing quite slowly with time. The bleed stream was then stopped and the nutrient feed rate reduced to 540 ml/hr in order to reduce the system pressure. Growth of cells continued. Very small samples of the culture were removed, just enough for OD readings. The results of this experiment are shown in Fig. 43 where the cell concentration is plotted against time. The filtrate was perfectly clear so that $N_F = 0$. The solution of Eq. (24) becomes straight forward when v_B is zero.

$$N = N_0 + \frac{v_f S_0}{\alpha v} t . \qquad (27)$$

Two straight lines have been drawn through the data for Run TJ and they appear to fit fairly well except for the last two points. The values of α calculated from the slopes are indicated on the figure. For the first line α is 7.3 and is within the range observed for the previous runs. The second value of α was 15 and is larger than those previously encountered. Furthermore, the data appear to be approaching a limit. In other words, there appears to be a maximum cell concentration which can be developed with the medium employed.

Samples of the broth taken during Run TI had to be centrifuged before the supernatent was stored for chemical analysis. This supernatent was clear for all samples taken for Run TI but when the broth taken from the fermenter following the termination of Run TJ was centrifuged, a clear supernatent did not result. Microscopic examination indicated the presence of many "ghosts", the remnants of lysed cells. Apparently, the fall-off in the rate of cell concentration increase was due to cell death although this has not been proven.

The filtrate from the fermenter was as clear as the nutrient feed so that the cellular remnants which would not centrifuge out could not pass through the membrane. How much influence these remnants had upon the OD is not known but it was probably small.

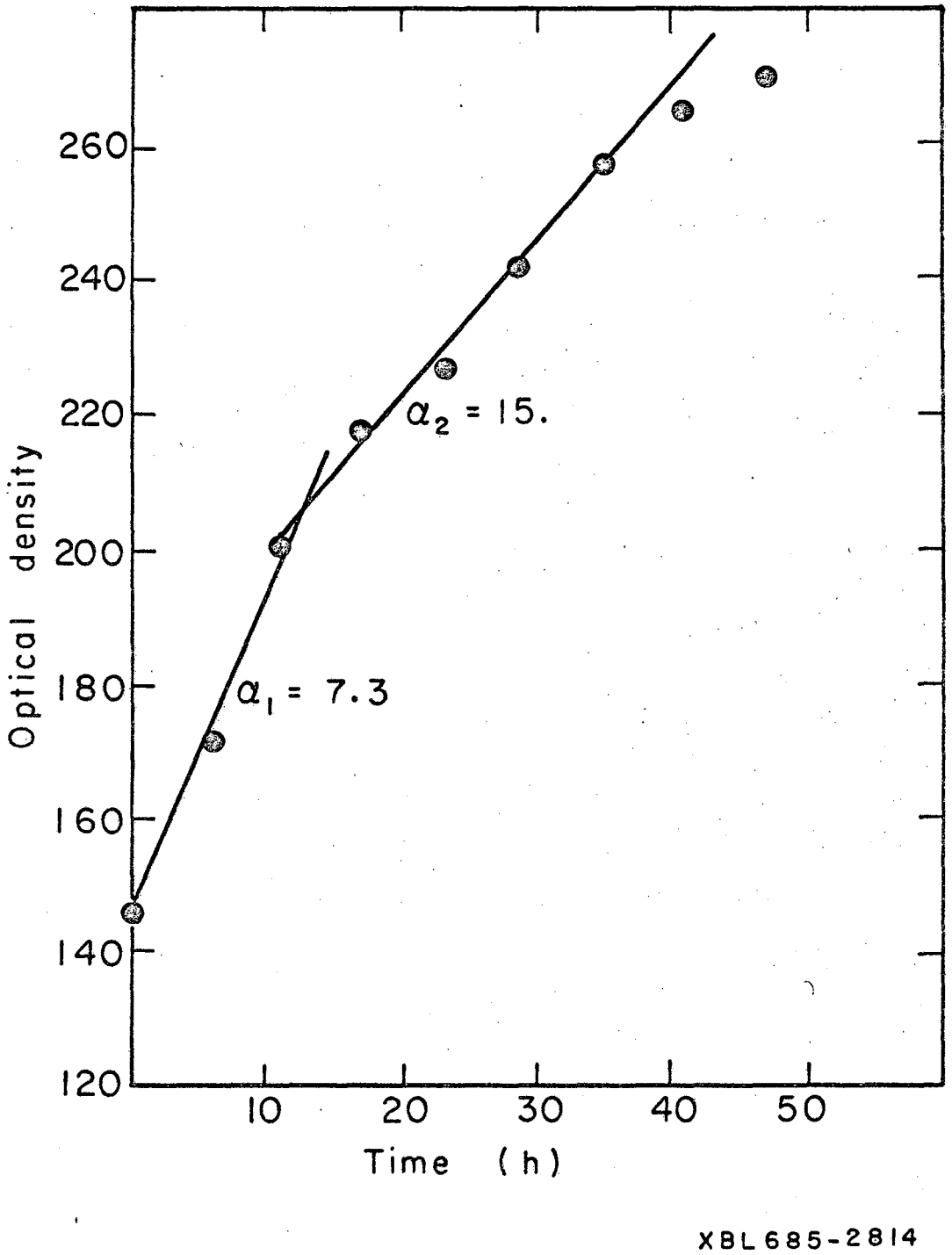

Fig. 43. The growth curve for the transient high density experimental Run TJ.

The run was terminated after two days. A sample of the broth was centrifuged at 16,000 g's for an hour and the packed cell volume was determined to be 40%. Figure 44 is a photograph of the broth before and after centrifugation together with a sample of the filtrate.

2. Lactate Yield Constant

The amount of glucose which was converted to lactate during the transient experiments could not be determined directly. The lactate concentration was time dependent and was influenced by the previous concentration history. However, during any time interval, the average lactate yield constant could be evaluated.

The product material balance is given by:

$$\frac{dP}{dt} = \left(\frac{dP}{dt}\right)_{Produced} - \frac{v_F}{V} P - \frac{v_B}{V} P \; . \tag{28}$$

The rate of lactate production is related to the rate of glucose consumption by a yield constant:

$$\left(\frac{dP}{dt}\right)_{produced} = - Y_{P/S} \left(\frac{dS}{dt}\right)_{consumed} \; . \tag{4}$$

The rate of substrate consumption is given by Eq. (19) with $dS/dt = 0$ and $S = 0$, then Eq. (19) becomes:

$$\left(\frac{dS}{dt}\right)_{consumed} = \frac{v_f}{V} S_0 \; . \tag{29}$$

Substitution of Eqs. (4) and (29) into (28) yields, after rearrangement:

$$\frac{dP}{dt} - P\left(\frac{v_F}{V} + \frac{v_B}{V}\right) = Y_{P/S} \frac{v_f}{V} S_0 \; . \tag{30}$$

For each time interval, the flow rates were known. If $Y_{P/S}$ is assumed to be constant for the time interval, $\Delta t_n = t_n - t_{n-1}$, then Eq. (30) can be integrated:

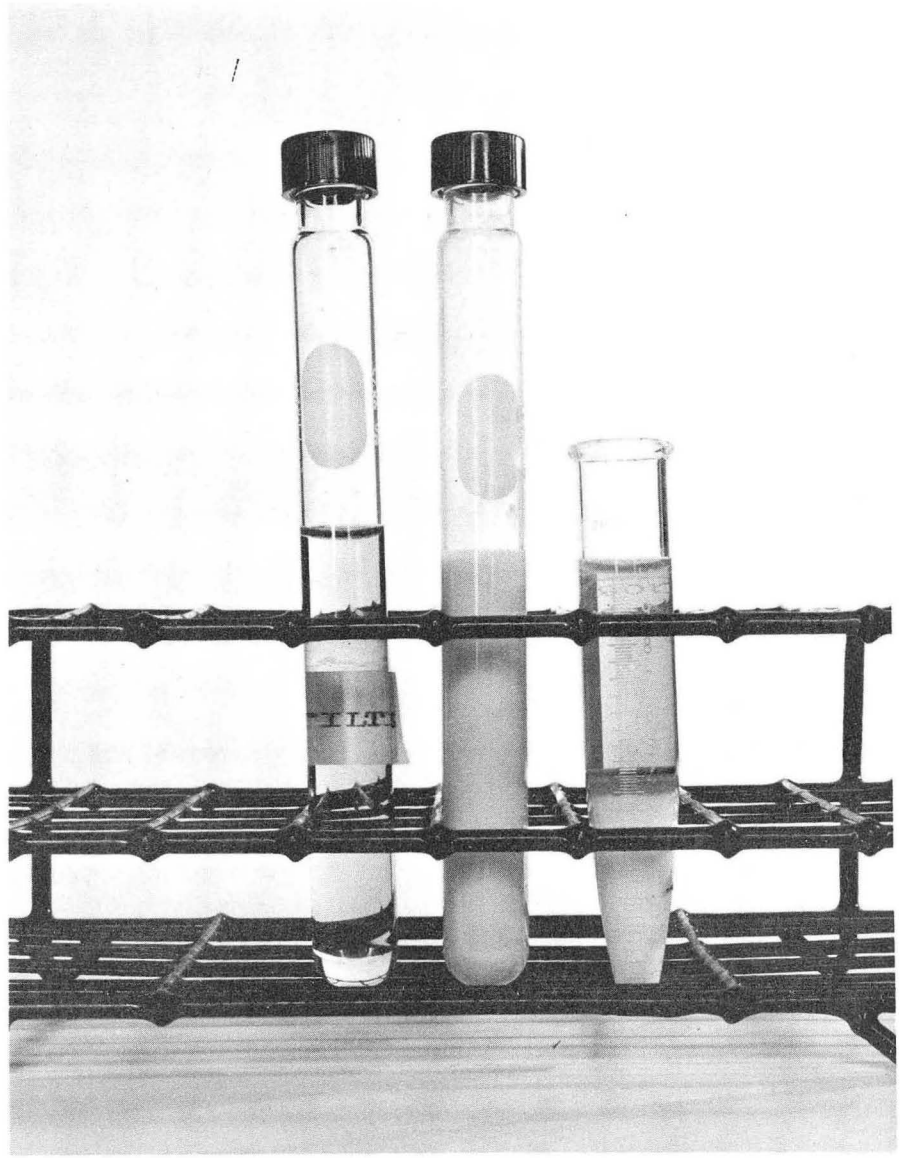

XBB 683-1029

Fig. 44. A photograph of the sample 8 taken from high density transient Run TJ. From left to right: the filtrate, the bacterial culture and a sample centrifuged at 16,000 g's for one hour which shows the packed cell volume attained.

$$P_n = Y_{P/S} E_n - (Y_{P/S} E_n - P_{n-1}) \exp(D'_n \Delta t_n) \qquad (31)$$

where:

$$E \equiv \frac{v_f S_0}{v_F + v_B}$$

$$D' \equiv \frac{v_F + v_B}{V} \quad .$$

Since the values of P are known from experimental measurement, the average value of the yield constant can be computed.

To illustrate the results obtained, the values of $Y_{P/S}$ for Run TI are presented in Fig. 45 as a function of time. Since the yield constants were average values, they were plotted at the median of the time interval when the time between samples was small. In Eq. (31), the exponential term for Δt's larger than two hours was small so that the initial lactate concentration had little influence on the terminal value. For samples where the time interval was greater than two hours, the yield constants were plotted at the end of the time period.

The yield constant curve closely follows the lactate concentration profile. The yield constant for the system just prior to the start of the transient run was 0.54 and is plotted at $t = 0$. The yield constant data for the initial portion of the run when extrapolated back to the $t = 0$ axis, gives a value for the initial yield very close to the stoichiometric one of 2.0. This observation was consistant for Runs TC, TD and TF where the initial cell concentration was small. Runs TE and TB displayed a similar shape but the $t = 0$ intercept was less than 2.0 because the initial cell concentration was larger causing a smaller initial specific growth rate. Apparently, just following the step change in feed rate, and therefore growth rate, an abrupt increase in yield occurs.

The points where the value of α changed have been indicated by arrows. Changes in α appear to correspond to alterations in the metabolism of the organisms, for after each change in α, the yield constant is quite drastically altered.

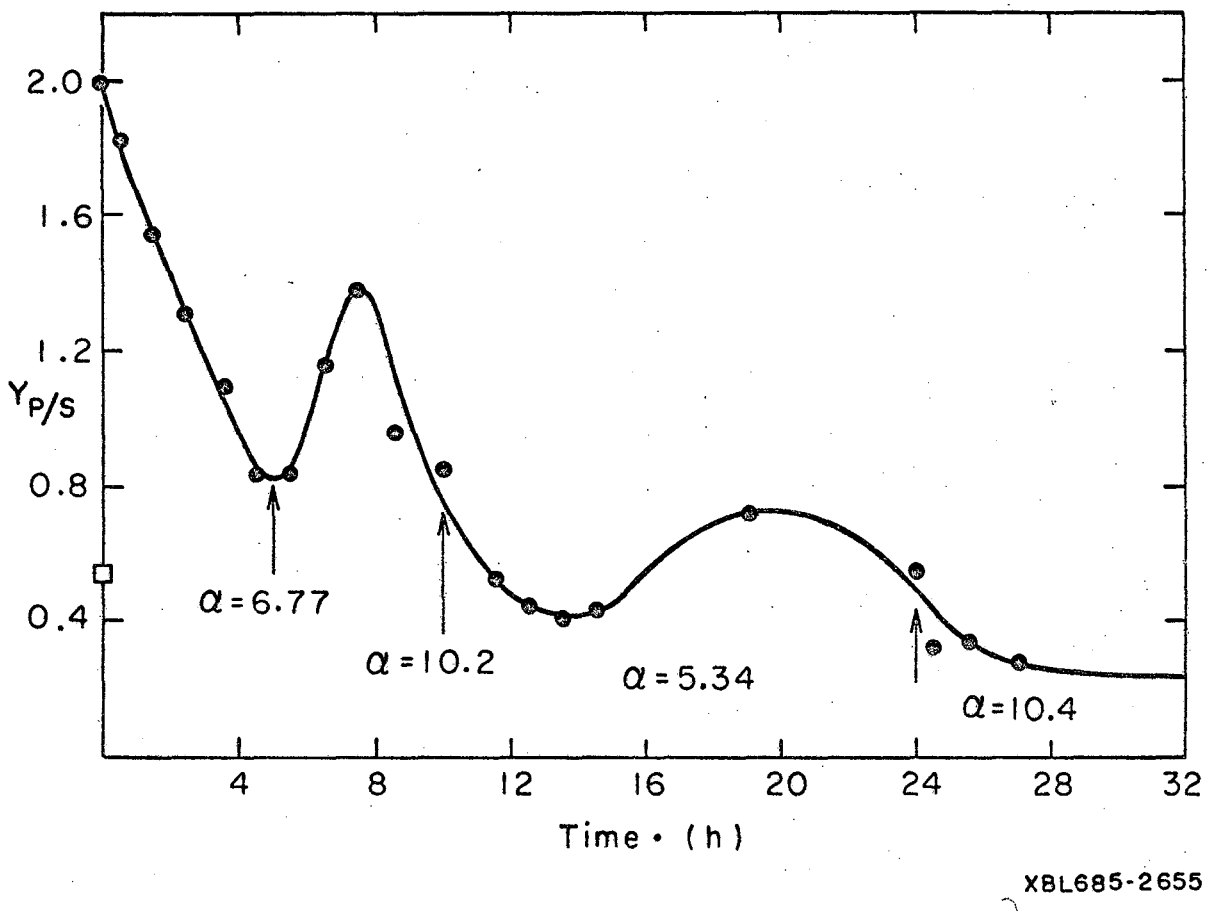

Fig. 45. The lactate yield constant calculated from Eq. 31 for the high density experimental Run AI.

E. Lactate Yield Constant as a Function of Specific Growth Rate

For all of the data for continuous fermentation, the decrease in lactate yield appeared to correspond to a decreasing specific growth rate as long as α was constant. The yield data for all the continuous runs were plotted as a function of specific growth rate to see if a unique relation existed.

Figure 46 contains the data for Runs CG, CJ and HDA. The values of $Y_{P/S}$ were calculated from the steady state concentrations. The specific growth rate, defined by Eq. (12) and (18), was equal to the cell dilution rate. The same general form is displayed for these runs; the yield constant is close to the stoichiometric value at high growth rates and becomes smaller as the growth rate decreases. At low growth rates, the yield constant decreases very rapidly. The data for Run CJ is quite consistent and forms a smooth curve, linear at high growth rates with a slow change of yield with μ and then decreasing abruptly. More scatter is present for Run CG. Although both have the same form, the two curves do not coincide, particularly at the high yield range. At low growth, they seem to approach a common asymptote. The high density run, HDA, had a much lower yield of lactate than the other two runs when compared at similar growth rates. The range of growth rates investigated was too small to see a distinct trend.

Also included in Fig. 46 are a few data points taken from the continuous fermentation studies of Rosenberger and Elsden[3] on S. faecalus. The range of dilution rates covered in their work was small but the same trend of decreasing lactate yield constant with decreasing dilution rate is evident.

The specific growth rates for the transient experiments were calculated from Eq. (23) and the yield and growth rate data are presented in Figs. 47, 48 and 49. Two characteristics are immediately apparent: first, the general shape of the curves are similar to those shown in the previous figure for the steady state experiments, and during the period of any run where α is unchanged, the data falls on a smooth curve which becomes linear at low growth rates. Second, all of the data, when extrapolated to the ordinate, intersect at a common value of specific growth rate.

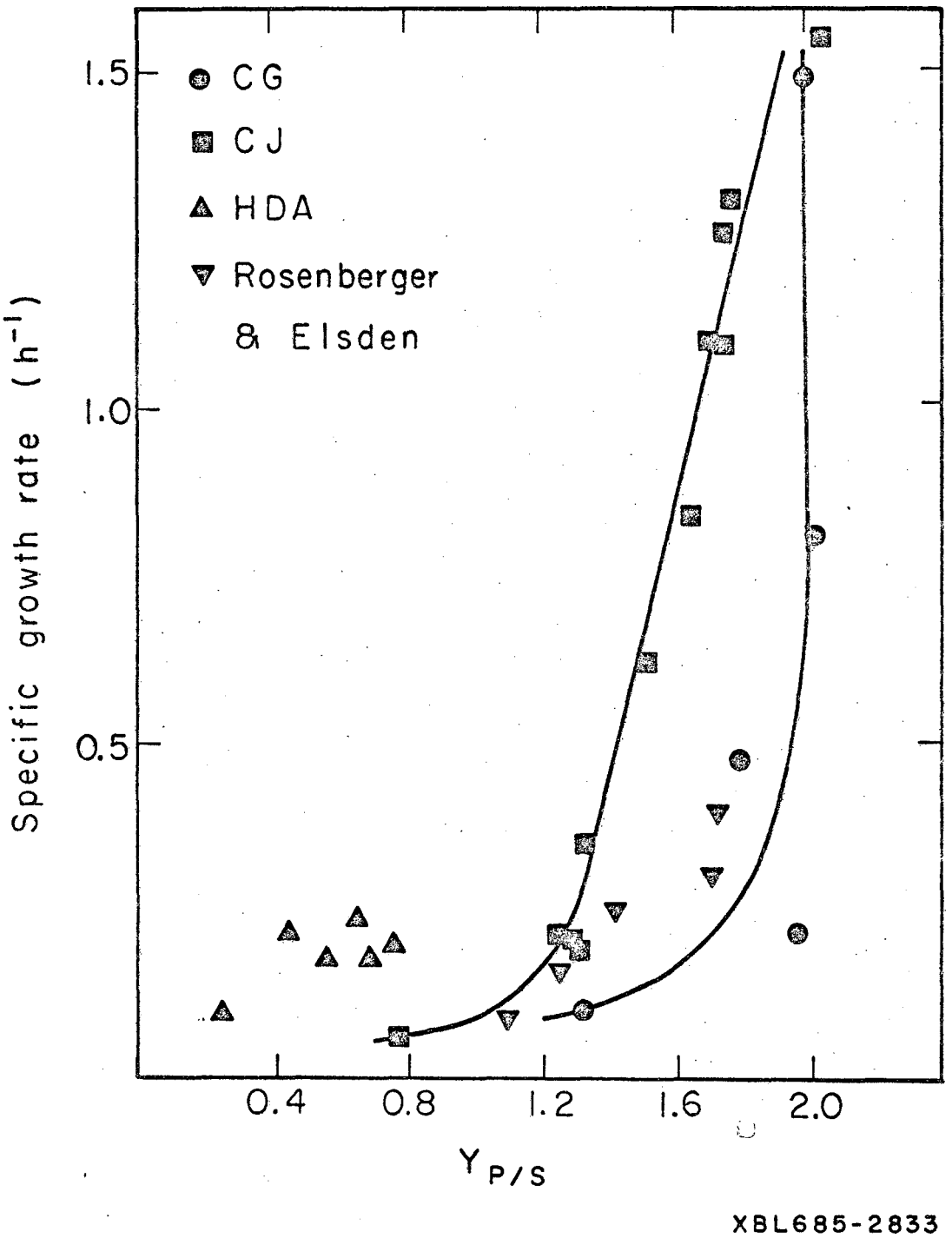

Fig. 46. The lactate yield constant plotted as a function of the specific growth rate for continuous stirred tank experimental Runs CG and CJ, the steady state high density Run HDA and the continuous stirred tank data of Rosenberger and Elsden[3] for S. faecalus.

Figure 47 contains the data for Runs TB, TE and TF. During the course of Run TB, no alteration in α occurred and a single curve resulted. Run TF contained a well defined change in α and two distinct yield curves resulted with the curve at higher α having a lower slope. Not enough data were collected during Run TE before the α change occurred to show whether two distinct curves would have resulted.

Figure 48 contains the results for Run TC and TD. Again, when α increases during Run TC, a new curve is formed with a much lower slope. Two data points for Run TC which lie between the curves were taken during the transition period and show the course of the transition.

The results for Run TI with its complex growth spectrum are plotted in Fig 49. The data for the different α regimes have been fitted with individual curves. The same type of behavior as encountered with the previous runs occurs. For the last part of the experiment where $\alpha = 10.4$, the data lie below the intercept value for μ. It is possible that the extrapolations which have been made and show that $Y_{P/S} = 0$ when $\mu = 0.07\ hr^{-1}$, is not correct. Whether $Y_{P/S}$ goes to zero is not known but evidence to show that it does not is given by the lactate yield determined from the final broth of Run TJ. The specific growth rate was about $0.007\ hr^{-1}$ and the value of $Y_{P/S}$ was 0.25; it would appear that even at such low growth rates some lactate is produced.

F. Viscosity of Dense Cultures

To determine the effect of the cell volume on viscosity, samples from Run TJ were diluted with a buffer solution and analysed in a Couette Viscosimeter. Not only were the viscosities of culture samples measured but also the supernatent of a centrifuged sample, the nutrient feed and a sample of the cells which were washed twice with buffer and resuspended in buffer to the same OD as the original. The results of these measurements are presented in Fig. 50 where the viscosity is plotted as a function of shear rate. The curves are designated by

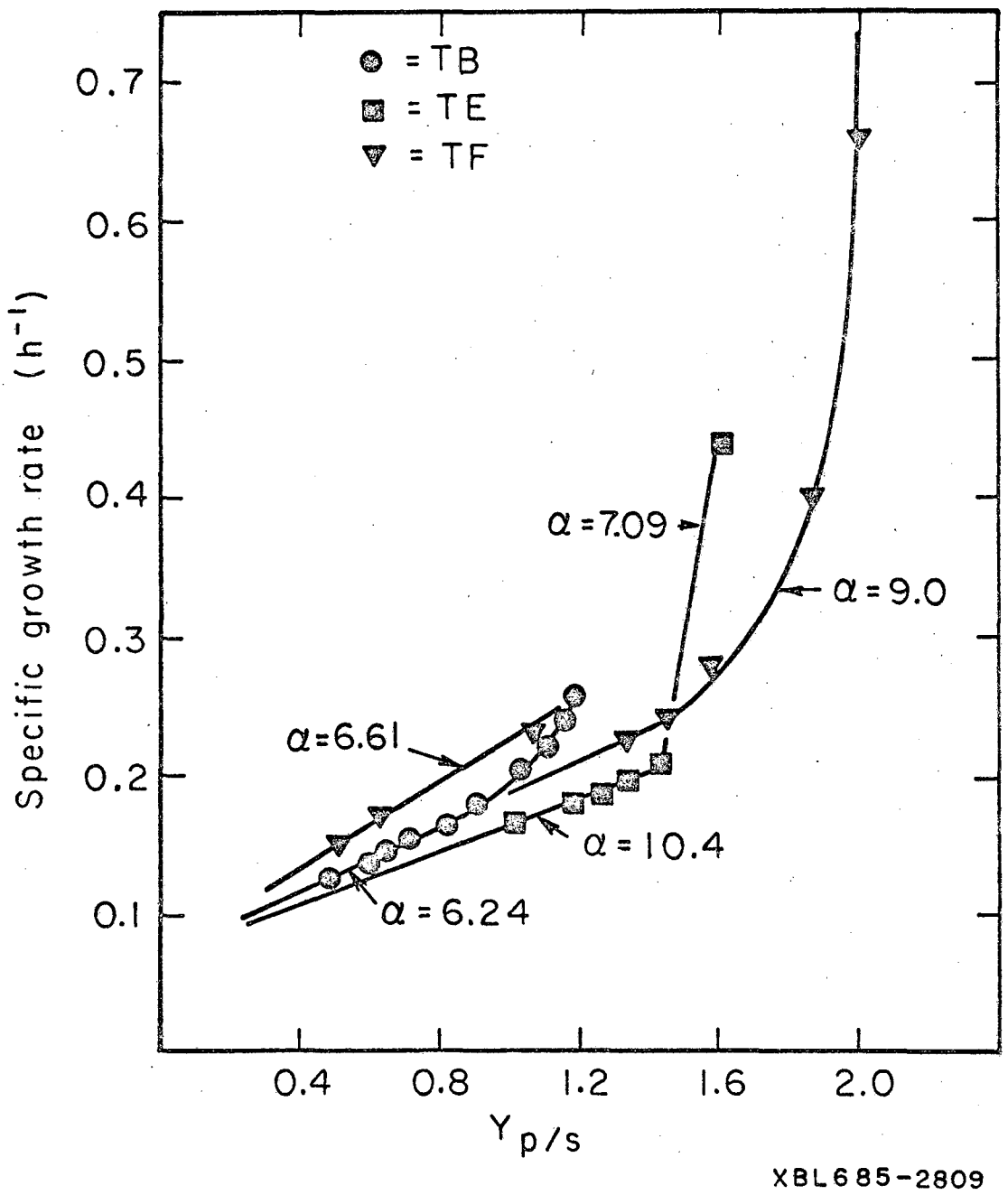

Fig. 47. The lactate yield constant plotted as a function of the specific growth rate for the transient high density Runs TB, TE and TF.

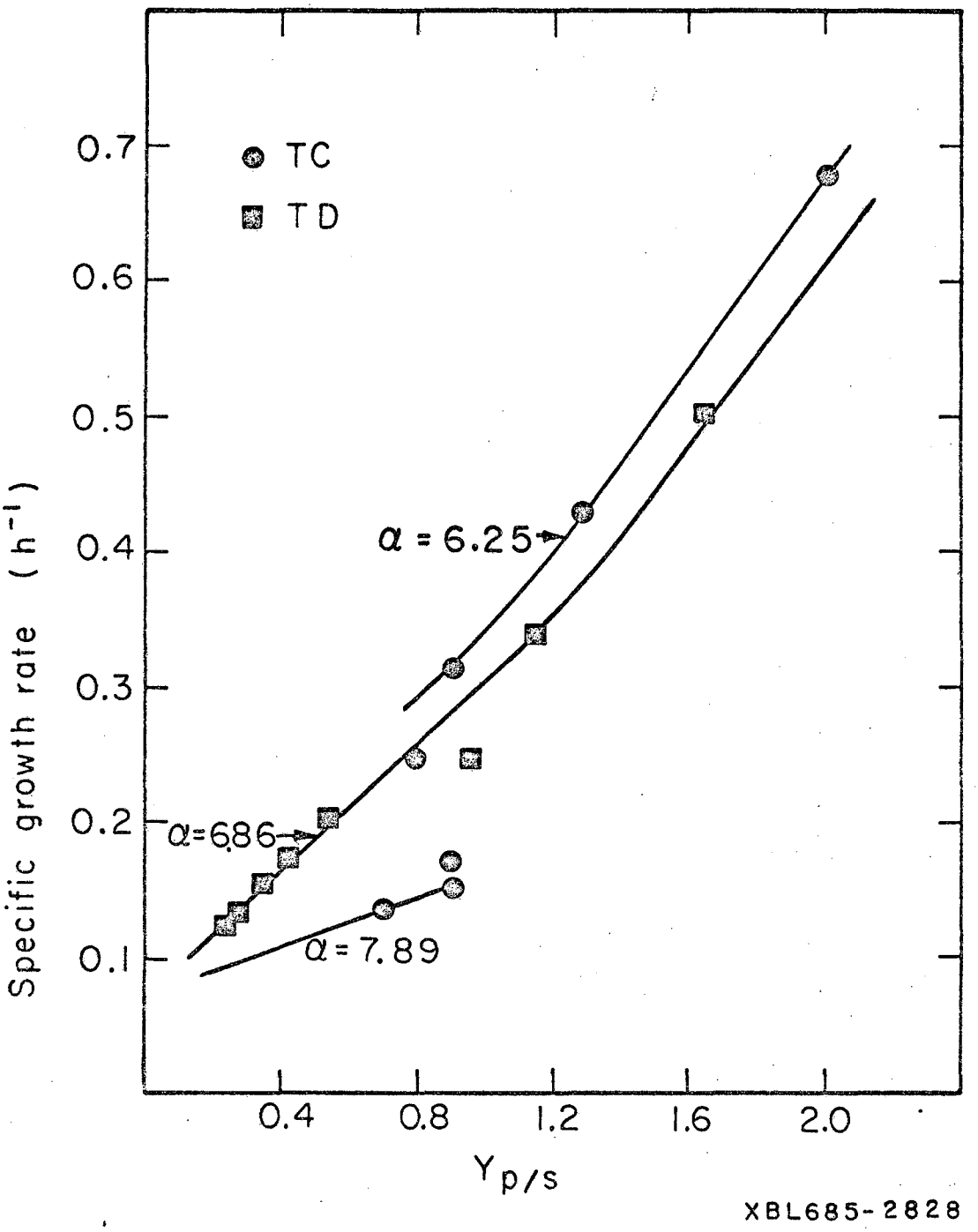

Fig. 48. The lactate yield constant plotted as a function of the specific growth rate for the transient high density Runs TC and TD.

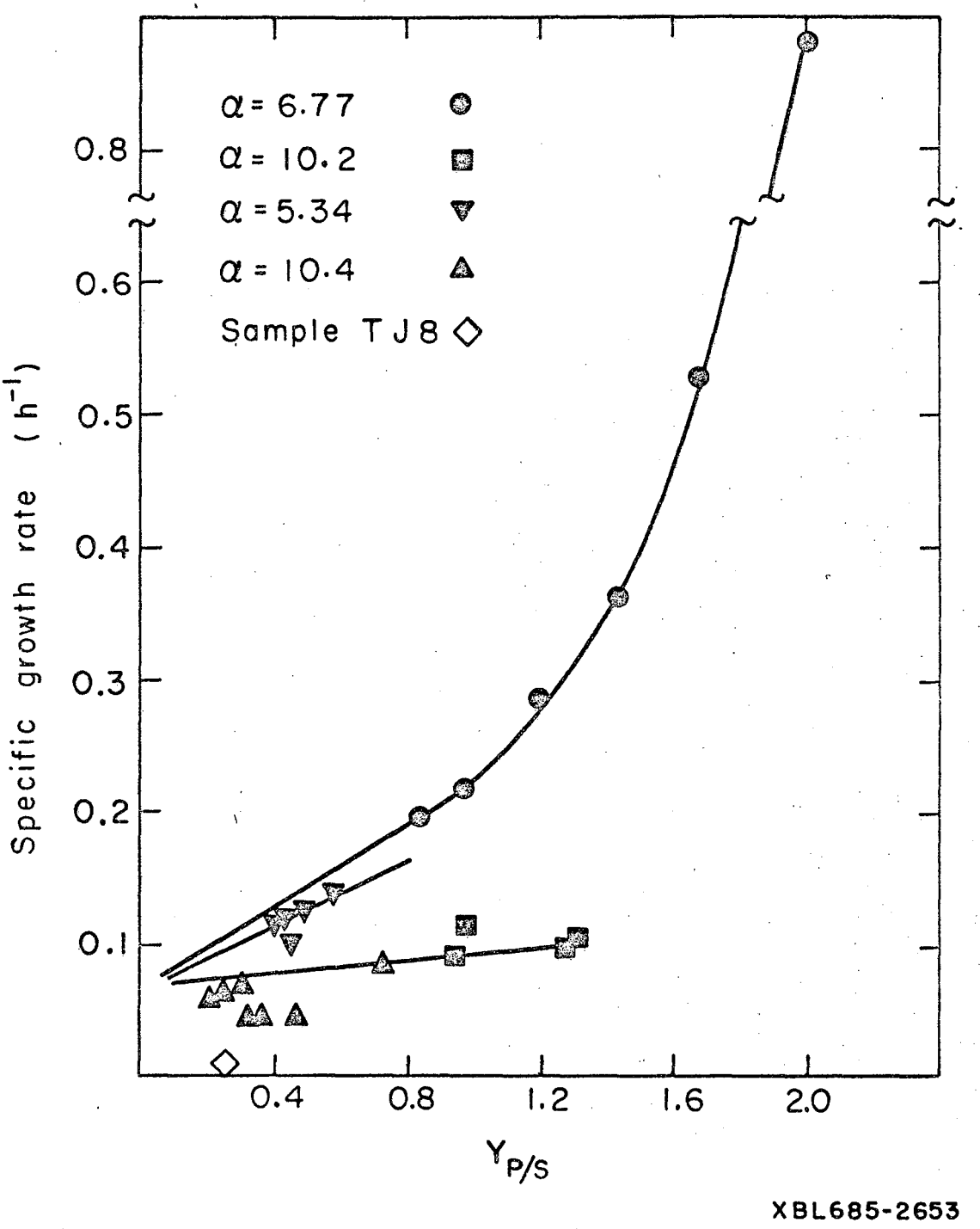

Fig. 49. The lactate yield constant plotted as a function of the specific growth rate for the transient high density Run TI and sample 8 of Run TJ.

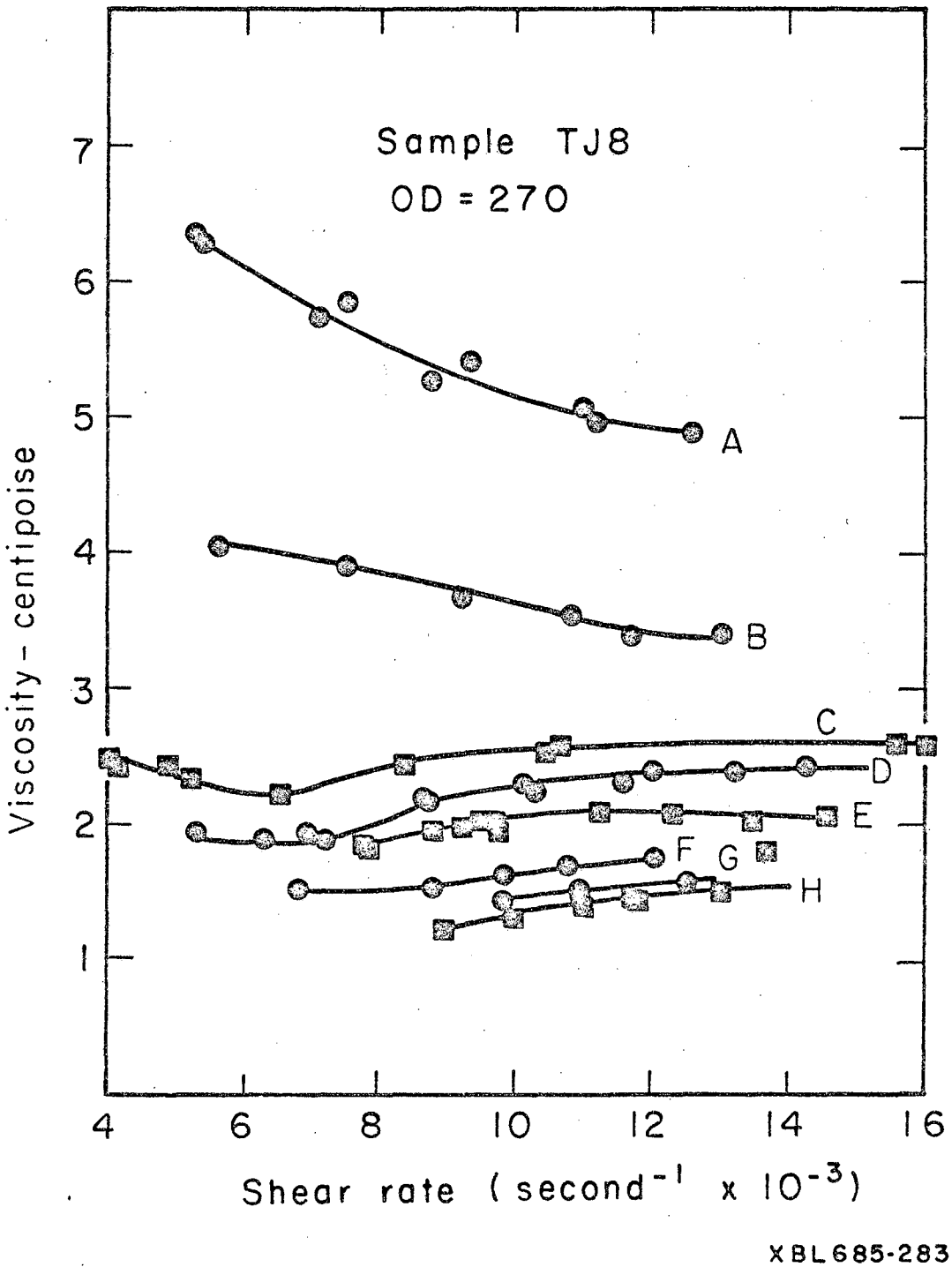

Fig. 50. Viscosity as a function of shear rate for sample 8 of the transient high density Run TJ. Curve A - no dilution. Curve B - sample washed twice and re-suspended in buffer. Curve C - 2:1 dilution after irreversible changes had occurred due to excessive shear rate. Curve D - 2:1 dilution. Curve E - supernatent of a centrifuged sample. Curve F - 5:1 dilution. Curve G - 10:1 dilution. Curve H - nutrient medium.

letters in order of decreasing viscosity. Curve A depicts the viscosity of the original sample and exhibits pseudo-plastic or shear thinning behavior. As the shear rate increases, the viscosity becomes less. Curves D, F, and G show the data for samples of broth which have been diluted 2:1, 5:1 and 10:1 respectively with buffer. The amount of viscosity decrease with dilution is not constant and the initial 2:1 dilution resulted in the largest reduction, from 5-6 cp. to 2-2.4 cp. The next dilution, 5:1, caused a further reduction of only 0.6 cp. while the 10:1 dilution reduced the viscosity additionally by only 0.2 cp.

Not only does dilution cause a drastic viscosity decrease but the functional relation with shear rate is reversed and the samples show a slight shear thickening, just the reverse of the undiluted sample. The same shear thickening behavior is also present in the nutrient feed shown by curve H.

During the measurements taken on the 2:1 dilution sample, the rate of shear was increased so far that irreversible changes occurred to the sample and the viscosity increased. The data for the 2:1 sample is given by curve D while the data for the same sample after the changes occurred is given by Curve C. The profile of curves C and D are similar but the presence of the irreversible changes due to shear are clearly evident. Measurements on a fresh 2:1 diluted sample were made and curve D was reproduced.

Viscosity measurements were made upon the supernatent of a centrifuged broth sample and they are shown by curve E. Some shear thickening is present but not to any large extent. The absolute value of the viscosity is approximately 40% greater than the nutrient feed and is assumed due to the remnants of dead cells which were not removed during centrifugation. The supernatent had a translucent appearance, not clear like the feed, and microscopic examination showed the presence of cellular debris as has been mentioned in a previous section. To eliminate the influence of this debris upon the viscosity, a sample of the culture was centrifuged, washed twice with buffer and resuspended in buffer to the

same OD as the original. The data are shown in curve B. The effect of washing and resuspension is clearly evident for the viscosity has been decreased by approximately 1.5 cp. or 30-35%. The same profile is retained although the amount of shear thinning has been reduced.

The presence of the cells appear to be responsible for the shear thinning although there is an effect of the debris upon the degree of shear thinning. The reason for reversal of the shear rate functionality with dilution is not readily apparent. The nutrient does have some shear thickening characteristics but it seems improbable that the predominance of the thickening action following dilution with buffer is due to the nutrient. The presence of cell debris may have an effect since there appears to be some interaction with intact cells. The difference between the data for washed and unwashed cell samples, Curves B and A, cannot be caused solely by the viscosity differences of the suspending fluid.

Although the presence of the cells at 40% packed cell volume does increase the viscosity of the broth by a factor of 5 or 6, the effect upon power input to the rotating filter was small.

G. Other Measurements of Bacterial Concentrations

1. Dry Weight Measurements

Optical density measurements were employed for determining cell concentration. The technique was rapid and the samples were adjusted by dilution to the range where optical density was shown to be linear with cell concentration. The decrease in the incident light intensity as it passes through the culture sample is caused by dispersion of the light beam by the individual microbial cells. The shape and size of the suspended particles does influence the OD. To check the OD-dry weight relationship, broth samples from most of the steady state runs were taken for dry weight measurements. The procedure for the determination has been described in Section II.F. The results of these measurements are summarized in Table IV where the dry weight/OD ratio and the specific growth rate for each sample is recorded.

Table IV. Dry weight measurements.

Run	Sample Number	Dry Weight (mg/ml)/OD	Specific Growth Rate, hr^{-1}
CG	5	0.348	0.222
	7	0.373	0.106
	8	0.383	0.469
	9	0.330	1.49
CJ	3	0.346	0.196
	4	0.348	0.351
	5	0.345	1.26
	6	0.344	0.209
	7	0.346	1.10
	8	0.342	1.31
	9	0.318	1.55
	10	0.337	0.222
	11	0.401	0.061
	12	0.321	0.621
	13	0.326	0.837
	14	0.395	1.09
HDA	1a	0.320	0.195
	2	0.333	0.179
	3	0.345	0.174
	4	0.318	0.234
	5	0.375	0.095
	6	0.353	0.216
	Average	0.347	
	Standard deviation	0.025	

The data were scattered about the average value of 0.347 mg/ml/OD but the standard deviation was fairly small, 0.025 mg/ml/OD. No consistent trend with specific growth rate was evident although the dry weight/OD ratio appeared to increase with decreasing growth rate. For example, samples CG7, CJ11 and HDA5 had small μ values and large dry weight/OD ratios, 0.37-0.40, while samples CG9 and CJ9 were rapidly growing and had dry weight/OD values around 0.32. Scatter in the data was too large to definitely demonstrate a trend.

2. Viable and Total Counts

Viable counts were determined for batch Run S and are shown in Fig. 7. The reasons for the variation in viable count per unit of optical density has been discussed in the section dealing with the batch growth experiments. The viable count/OD ratio was computed for each sample and they are summarized in Table V. The change in the average size of the discrete cellular particle is reflected in the change in viable count/OD. The results appear in agreement with the size distribution data (Figs. 22, 23 and 24) which showed that the cell size went through a minimum, as the fermentation progressed.

It is of interest to know what fraction of the cells present are viable in dense cultures. Gallup and Gerhardt[16] have measured the total and viable count for their dialysis system with results indicating that most of the cells were viable. In order to see if nonviable cells represented a large fraction in the present system, samples were taken from Run HDA for viable and total count and a few from Runs TI and TJ for viable count. The percent viability, the viable count/OD ratios and total count/OD ratios were computed and they are summarized in Table V with the results from Run S. The fraction of viable cells for Run HDA was between 80 and 90% with the exception of sample HDA5. The total count appeared to be too large by a factor of two for both samples HDA5 and HDA6 for the computed total count/OD values were about twice those for the other samples. Probably an error in dilution was responsible.

The viable count per unit of optical density was larger for the high density runs than for the batch run. This was due to the increased

Table V. Viable and total counts.

Run	Sample Number	Viable Count/OD X 10^{-8}	% Viable	Total Count/OD X 10^{-8}	Specific Growth Rate hr^{-1}
S	1	2.30			1.79
	2	2.46			1.79
	3	3.17			1.73
	4	3.29			1.34
	5	2.42			.95
	6	2.22			.61
	7	1.62			.34
	8	1.65			.28
	9	1.93			.25
	10	1.70			.22
HDA	1	-	-	7.0	.195
	2	4.17	77	5.4	.179
	3	8.22	90	9.1	.174
	4	5.35	87	6.1	.234
	5	7.18	57	12.5	.094
	6	-	-	12.7	.216
TI	19	6.65			.069
TJ	6	7.75			.008
	7	8.07			.008
	8	7.77			.007

number of singlet cells present in the high density culture. This is illustrated by the photomicrographs shown in Fig. 51. The upper picture shows a sample taken from a continuous fermentation run and the lower is a photograph of a 50:1 dilution of sample TJ8. There was a striking increase in the number of single cells in the high density experiment.

The size distribution of cell samples taken from continuous nonfiltration runs showed a much broader profile than did those taken from the batch experiments. The distribution was similar to that for sample S1 shown in Fig. 22. Photomicrographs of log phase batch cultures displayed cell aggregates midway between the two cases shown in Fig. 51. The singlet and dumbbell forms were quite numerous in the batch experiment but there were longer chains present also. Chains were almost completely absent in the high density sample TJ8.

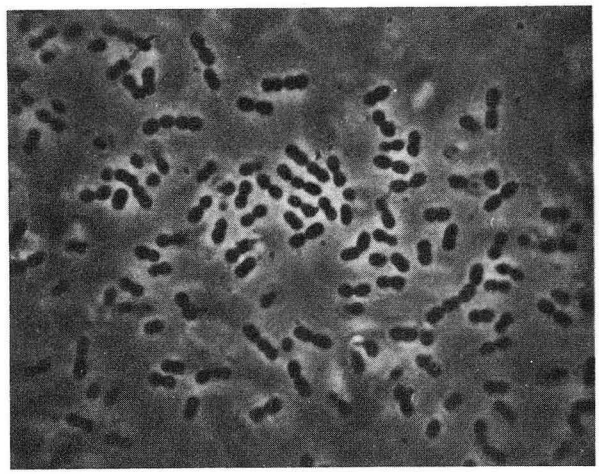

Fig. 51a. A sample of S. faecalus from continuous stirred tank experiment: phase contrast X 1600.

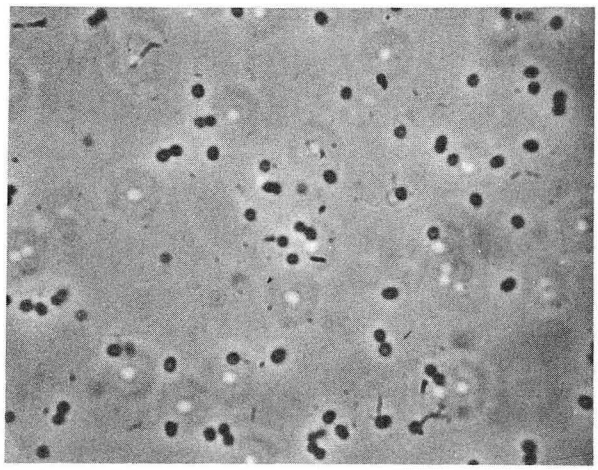

XBB 685-2582

Fig. 51b. S. faecalus from sample 8 of transient high density Run TJ: phase contrast X 1600.

IV. GENERAL DISCUSSION

One of the primary objectives of this research program was to develop an experimental apparatus for the production of a cellular concentration much higher than can be obtained in simple batch growth. The fermentation system for this purpose using the micro-filtration technique has been described thus far with primary emphasis on the bacterial kinetics. Little information pertaining to the operating characteristics of the filter have been presented as yet. In the following section, the fermentation system and its operating characteristics are discussed in some detail.

The data from the experimental program have been presented in the previous section. Each mode of operating the fermenter resulted in different information. A section of this General Discussion is devoted to summarizing these findings and to interpretation of the results.

A. The Experimental Apparatus

The fermenter system for this study was developed primarily for the continuous growth of micro-organisms to concentrations many times larger than those which could be obtained by the usual techniques of stirred tank or batch fermentations. The fermenter accomplished this objective successfully with a maximum concentration factor of 45 over batch culture. The investigation of dense cultures at specific growth rates larger than those obtained was prevented by the upper limit on the filtration rate which could be achieved and maintained for long periods of time without development of excessive pressures. The equipment was designed to withstand 30 to 40 psi but the maximum pressure used did not exceed 20 to 25 psi and was usually much less.

1. The Filter Membranes

Millipore membranes are fairly fragile and care had to be employed in handling them. Several types of membrane materials are produced by Millipore; of these, the teflon and nylon materials appear to have much better physical and chemical properties than the Microweb type employed

here. Unfortunately, the pore diameters available in the former types are not small enough to remove the cells from the filtrate. One type of membrane material which had excellent chemical resistance and could have been steam sterilized in place was much too fragile and was almost impossible to handle.

The Microweb membranes had quite good handling characteristics although some lots were better than others. With care and experience, filter membranes could be attached to the support screen, sealed tight and sterilized in a reproducible fashion. The technique employed was quite important to success. The glue had to be flexible so that the membrane would not crack along the joint. The ends sealed by the "O" rings had to have a layer of glue to give mechanical strength to prevent development of cracks in the membrane.

The membrane had to be assembled dry for the glue to stick and since it expands when wet, the filter did not adhere very tightly to its support screen. When the filter was rotated with little or no pressure drop, flapping occurred like a flag in the wind. At high initial rotational speeds with a new membrane, such flapping caused membrane failure. To minimize this problem, the membrane was supported by 5 or 6 elastic bands distributed along its length and the initial rotational speed was kept as low as possible, about 600 rpm. The torque characteristics of the filter motor were poor at low speeds and 600 rpm was the smallest which could be maintained.

After a pressure drop had developed across the membrane, flapping became no problem and the speed could be increased. As previously mentioned, the effect of rotational speed on filtering characteristics was small and the lowest possible speed was used. The rotor had been operated briefly at 1800 rpm without membrane failure.

2. Filtration Characteristics

A thorough study of the filtration as a function of time, rotational speed and cell concentration was not made but data taken during the runs revealed the general characteristics. The results of Bhagat and Wilke[22] showed that, for small polystyrene spheres, the steady state

rate of filtration was almost independent of pressure drop and was proportional to the square of the rotational speed. The experimental configuration, the particles and the mode of operation used by Bhagat were quite different from those encountered here. Bhagat employed a constant pressure drop through the membrane and filtration rate was the dependent variable. A cake of particles was very rapidly built up until an equilibrium condition resulted where the rate of attrition of particles equalled their rate of transport to the membrane by flow of filtrate. In the present work, flow rate was fixed and pressure drop was the dependent variable. Cake was formed very slowly and the pressure increased gradually and a steady state pressure appeared to be reached so long as the cell density did not change. This was observed during the HDA run where operation continued for many hours at constant cell concentrations with no pressure increase with time. The maximum filtration rate employed was approximately 3 ml/hr/cm^2 at a cell concentration of 43 OD and a pressure of 7 psi. At a filtration rate of about 1.8 ml/hr/cm^2 and an OD of 42, the pressure was approximately 4 psi. From these two examples, it would appear that the steady state filtration rate is a function of pressure drop for the present system rather than independent of it as observed in Bhagat's system.

A further deviation from the results of Bhagat was found in the filtration rate increase with rotational speed. He found that the filtration rate varied with the square of the rotational speed. However, in the bacterial filtration increases in flow rate due to an increase in rotor speed were fairly small.

A possibly important difference between the present system and that used by Bhagat is that the organism layer formed during the filtration was slimy and not particulate like the layers formed by the plastic particles.

The bacterial filtration rate was somewhat time dependent as small particles penetrated the pores and gradually blinded the membrane. This effect was not very noticeable over time periods of several days. The effect of cell concentration had a larger effect on the pressure

required to affect a fixed filtration rate. To illustrate the behavior observed, the pressure and OD for Run TI will be described. The rotational speed of the filter was 650 rpm and the filtration rate was 980 ml/hr. The initial pressure was very small and gradually increased to 3 psi and the cell concentration grew to 128 OD at sample TI-15. During the five hour time period between TI-15 and TI-16, the OD did not change while the pressure increased by 6 or 7 psi. The rpm was increased to 1100 and the pressure decreased by 1 or 2 psi. From this time to the end of the run, the OD increased to 146 and the pressure increased by only 1 or 2 psi. Following the termination of the runs with this filter membrane, the system was thoroughly cleaned with detergent to remove cells from the surface of the membrane but the filtration rates with pure water could not be returned to the "new membrane" state. Examination of the membrane showed that no visible layer remained but the discolored appearance suggested that the pores were partially plugged.

The influence, then, of OD on filtration rate was small until cell concentrations of 125 OD were reached. The pressure increase noticed at this time could have been caused directly by the cell concentration but the progressive partial plugging of the pores could also have been responsible.

3. The Control Systems

The control systems worked very well once they had been debugged. Control of pH was better than ±0.05 pH units and the electrode drift was negligible. Grab samples were periodically taken to insure against deviations from the pH meter reading but corrections to the ascentric potential on the analyser were seldom necessary.

Reactor temperature control using the heating tapes wrapped around the outside of the fermenter gave excellent temperature control as measured by the thermocouple. To keep the broth at a uniform temperature, stirring was required to increase the heat transfer from the

glass walls and to keep the thermowell in contact with the fluid during batch growth where the fermenter volume was not completely filled with broth.

The control of nutrient feed rates in some runs was not as accurate as desired because the speed control mechanism on the pump was wearing out. Once it had been replaced, long term stability within a few percent was achieved. Peristaltic pumps are not the best type for long term operation or for accurate setting of predetermined flow rates. The nutrient pumping system, as originally designed, had a positive displacement piston pump with a manual motor speed control similar to that employed for the NaOH supply. The speed was measured using a tachometer-generator and millivolt recorder in a manner identical to the NaOH system. Flow rates could be very accurately set and fine adjustments made. Unfortunately, this pump could not be successfully sterilized and had to be replaced by the peristaltic pump.

The control of the bleed flow rate was a problem solved with difficulty. Originally, a combination pressure-regular and fine metering valve built by the Milliflow Corp. was employed but with no success. Flow rates could not be controlled at all. During the development stages of the pH control system, a peristaltic pump had to be designed to recirculate broth through the external pH electrode holder. This pump worked so well that a second one was built and employed to meter broth from the system. The volume pumped was quite independent of the system pressure because of the heavy walled rubber tubing used in the device. The pumping rate could be varied over a very wide range by using a DC motor with a variable voltage power supply and a combination of gear reduction boxes. This pump, together with a buret to collect the cell effluent, provided accurate metering of the flow of bleed from the system. As mentioned in a previous section, continuous attention had to be paid to the effluent volume collected versus time because some gas was evolved from time to time and because the setting of the motor speed to the correct value was difficult at the low pumping rates used. Small adjustments had to be made periodically to ensure that the pumped volume

accurately adhered to the predetermined rate. At no time did the amount of effluent deviate more than a milliliter from the desired volume versus time profile.

4. Batch and Continuous Stirred Tank Operation

The fermentation system, though specifically designed for high density operation, was equally suited for batch and continuous stirred tank cultures. The external recycle line was convenient for sample removal and addition of small quantities of liquid, like the seed culture. The diameter to height ratio was much smaller than usually used for regular fermentation but the use of a stirring shaft with several impellers spaced along its length gave excellent mixing. Residence time distribution measurements showed that complete mixing was closely adhered to. In fact, the fermenter volume calculated using residence time distribution data agreed with the direct measurement to within less than 1%.

5. Uses of Filtration-Fermenter Combinations

This type of apparatus has been shown by the experimental program described here to be uniquely suited to the investigation of microbial growth characteristics. The advantage of the high density device over continuous stirred tank fermentation as a research tool is due mainly to the differing modes of operation. Continuous culture yields steady state data and the amount of information derived per unit time is small, for 4 to 6 residence times are required to change steady states. With filtration, the fermenter can be operated so that cell concentration is in a transient state while the limiting substrate concentration is essentially zero. Changes in the cell yield are readily apparent, particularly in instances where diversion of substrate to cell maintenance is negligible. With a maintenance energy requirement, this mode of operation is still applicable although the graphical presentation is not as descriptive and changes in cell yield and maintenance energy constants are not as evident.

The Luedeking maintenance energy model given by Eq. (5) can be used in the substrate material balance, Eq. (19), to express the rate of glucose consumption.

$$-\frac{dS}{dt} = \frac{v_f}{V} S_0 - \alpha \mu N - \beta N - \frac{v_F}{V} S - \frac{v_B}{V} S . \qquad (32)$$

With S and dS/dt equal to zero, Eq. (32) can be solved for μ .

$$\mu = \frac{v_f S_0}{\alpha V N} - \beta/\alpha . \qquad (33)$$

Equation (33) can be combined with the cell material balance expressed by Eq. (17).

$$\frac{dN}{dt} = -\left(\frac{v_B}{V} + \frac{\beta}{\alpha}\right) N + \frac{v_f S_0}{\alpha V} - \frac{v_F}{V} N_F . \qquad (34)$$

Assuming that the flow conditions remain constant, Eq. (34) can be solved to give the cell concentration as a function of time.

$$N = C - (C - N_0) \exp\left[-\left(\frac{v_B}{V} + \frac{\beta}{\alpha}\right) t\right]$$

$$C \equiv \left(\frac{v_f S_0}{\alpha V} - \frac{v_F}{V} N_F\right) \Big/ \left(\frac{v_B}{V} + \frac{\beta}{\alpha}\right) . \qquad (35)$$

As time becomes large, the cell concentration approaches the value C, the steady state cell concentration. Because the ratio of β/α enters into the exponential, a plot of $\exp(-\frac{v_B}{V} t)$ versus N would not be linear but would bend towards the N axis and asymptotically approach the steady state cell concentration. Once the steady state value is known, a suitable rearrangement of the mathematics results in a linear curve when ℓn (N steady state - N) is plotted as a function of time.

$$\ell n(N_{\text{steady state}} - N) = \ell n(N_{\text{steady state}} - N_0) - \left(\frac{v_B}{V} + \frac{\beta}{\alpha}\right) t \qquad (36)$$

where: N steady state = C. The slope of this curve is $-\left(\frac{v_B}{V} + \frac{\beta}{\alpha}\right)$. From the experimentally determined steady state cell concentration and this slope, the values of α and β can be readily computed.

Applications for the filtration-fermenter in the fermentation industry are probably very limited. Almost all of the major industrial fermentations are conducted batchwise with only limited use of continuous culture. Use of high density culture with its much more complex operating requirements, would necessitate the presence of special conditions. For example, the removal of a cell-free effluent could be advantageous in those instances where the cell material interferes with product recovery.

The productivity of a continuous fermenter normally increases with dilution rate until the cell and product concentration begin to decrease due to washout. For a continuous stirred tank fermenter (CST), the rate of cell formation per unit fermenter volume (Productivity, CST) can be expressed by the following relationship.

$$\text{Productivity, CST} = \frac{v}{V} N \tag{37}$$

where: v = effluent flow rate
N = cell concentration
V = fermenter volume.

Since

$$\frac{v}{V} = \mu$$

from Eq. (12), then:

$$\text{Productivity, CST} = \mu N . \tag{38}$$

For the high density system (HD),

$$\text{Productivity, HD} = \frac{v_B}{V} N \tag{39}$$

where:

v_B = bleed flow rate.

From Eq. (18),

$$\frac{v_B}{V} = \mu$$

assuming that no cells are lost in the filtrate. At the same specific growth rate, the ratio of the productivity for the high density with filtration to the productivity of the continuous stirred tank with no filtration is:

$$\text{Productivity Ratio (PR)} = \frac{N_{HD}}{N_{CST}} . \tag{40}$$

The cell concentration for the CST is given by Eqs. (9) and (13) and is equal to the following expression assuming no substrate is present in the effluent.

$$N_{CST} = \frac{v_f}{V} \frac{S_0}{\alpha\mu} \tag{41}$$

where v_f = the feed flow rate. From the material balance on the flow rates,

$$v_f + v_{NaOH} = v .$$

The amount of base added to the system is proportional to the feed rate.

$$v_{NaOH} = k\, v_f . \tag{42}$$

Therefore,

$$v_f = \frac{v}{1 + k} . \tag{43}$$

And,

$$N_{CST} = \frac{v}{V} \frac{S_0}{\alpha\mu} \frac{1}{1 + k} = \frac{S_0}{\alpha(1+k)} \tag{44}$$

The cell concentration for the high density case is given by Eq. (21) assuming that no cells are lost in the filtrate.

$$N_{HD} = \frac{v_f S_0}{\alpha v_B} . \tag{21}$$

In this case, the material balance on the flow rates gives,

$$v_f + v_{NaOH} = v_B + v_F . \tag{45}$$

Using Eqs. (42) and (45), the following expression for the cell concentration in the high density case results:

$$N_{HD} = \frac{v_B + v_F}{v_B} \quad \frac{S_0}{\alpha(1+k)} . \tag{46}$$

Assuming that the cell concentration does not influence α, the substitution of Eq. (44) and (46) into (40) for the productivity ratio gives:

$$PR = 1 + \frac{v_F}{v_B} . \tag{47}$$

Since

$$\frac{v_B}{V} = \mu ,$$

then

$$PR = 1 + \frac{v_F}{V} \frac{1}{\mu} . \tag{48}$$

The productivity ratio depends strongly on the filtrate rate per unit fermenter volume and on the specific growth rate at which the system is operated. If the present high density system is operated at low bleed rates such as in Run TI, the productivity ratio at steady state will be approximately 34.

For a continuous stirred tank fermenter, the maximum productivity occurs near washout where the increase due to increasing flow rates is counteracted by decreasing cell concentrations. For S. faecalus the optimum specific growth rate for maximum productivity in a continuous stirred tank was found to be near 1.25 hr^{-1}. Therefore, the productivity ratio for S. faecalus grown in the experimental apparatus at the optimum specific growth rate and at the maximum obtainable filtration rate of 1 liter per hour, was computed to be 2.3.

S. faecalus grows much faster than most organisms and the improvement in productivity is not large. Very much larger increases are possible with slow growing organisms for which this type of apparatus may be particularly useful.

The productivity of a filtration-fermenter is proportional to the limiting rate of filtration which can be achieved. With the Millipore membranes, flow rates are small so that a large filter area is required per unit fermenter volume. The required mechanical design is complicated and the equipment is expensive. Also the power consumption could be considerable depending upon the fluid viscosity and the size and rotational speed of the filters.

The handling characteristics of the Millipore membrane are poor for this purpose; they are fragile and some types cannot be steam sterilized. The membrane material is costly, $4.50 per square foot for the least expensive. Amicon Corp. produces another type of membrane for micro-filtration which is claimed to be superior to Millipore in handling and long term filtration characteristics, with plugging not a problem if the system is well agitated. The filtration rates claimed by Amicon are much higher than those found for Millipore. The filtration conditions were quite different for the Amicon tests used water rather than fermentation broth. How much difference in filtration rates would occur when a thick bacterial suspension was used is not known but the rates could be considerably reduced. The Amicon membrane costs as presently quoted would seem prohibitive.

Further research seems necessary to determine the feasibility of applying high density filtration culture to industrial fermentations. Availability of low cost--high filtration rate membranes could make the increased productivity which is possible with this technique economically attractive, particularly for systems employing very slow growing organisms.

An important factor is the power requirement for this type of device. In the present system power requirements estimated from existing correlations were on the order of 500 horsepower per thousand gallons, an excessive value for industrial practice. However, it seems likely that alternate designs might be possible for large scale systems which would reduce the volumetric power input. This remains an important variable for future investigation.

B. Experimental Results

1. Growth Characteristics

Streptococcus faecalus is an anaerobic, supposedly homo-fermentive, lactic acid bacterium with strict nutritional requirements. The complexity of these requirements was amply illustrated by the batch experiments. The semi-defined medium with its many components was still deficient in that the log period of growth was not adequately reproducible in either rate or duration. A trace constituent in casein, the amino acid source, appeared to be responsible for the nonreproducibility. The casein which was an enzyme hydrolysate, was not vitamin-free. Use of a vitamin-free casein product would have been prohibitive in cost and the nutritional studies required to determine the trace component in the casein which had such a vast influence on growth, would have required a considerable investment in time. The principle purpose of the batch experiments was to develop a nutrient medium which would support good growth in a reproducible fashion with a known component, glucose, as the growth limiting constituent. The complex medium containing yeast extract appeared to satisfy these requirements.

The batch growth characteristics of S. faecalus were very similar for the semi-defined and complex media. The main difference between the

two was the presence of a lag phase with the complex medium while none was observed with the semi-defined recipe. The seed culture used for the complex nutrient growth experiments contained yeast extract, buffer and glucose but not the vitamins. Subsequent experiments during continuous growth runs showed that these vitamins had a beneficial influence on growth and the lack of them in the seed culture medium was probably the cause of this lag phase. The effect of the added vitamins was rather surprising for one would assume that yeast extract at 20 g/l should supply ample quantities of growth factors.

The size distributions for samples taken during batch experiments shows the presence of two distinct particle sizes. This is a surprising phenomenon and is undoubtedly due to the propensity of the organism to form small cocci chains. For cultures in the stationary phase or growing at low rates, the distribution was broad with a maximum near the doublet size. As the culture begins to grow at the maximum rate, the chains begin to decrease in number and in length until the vast majority approach the singlet size. The doublet peak almost disappears and remains as a shoulder on the singlet peak. It must be emphasized that the terms "singlet" and "doublet" are used by analogy to the standard calibrating spheres where genuine singlets and doublets are present. The bacterial singlets and doublets do not refer to single cells and two-cell chains for the cells under the singlet peak are undoubtedly dumbbell in shape showing the beginning of duplication while the doublet peak represents two finished daughter cells which may also show the beginnings of duplication. In any event, during the initial stages of batch growth, the position of the doublet peak displays a cell volume approximately twice that of the singlet. As growth proceeds, the increasing volume of the singlet maximum demonstrates that the dumbbell shaped cells begin to predominate.

Two batch experiments were conducted to determine the absolute glucose requirement for growth; one with the semi-defined medium and one with yeast extract. Both experiments involved the incubation of nutrient media without glucose for a period of time followed by the addition of glucose. No growth occurred with the semi-defined medium until glucose was added. Following the addition of glucose, growth began and the normal

batch curve resulted although the specific rate was lower than normal. With yeast extract, some growth resulted without glucose. After a stationary phase was reached, glucose was added and growth was again observed but at a much lower rate than usually occurred with this medium. It is not known whether an important nutrient was consumed during the incubation without glucose and was not available when the glucose was added or whether the cells underwent some change during this period which affected their performance.

The continuous stirred tank experiments grown on the complex medium with 7 g/l glucose displays the usual dependence of cell concentration on dilution rate. The cell concentration was limited by the available glucose until the dilution rate approached washout where the concentration decreased rapidly. For dilution rates below 1.2 hr^{-1}, the measured glucose was zero by the Glucostat analysis which could detect less than 0.1 mg/ml glucose. During this period when all the glucose was being consumed, the cell concentration profile showed a slight increase of OD with decreasing dilution rate. This increase was too small to influence the graphical determination of α from Eq. (14). Some utilization of nutrient components other than glucose for energy may have occurred since the yeast extract medium would support some growth in the absence of glucose.

2. Cell Yield

The rate of consumption glucose to provide the energy for the increase in cellular mass was found to be directly proportional to the rate of cell growth as long as glucose was present in limiting amounts. Evidence to support this statement is contained in the steady state data for both normal and high density continuous experiments. There was no apparent effect of cell concentration on the specific rate of glucose consumption. During the batch experiments where an excess was present, glucose catabolism became uncoupled from cell growth and the energy derived therefrom was dissipated. The Luedeking et al.[36] maintenance model fitted the batch data but gave widely differing maintenance energy terms from one experiment to the next. For steady state continuous experiments, it failed completely.

It was stated in the section dealing with batch results, that the cell relationship between cell concentration and glucose consumption (or product formation under conditions of stoichiometric conversion) could be explained by either the maintenance energy concept or by energy dissipation. To illustrate the general form obtained, refer to Fig. 11 which contains the data for Run S. The curve is linear at low cell concentrations and begins to increase after an OD near 3.5 is reached. This linear region can be accounted for by the Luedeking model if, and only if, the specific growth rate is constant. During this period, the glucose consumed is linear with OD:

$$S_0 - S = K N . \tag{49}$$

Differentiating with respect to time,

$$- \frac{dS}{dt} = K \frac{dN}{dt} . \tag{50}$$

Luedeking's model is given by Eq. (5):

$$- \frac{dS}{dt} = \alpha \frac{dN}{dt} + \beta N . \tag{5}$$

Substituting Eq. (50) into (5),

$$K \frac{dN}{dt} = \alpha \frac{dN}{dt} + \beta N. \tag{51}$$

Now, from Eq. (1),

$$\frac{dN}{dt} = \mu N . \tag{1}$$

Therefore,

$$K \mu N = \alpha \mu N + \beta N \tag{52}$$

or,

$$K = \alpha + \beta/\mu \ . \qquad (53)$$

For this equation to hold, as long as K is a constant, the specific growth rate, μ, must also be unchanging. Therefore, for the Luedeking model to be valid, the dissociation of energy production must coincide with a change in growth rate. With the sole exception of Run AI, the ratio of OD at the end of the log phase to the OD where dissociation occurred was 0.7 or less.

The amount of glucose consumed which went to support new growth was subject to abrupt changes. These changes were not evident from the batch and steady state experiments for fluctuations in α from run to run were quite small. The only exception to this occurred during the last few data points for Run CJ. All of the α values determined from the experimental results reported here, are summarized in Table VI. These values have been grouped into four catagories; the first group includes all the values for the batch and steady state runs (except for $\alpha 2$ of Run CJ) together with those from the transient experiments which were in the same neighborhood. The average value is 6.77 mM glucose/l/OD with a standard deviation of 6.3%. The second group contains the larger values from the transient runs while group three contains only the smallest value, $\alpha 3$ for Run TI. Group four includes those values intermediate to groups one and two. The groupings were somewhat arbitrary, particularly group four which could possibly be distributed between one and two although there seems to be a gap separating group four from either one or two. The separation of group three from group one appeared to be justified due to the large gap between them. The average value for each group did bear a simple relationship from group to group. The ratios of groups 3:1:4:2 were approximately 4:5:6:8. The reason why α values fell into these groupings could not be determined from the experimental data.

Without the transient growth experiments, the conclusion must be that α is a constant, for the 6.3% standard deviation found for group one is quite reasonable considering the possible experimental

Table VI. Summary of values.

Run	mM Glucose/l/OD	
S	6.95	(1)
AB	7.45	(1)
AC	7.15	(1)
AE	6.35	(1)
AI	6.80	(1)
CG	7.46	(1)
CJ α 1	7.25	(1)
α 2	8.40	(4)
HDA	7.05	(1)
TB	6.24	(1)
TC α 1	6.25	(1)
α 2	7.89	(4)
TD	6.86	(1)
TE α 1	7.09	(1)
α 2	10.4	(2)
TF α 1	9.0	(4)
α 2	6.61	(1)
TI α 1	6.77	(1)
α 2	10.2	(2)
α 3	5.34	(3)
α 4	10.4	(2)
TJ α 1	7.3	(1)
α 2	15.	*

Group (1) - Average α = 6.77
Standard Deviation = 0.43
= 6.3%

Group (2) - Average α = 10.4

Group (3) α = 5.34

Group (4) - Average α = 8.42

errors. The α 2 value for Run CJ could be accepted as resulting from differences in medium following the preparation of more nutrient after sample CJ11, for the organisms have complex requirements and the medium was undefined due to the presence of yeast extract. However, it became clear during the transient experiments that α could and did quite abruptly change. These changes were not caused by fluctuations in operating variables or nutrient composition for flow rates and the other system variables were monitered continuously and the nutrient was withdrawn from a single, well agitated vessel. Furthermore, the lactate yield constant also indicated that a metabolic pathway alteration had been made.

The reason for the pathway shift was not apparent from the experimental data obtained. No effect of cell concentration was found, for in a duplicate set of experiments, Runs TE and TF, a change in α occurred but the values before and after were completely reversed. In another set of duplicate runs, a change occurred in one, Run TC, but not in the other, Run TD.

3. Product Yield

The pathway alteration signified by the α changes seem to be tied to the product formation but the α - $Y_{P/S}$ variation is superimposed on the μ - $Y_{P/S}$ relationship and complicates interpretation. The material balances for all of the batch experiments showed near stoichiometric conversion of glucose to lactate. In these runs, glucose was present in excess. When glucose was limiting, the conversion of glucose to lactic acid was a strong function of specific growth rate, particularly at low rates. The lactate yield constant curves extrapolate to a single specific growth rate values at $\mu = 0$, of $0.07\ hr^{-1}$ and at high rates, the yield asymptotically approaches the stoichiometric value of 2.0. The slope of the linear portion of the $Y_{P/S}$ curve varied from run to run as well as with changes in α during a run. There was no consistent correlation between this slope and α when all runs were considered. During any one run, a decrease in α resulted in a new curve with increased slope, and visa versa.

The metabolic pathway for the catabolism of glucose has been presented in the introductory section dealing with the published information on S. faecalus. In order to understand more fully the results found in this experimental program, a brief summary of the glycolytic pathway is presented here.

Glucose is converted via a series of enzymatically catalized steps to pyruvate.

$$\text{Glucose} + 2\ \text{ADP} + 2\ \text{Pi} + 2\ \text{NAD}^+ \rightarrow 2\ \text{pyruvate} + 2\ \text{ATP} + 2\ \text{NADH} + 2\ \text{H}^+.$$

In this sequence of steps, two moles of ATP and 2 moles of NADH are produced per mole of glucose. ATP is the common energy currency for the biosynthetic pathways, while NAD^+ is a hydrogen acceptor required during the glycolytic sequence. During the conversion of pyruvate to lactate, the NADH is oxidized and recycled.

$$\text{pyruvate} + \text{NADH} + \text{H}^+ \rightarrow \text{lactate} + \text{NAD}^+$$

Since NAD^+ is present in minute quantities, this co-factor must be regenerated. If pyruvate is converted to formate plus acetate, one mole of ATP is formed, but no NADH is oxidized.

$$\text{pyruvate} + \text{ADP} + \text{Pi} \rightarrow \text{formate} + \text{acetate} + \text{ATP}$$

Therefore, to ensure that the glycolytic sequence does not stop due to a lack of NAD^+, some other means of oxidizing NADH must occur. There are two possibilities. The first one involves the conversion of pyruvate to ethanol which would use a mole of NADH. Rosenberger and Elsden[3] found only formate and acetate when they grew S. faecalus in continuous culture. Almost identical results were found when the data of Rosenberger and Elsden were compared to those found here for the fraction of glucose which could be accounted for in the samples taken from the present steady state runs. Rosenberger and Elsden analysed for formate and acetate directly while in the present study the titration for total acid production was used together with the measured lactate concentration to

compute the other acids produced. Several samples from a high density transient run were analysed on a gas chromatograph and considerable quantities of ethanol were present. Unfortunately, the samples were old and the results were erratic. For these transient runs, the titration method for estimating the acid production was inaccurate due to the rapid changes in lactate production. However, the same type of relation was found between the NaOH consumed and the lactate produced, i.e., a decreased yield of lactate corresponded to an increase in the total base consumed. At very low lactate yields, only about 70-75% of the glucose could be accounted for and the remaining amount may be appearing as alcohol. The appearance of more than 2 moles of acid per mole of glucose indicates that some acetate and formate was produced so that NADH must be oxidized by some other means.

The second possibility assumes that the NADH is oxidized by a component in the nutrient medium. With 20 gm/l yeast extract in the medium, it is quite possible that sufficient material is available to act as a hydrogen acceptor. During the anaerobic fermention of S. faecalus using glycerol as substrate, Gunsalus[35] has demonstrated that yeast extract does contain a hydrogen acceptor. Although no direct evidence for a similar regeneration of NAD^+ was obtained here, such a reaction sequence is quite possible.

While the excess NADH appears to be accounted for, the additional energy produced during the formation of acetate and formate from pyruvate has not been. In fact, from the experimental data, no consumption of this ATP is evident for the amount of new cells produced per glucose consumed remains unchanging during periods where the lactate yield constant is drastically altered. Although changes in cell yield per mole of glucose do occur and they appear to be somehow connected with alterations in lactate yields, no direct correlation between them is evident. To illustrate this point, consider the results for Run TI which are shown in Fig. 46. At least four changes in α occur and they are accompanied by alterations in the lactate yield profile but there is no consistent relation between them. When

α increases from 6.77 to 10.2, a maximum in $Y_{P/S}$ results. A similar maximum occurs when α decreases from 10.2 to 5.34. It would appear, therefore, that whatever relationship exists, it must be rather tenuous.

Since the changes in α do not appear to be caused by changes in the distribution of metabolic end products of glucose catabolism, a complex interaction of the cell with its environment must be responsible. Whether the cell density has an effect is not known for no consistent correlation exists. To investigate the complicated interrelation of the catabolic and anabolic pathways, a much more intensive investigation using a completely defined medium would have to be undertaken with particular attention being paid to the analysis of the fermentation products.

SUMMARY

An experimental filtration-fermenter combination was designed and constructed for the investigation of microbial growth characteristics in batch, continuous and high cell density cultures. The micro-filtration technique for removal of cell-free product from the fermenter was successful. Filtration rates in excess of a liter per hour (2.2 ml/cm^2 hr) were maintained for several days with cell concentrations up to 20% packed cell volume. The maximum cell density obtained was 40% packed cell volume, a factor of 45 larger than could be obtained in the usual batch culture. Excellent filtration efficiency was achieved; the concentration of cells in the filtrate was six orders of magnitude smaller than in the fermenter.

The filtration-fermenter combination has a larger productivity per unit volume than a continuous stirred tank fermenter when both are operated at the same specific growth rate. The advantage of the filtration-fermenter over the continuous stirred tank increases with decreasing specific growth rate and with increasing filtration rate. Very large increases in productivity are possible at low specific growth rates. The application of high density fermentation to industrial processes will depend largely on the cost of filtration membranes which are expensive at present. The presence of a cell-free effluent is advantageous when product recovery systems require the separation of cells from the fermentation broth. The filtration equipment is more complex than a stirred tank but the added cost is offset by the smaller size required for the same throughout.

The anaerobic growth characteristics of S. faecalus were investigated at 37°C and pH 7.0. In batch culture, glucose was converted almost stoichiometrically to lactic acid. When an excess of glucose was present, dissociation of the rate of glucose consumption and growth rate occurred as the culture entered stationary phase. In continuous culture with glucose limitation, the fraction of glucose going to lactate decreased with dilution rate. The consumption of glucose for cell maintenance was negligible. Results in terms of substrate conversion, yields, viability, etc., from steady state high density experiments were similar to those obtained from low density continuous culture.

The transient high density experiments showed that the yield of cells per mole of glucose changed quite abruptly as a run progressed. Complex interactions between the cell and its environment were probably responsible. No consistent correlation between these yield changes and cell density was evident. The changes in cell yield were usually accompanied by alteration in the lactate yield constant but no correlation could be developed.

The transient technique of operating the filtration-fermenter and the plotting methods employed for the data obtained, can be used for the rapid determination of changes in metabolic pathways which affect cell and product yield constants.

PROPOSALS FOR FUTURE WORK

1. A definitive study of the filtration rate as a function of time, cell concentration and pressure drop should be undertaken.

2. The filtration of mycelial cultures using the rotating filter should be investigated. The viscosity of such cultures is primarily due to the inter-connecting mycelial strands. Little breakage of these strands should occur with the filter and a high flow rate may be possible without excessive power consumption.

3. Other filter membranes such as those produced by the Amicon Corp. should be tested. Greatly increased filtration rates may be possible.

4. The Amicon membranes can be used to separate macro-molecules such as proteins. A rotary filtration device may prove to have application in the large scale preparation of protein fractions.

5. The high density transient growth of S. faecalus should be continued using a completely defined medium in order that the inter-relationship between cell yield and lactate yield can be elucidated. These studies should also determine if the changes in cell yield still occur using the defined medium.

ACKNOWLEDGMENTS

Contributions to this study were made by many individuals and it is possible to mention only a few. The authors extend special thanks to Gene Powers for his assistance in the design and installation of the electronic equipment, to G. G. Young for his aid in solving the many mechanical problems which arose, to Ronald O'Dor for his assistance with several phases of the experimental program, and to S. Shapiro for performing the viscosity measurements.

This work was performed under the auspices of the United States Atomic Energy Commission.

REFERENCES

1. Robert Luedeking, The Lactic Acid Fermentation at Controlled pH; Kinetics of the Batch Process and Continuous Flow Theory and Experiments. (Ph.D. thesis) Univ. of Minnesota, September 1956.
2. Peter J. Reilly, Kinetics of Lactic Acid and Gluconic Acid Fermentations (Ph.D. thesis) University of Pennsylvania, 1964.
3. R. F. Rosenberger and S. R. Elsden, The Yields of S. faecalus Grown in Continuous Culture, J. Gen. Microbio. 22, 457 (1960).
4. J. Monod, La Technique de Culture Continue; Theorie et Applications. Ann. Inst. Pasteur 79, 330 (1950).
5. L. Michaelis and M. L. Menten, Biochem. Z. 49, 333 (1913).
6. D. Herbert, Continuous Culture of Micro-organisms; Some Theoretical Aspects, in Continuous Culture of Micro-organisms, edited by I. Malek, Academy of Science, Prague, (1958) p. 45.
7. Robert Luedeking and Edgar L. Piret, Transient and Steady States in Continuous Fermentation, Theory and Experiment, J. Biochem Microbiol. Tech. Eng. 1, 431 (1959).
8. Jack I. Northam, A Course of Bacterial Population Growth in Batch and Continuous Culture According to the Theory of Monod, J. Biochem. Microbiol.Tech. Eng. 1, 349 (1959).
9. I. Malek and Z. Fencil, Continuous Culture of Micro-organisms, a Review, Folia Microbiologica, 6 192 (1961)
10. Victor Henry Edwards and C. R. Wilke, Analytical Methods in Bacterial Kinetics, UCRL-16398, January 1967.
11. Ping Shu, Mathematical Models for the Product Accumulation in Microbiological Processes, J. Biochem. Microbiol. Tech. Eng. 3, 95 (1961).
12. A. G. Fredrickson and H. M. Tsuchiya, Continuous Propagation of Micro-organisms, A. I. Ch. E. J. 9, 459 (1963).
13. H. M. Tsuchiya, A. G. Fredrickson and R. Aris, Dynamics of Microbial Cell Populations, Adv. Chem. Eng. 6, 125 (1966).
14. Proceedings of the U. S. - Japan Seminar on Dynamics of Microbial Populations, J. Ferm. Tech. 44 (1966).
15. Philipp Gerhardt and D. M. Gallup, Dialysis Flask for Concentrated Cultures of Micro-organisms, J. Bacteriol. 86, 919 (1963).

16. D. M. Gallup and Philipp Gerhardt, Dialysis Fermentation Systems for Concentrated Culture of Micro-organisms, Appl. Microbiol. 11, 506 (1963).
17. Philipp Gerhardt and Jerome S. Schultz, Dialysis Culture, J. Ferm. Technol. 44, 349 (1966).
18. Philipp Gerhardt, J. U. Pedersen, H. E. B. Humphrey, Jr., and J. S. Schultz, The Biodialyser; A Multiple-Plate Exchanger for Dialysis Fermentations, 152nd Meeting of the American Chemical Society (Division of Microbial Chemical and Technology) New York, New York, September 1966.
19. H. E. B. Humphrey, Jr. and Philipp Gerhardt, Performance Characteristics of a Prototype Biodialyser, Ibid.
20. J. Downs Herold, J. S. Schultz Philipp Gerhardt, Differential Dialysis Culture for Separation and Concentration of Cells and Macro-molecular Products, Ibid.
21. J. S. Schultz and Philipp Gerhardt, Kinetics of Dialysis Culture, ibid.
22. Ashok Kumar Bhagat and C. R. Wilke, Filtration Studies with Ultrafine Particles, UCRL-16574, September 1966.
23. I. C. Gusalus and C. F. Niven, The Effect of pH on the Lactic Acid Fermentation, J. Biol. Chem. 145, 131 (1942).
24. M. Gibbs, J. T. Sokatch and I. C. Gunsalus, Product Labeling of Glucose-1-C^{14} Fermentation by Homo-fermentative and Hetero-fermentative Lactic Acid Bacteria, J. Bact. 70, 572 (1955).
25. T. B. Platt and E. M. Foster, J. Bact. 75, 453 (1958).
26. T. Bauchop and S. R. Elsden, The Growth of Micro-organisms in Relation to Their Energy Supply, J. Gen. Microbiol. 23, 457 (1960).
27. Henry R. Mahler and Eugene H. Cordes, Biological Chemistry (Harper and Row, 1966) p. 436.
28. G. Toennies and G. D. Shockman, Growth Chemistry of S. faecalus, Proc. Intern. Cong. Biochem. 4th Vienna, 13, 365 (1959).
29. Boguslaw Wojciech Kusmierek, The Transient Response of a Continuous Fermentation (M.S. thesis) Massachusetts Institute of Technology, August 1959.

30. B. E. Baber and N. A. Khan, Quantitative Determination of Amino Acids in Undesalted Hydrolysates by Buffer Filter Paper Chromatography, J. Sci. Food Agri. 8, 217 (1957).

31. Allen G. Marr, E. H. Nilson and D. J. Clark, The Maintenance Requirement of Escherichia coli, Ann. New York Acad. Sci. 102, 536 (1963).

32. E. A. Dawes and D. W. Ribbons, Studies on the Endogenous Metabolism of Escherichia coli, Biochem. J. 95, 332 (1965).

33. S. J. Pirt, The Maintenance Energy of Bacteria in Growing Cultures, Proc. Roy. Soc., Ser. B 163, (991) 224 (1965).

34. E. A. Dawes and D. W. Ribbons, Bact. Rev. 28, 126 (1964).

35. I. C. Gunsalus, Products of Anaerobic Glycerol Fermentation by S. faecalus, J. Bact. 54, 239 (1947).

36. Robert Luedeking and Edgar L. Piret, A Kinetic Study of the Lactic Acid Fermentation: Batch Process at Controlled pH. J. Biochem. Microbiol. Tech. Eng. 1, 393 (1959).

NOMENCLATURE

Variables

k	proportionality constant
K	proportionality constant
N	bacterial density, optical density units
P	product concentration, mM/l.
PR	productivity ratio
S	substrate concentration, mM/l.
t	time, hours
V	fermenter volume, liters
v	flow rate, liters/hour
Y	yield constant

Subscripts.

F	filtrate
f	feed
B	bleed
0	initial quantity
P/S	product from substrate
G	growth
C/S	cells from substrate

Greek Letters

μ	specific/growth rate, $hours^{-1}$
α	substrate consumed/yield of new cells, mM/l/OD
β	maintenance term, mM/l/OD hr.

APPENDIX

Nutrient Composition

The nutrient medium contained many components. To simplify formulation, the constituents were divided into several groups so that those present in small amounts could be made up in high concentration and then added to the nutrient medium in small aliquots. The vitamin solution, also called the trace component solution, TCS, and the mineral solution were used for both the semi-defined and the complex media. In the following section where the numerical data are presented, alterations, if any, to the standard nutrient recipe for each run is given.

Tables I and II contain the vitamin and mineral solution compositions respectively. Table III contains the recipe for the semi-defined medium and Table IV shows the composition of the complex medium.

The sources for the chemicals were:

1. Yeast Extract - Difco Labs, Detroit, Michigan
2. Minerals and Salts - B & A Quality, General Chemical Div., Allied Chemical Co.
3. Glucose (Anhydrous Dextrose) - Mallinckrodt Chemical Works, St. Louis, Mo.
4. Vitamins and other biological chemicals - Calbiochem, Los Angeles, Calif.

Table A-I. Trace Component Recipe.

Component	mg/liter final medium
Nicotinamide	1.
Ca Pantothanate	1.
Riboflavin	1.
Pyrodoxin · HCℓ	2.
Folic Acid	0.1
Biotin	0.1

This recipe was made up in a 1/2 normal HCl solution to a concentration 400 times that in the final medium and added to the nutrient at the rate of 2.5 ml/liter.

Table A-II. Mineral Solution

Component	gm/liter of Stock Solution
MgO	10.75
$CaCO_3$	2.0
$FeSO_4 \cdot 7H_2O$	4.5
$ZnSO_4 \cdot 7H_2O$	1.44
$MnSO_4 \cdot H_2O$	.80
$CuSO_4 \cdot 5H_2O$	0.25
$CoSO_4 \cdot 7H_2O$	0.28
H_3BO_3	0.06
HCl, Concentrated	51.3 ml.

This solution is added to the final medium at the rate of 5.0 ml/l.

Table A-III. Semi-defined Medium.

Component	gm/liter final medium
Enzymatic Hydrolysed Casein	10.0
Cysteine · HCℓ	0.2
Tryptophan	0.2
Asparagine·H_2O	0.2
Adenine	0.03
Uracil	0.03
Guanine	0.03
Sodium Acetate, Anhydrous	4.0
Ammonium Sulfate	2.0
Postassium Monohydrogen Phosphate · 3 H_2O	3.0
Postassium Dihydrogen Phosphate	1.5
Vitamin Solution	2.5 ml.
Mineral Solution	5.0 ml.
Glucose	15.0

Table A-IV. Complex Medium.

Component	gm/liter final medium
Yeast Extract	20.0
Sodium Acetate, Anhydrous	4.0
Ammonium Sulfate	2.0
Potassium Monohydrogen Phosphate · $3H_2O$	6.0
Potassium Dihydrogen Phosphate	1.5
Vitamin Solution	1.5 ml
Mineral Solution	2.0 ml
Glucose	7.0

Numerical Data

Batch Experiments. The batch experiments were conducted using slightly differing medium compositions. The details for the different runs are described below with the alterations in composition as noted.

Run S: semi-defined medium.

Run AB: complex medium with 3 gm/l dihydrogen phosphate, 15 gm/l monohydrogen phosphate respectively, 10 gm/l glucose, initially. 6 gm/ℓ glucose added later.

Run AC: complex medium with 3 gm/l dihydrogen phosphate, 12 gm/l monohydrogen phosphate and 30 gm/l glucose.

Run AE: complex medium with 30 gm/l yeast extract, 1 gm/l dihydrogen phosphate, 4 gm/l monohydrogen phosphate and 30 gm/l glucose.

Run AI: complex medium.

The substrate and product concentrations and the amount of NaOH added to the broth are tabulated in Tables 5 through 9 on the basis of 1 liter of nutrient medium.

Table A-V. Batch Experimental Run S.

Sample number	time (hr.)	cell concentration (OD)	viable count per ml	glucose concentration (mM/l)	lactate concentration (mM/l)	NaOH added between sample times (mM/l)	Total NaOH added (mM/l)	NaOH addition[1] rate, d(NaOH)/dt (mM/l hr.)	specific growth[2] rate, μ ($hr.^{-1}$)
1	.5	.094	2.16×10^7	75.2	2.1		0	1.8	1.79
2	1.	.234	5.77×10^7	70.5	4.0	1.5	1.5	5.4	1.79
3	1.5	.583	1.86×10^8	72.1	8.8	4.7	6.2	13.9	1.73
4	2.	1.22	4.01×10^8	65.5	16.2	9.6	15.8	23.2	1.34
5	2.5	2.24	5.41×10^8	57.2	32.8	13.8	29.6	29.8	.95
6	3.	3.32	7.39×10^8	48.6	46.8	15.4	45.0	33.8	.61
7	3.5	4.17	6.77×10^8	36.5	72.3	18.1	63.1	36.8	.34
8	4.	4.85	8.02×10^8	26.9	89.3	21.4	84.5	39.3	.28
9	4.5	5.34	1.03×10^9	13.9	116.4	16.8	103.3	41.4	.25
10	5.	6.19	1.05×10^9	4.1	139.6	21.3	124.6	43.2	.22

(1) d(NaOH)/dt was determined from a smoothed semi-log plot.

(2) μ was determined from the slope of a semi-log plot.

Table A-VI. Batch Experimental Run AB.

Sample number	time (hr.)	cell concentration (OD)	glucose concentration (mM/l)	lactate concentration (mM/l)	NaOH added between sample times (mM/l)	Total NaOH added (mM/l)	NaOH addition (1) rate, d(NaOH)/dt (mM/l hr.)	specific growth (2) rate, μ ($hr.^{-1}$)
0	0	0.051	49.4	0	0	0	-	-
1	0.5	0.053	52.8	2.2	0	0	2.36	-
2	1.	0.106	50.2	-	0	0	4.32	1.38
3	1.5	0.218	48.5	4.8	4.5	4.5	7.9	1.73
4	2.	0.546	46.9	11.5	6.0	10.5	14.4	1.73
5	2.5	1.26	39.1	18.6	9.6	20.1	26.2	1.58
6	3.	2.63	30.8	39.1	18.2	38.3	47.6	1.31
7	3.5	4.81	18.3	70.7	32.3	70.6	72.8	.84
8 (3)	4.	6.43	2.2	98.3	35.8	106.4	78.5	.52
9	4.5	8.27			42.0	148.4	75.0	.32
10	5.	9.07			34.7	183.1	60.	.12

(1) d(NaOH)/dt was determined from a smoothed semi-log plot.

(2) μ was determined from the slope of a semi-log plot.

(3) 6 gm/l glucose added to fermenter.

Table A-VII. Batch Experimental Run AC.

Sample number	time (hr.)	cell concentration (OD)	glucose concentration (mM/l)	lactate concentration (mM/l)	NaOH added between sample times (mM/l)	Total NaOH added (mM/l)	NaOH addition rate, d(NaOH)/dt [1] (mM/l hr.)	specific growth rate, μ [2] ($hr.^{-1}$)
0	0	.045	161.	0	0	0	-	-
1	.5	.052	141.5	2.1	0	0	.9	-
2	1.	.088	159.	-	1.2	1.2	1.85	1.32
3	1.5	.197	159.	5.0	1.5	2.7	4.55	1.70
4	2.	.508	150.5	8.8	3.6	6.3	11.2	1.70
5	2.5	1.14	150.	16.3	8.5	14.8	25.2	1.70
6	3.	2.34	122.	35.0	17.6	32.4	49.5	1.41
7	3.5	4.49	128.	69.4	31.8	64.2	83.	1.10
8	4.	7.17	95.7	108.	49.0	113.2	125.	.73
9	4.5	9.87	75.0	162.	71.	184.	146.	.50
10	5.	11.7	39.6	230.	73.	257.	152.	.37
11	5.5	14.4	6.5	283	77.	334.	158.	.25

(1) d(NaOH)/dt was determined from a smoothed semi-log plot.

(2) μ was determined from the slope of a semi-log plot.

Table -VIII. Batch Experimental Run AE.

Sample number	time (hr.)	cell concentration (OD)	glucose concentration (mM/l)	NaOH added between sample times (mM/l)	Total NaOH added (mM/l)	NaOH addition rate, d(NaOH)/dt (mM/l hr.) [1]	specific growth rate, μ ($hr.^{-1}$) [2]
0	0	0.05		0.0	0.0	-	-
1	0.5	0.057	155.	1.7	1.7	1.1	-
2	1.	0.097	155.	3.4	5.1	2.2	1.44
3	1.5	0.259	156.	4.8	9.9	4.5	1.44
4	2.	0.521	152.	6.7	16.6	9.0	1.44
5	2.5	1.06	147.	7.3	23.9	17.9	1.44
6	3.	2.24	126.	12.8	36.7	36.3	1.42
7	3.5	4.16	128.	25.8	62.5	69.0	1.15
8	4.	6.79	105.	42.1	104.6	96.0	0.68
9	4.5	8.58	79.6	52.8	157.4	110.	0.37
10	5.	9.87	50.5	55.9	213.3	110.	0.17
11	5.5	10.3	-	52.4	265.7	98.5	0.0
12	5.92	10.1	3.4	37.7	303.4	80.	0.0

(1) d(NaOH)/dt was determined from a smoothed semi-log plot.

(2) μ was determined from the slope of a semi-log plot.

Table A-IX. Batch Experimental Run AI.

Sample number	time (hr.)	cell concentration (OD)	NaOH added between sample times (mM/l)	Total NaOH added (mM/l)	NaOH addition rate, d(NaOH)/dt (1) (mM/l hr.)	specific growth rate, μ (2) ($hr.^{-1}$)
0	0	0.055	0.0	0.0	-	-
1	0.5	0.068	0.0	0.0	1.05	-
2	1.	0.111	1.1	1.1	2.25	1.26
3	1.5	0.226	1.1	2.2	4.8	1.52
4	2.	0.482	3.6	5.8	10.5	1.52
5	2.5	1.074	7.7	13.5	21.8	1.52
6	3.	2.31	15.8	29.3	44.5	1.52
7	3.5	4.41	29.8	59.1	68.	1.05
8	3.7	4.99	14.2	73.3	-	-

(1) d(NaOH)/dt was determined from a smoothed semi-log plot.

(2) μ was determined from the slope of a semi-log plot.

Note: Initial glucose concentration was 38.0 mM/l.

Continuous Stirred Tank Numerical Data

The nutrient for the continuous experiments was the complex medium shown in Table IV. The numerical data for these runs are presented in Tables 10 and 11.

Table A-X. -Continuous Stirred Tank Experimental Run CC.

Sample number	Effluent flow rate / Nutrient flow rate (v/v_f)	Dilution rate, v/V ($hr.^{-1}$)	Glucose concentration (mM/l)	Lactate concentration (mM/l)	NaOH[1] addition (mM/l)	Cell concentration (OD)	Cell concentration (dry weight mg/ml)	Dry weight / OD (mg/ml·OD)	Lactate yield constant, $Y_{P/S}$ (mM lactate/ mM glucose)	Acetate + formate (by titration method) (mM/l)	Fraction of Glucose fed accounted for in the effluent (from Eq. 10)
5	1.051	0.222	0.	65.3	87.1	4.52	1.54	0.348	1.95	15.9	1.08
6	1.024	0.809	0.	67.5	79.0	4.42	-	-	2.01	5.8	1.04
7	1.101	0.106	0.	44.0	96.5	4.60	1.71	0.373	1.33	48.1	0.99
8	1.031	0.469	0.	59.5	86.3	4.50	1.73	0.383	1.78	20.9	1.04
9	1.046	1.49	15.3	45.0	40.8	2.90	0.96	0.330	1.99[2]	0.	1.14

(1) NaOH addition per liter of nutrient feed.

(2) Based on NaOH added.

Note: Glucose concentration in the nutrient feed was 36.5 mM/l.

Table A-XI. Continuous Stirred Tank Experimental Run CJ.

Sample number	Nutrient feed rate / Nutrient flow rate (v/v_r)	Dilution rate, v/V ($hr.^{-1}$)	Glucose concentration (mM/l)	Lactate concentration (mM/l)	NaOH[1] addition (mM/l)	Cell concentration (OD)	Cell concentration (dry weight mg/ml)	Dry weight (OD) (mg/ml·OD)	Lactate yield constant, $Y_{P/S}$ (mM lactate/ mM glucose)	Acetate + formate (by titration method) (mM/l)	Fraction of Glucose fed accounted for in the effluent (from Eq. 10)
3	1.103	0.196	0.	45.7	100.0	5.31	1.84	0.346	1.30	49.6	0.968
4	1.092	0.351	0.	46.6	95.3	5.41	1.88	0.348	1.31	43.8	0.940
5	1.082	1.26	0.6	61.7	78.7	4.87	1.68	0.345	1.75	19.9	1.01
6	1.092	0.209	0.	45.8	91.5	5.39	1.85	0.344	1.29	41.5	0.910
7	1.081	1.10	0.	61.0	78.8	4.97	1.72	0.346	1.69	12.9	0.932
8	1.068	1.31	3.5	58.8	65.3	4.45	1.52	0.342	1.78	2.5	0.920
9	1.082	1.55	22.1	31.7	27.9	2.17	.69	0.318	2.03	0.	1.00
10	1.099	0.222	0.	43.6	94.5	5.43	1.83	0.337	1.23	46.6	0.917
11	1.110	0.061	0.	27.5	109.2	4.09	1.64	0.401	0.78	78.7	0.900
12	1.092	0.621	0.	51.8	89.3	4.23	1.36	0.321	1.50	32.7	0.956
13	1.088	0.837	0.	57.2	86.0	4.17	1.36	0.326	1.64	23.8	0.980
14	1.084	1.09	0.	61.1	81.8	4.17	1.65	0.395	1.75	15.6	0.978

(1) NaOH addition per liter of nutrient feed.

Note: Glucose concentration in the nutrient feed was 38.9 mM/l for samples 3 to 11 and 37.8 mM/l for samples 12 to 14.

Continuous Stirred Tank Experiments with Filtration

The data for the steady state fermentation with filtration are shown in Table 12. The data for the transient high density experiments are summarized in Tables 13 to 19 inclusive. The nutrient for these runs was the complex medium presented in Table 4. The glucose concentration in the effluent of all of the high density experiments was essentially zero.

The concentration of the NaOH was 1.03 normal and 2.4 mℓ was required to adjust a liter of nutrient feed to 7.0 pH.

Table XII. Steady State High Density Experimental Run HEA.

Sample number	Filtrate flow rate (ml/hr)	Bleed flow rate (ml/hr)	NaOH flow rate (ml/hr)	Nutrient flow rate (ml/hr)	Dilution rate, v_B/V (hr^{-1})	glucose concentration in nutrient feed (mM/l)	lactate concentration (mM/l)	NaOH[1] addition (mM/l)	cell concentration in bleed (OD)
1a	144	121	21.4	244	0.195	38.9	53.4	88.0	11.0
2	374	111	41.4	444	0.179	38.9	39.0	93.7	22.1
3	803	108	74.3	837	0.174	39.3	48.2	89.1	42.6
4	1330	145	125	1350	0.234	39.3	44.9	93.1	42.8
5	342	58.3	37.8	362	0.094	39.3	16.4	105.2	32.8
6	181	134	30.0	285	0.216	38.7	30.1	106	11.8

Sample number	cell concentration in filtrate (OD)	cell concentration in bleed (dry weight mg/ml)	cell concentration in bleed (viable count/ml)	cell concentration in bleed (total count/ml)	percent viable	dry weight/OD (mg/ml)	lactate yield constant, $Y_{P/S}$ (mM lactate/ mM glucose)	formate + acetate(by titration method) (mM/l)	fraction of glucose fed accounted for in the effluent (from Eq. 10)
1a	0.81	3.52	-	7.7×10^9	-	0.320	0.745	30.0	0.938
2	0.61	7.36	9.22×10^9	1.2×10^{10}	77	0.333	0.546	51.1	0.876
3	0.01	14.7	3.50×10^{10}	3.9×10^{10}	90	0.345	0.669	36.6	0.902
4	0.41	13.6	2.28×10^{10}	2.6×10^{10}	87	0.318	0.625	44.1	0.903
5	0.04	12.3	2.35×10^{10}	4.1×10^{10} *	57	0.375	0.231	87.1	0.785
6	0.0	4.16	-	1.5×10^{10}	-	0.353	0.430	73.0	0.901

(1) NaOH addition per liter of nutrient feed.

* A dilution error may have occurred, for this value appears to be too large by a factor of two.

Table XIII. Transient High Density Experimental Run TB.

Sample number	time (hr.)	filtrate flow rate (ml/hr)	bleed flow rate (ml/hr)	NaOH flow rate (ml/hr)	nutrient flow rate (ml/hr)	lactate concentration (mM/l)	NaOH[1] addition (mM/l)	cell concentration in bleed (OD)	α (mM/l glucose /OD)	specific growth[2] rate, μ (hr^{-1})	lactate yield[3] constant, $Y_{P/S}$ (mM lactate/ mM glucose)
0	0							36.6	-	0.259	1.19
1	0.5	972	55.7	92.3	936	32.7	99.2	38.0	6.24	0.239	1.15
2	1.	953	55.7	91.8	917	36.4	100.7	40.2	6.24	0.222	1.11
3	2.	953	49.0	90.9	911	38.0	100.6	46.0	6.24	0.203	1.03
4	3.	947	54.3	92.6	908	35.7	102.8	50.0	6.24	0.180	0.93
5	4.	950	58.4	95.0	913	31.8	104.7	55.4	6.24	0.163	0.81
6	5.	952	55.1	95.8	911	27.5	105.9	60.4	6.24	0.154	0.71
7	6.	962	56.9	96.3	923	27.4	105.	66.8	6.24	0.144	0.64
8	7.	960	54.7	98.2	917	22.6	107.8	66.0	6.24	0.138	0.59
9	9.	960	57.9	95.4	923	25.2	104.	73.6	6.24	0.125	0.49

Note: a) Glucose concentration in the nutrient feed was 38.7 mM/l.
b) Cell concentration in filtrate was essentially zero.

(1) NaOH addition per liter of nutrient feed.

(2) Calculated using Eq. (23).

(3) Taken from smoothed curve of $Y_{P/S}$ (calculated from Eq. (31)) versus time.

Table XIV. Transient High Density Experimental Run TC.

Sample number	time (hr.)	filtrate flow rate (ml/hr)	bleed flow rate (ml/hr)	NaOH flow rate (ml/hr)	nutrient flow rate (ml/hr)	lactate concentration (mM/l)	NaOH[1] addition (mM/l)	cell concentration in bleed (OD)	α (mM/l glucose /OD)	specific growth[2] rate, μ (hr^{-1})	lactate yield[3] constant, $Y_{P/S}$ (mM lactate/ mM glucose)
0	0							11.8	6.25	0.682	2.0
1	1.0	872.	28.	78.1	822.	56.5	106.	18.7	6.25	0.430	1.28
2	2.	867.	28.	82.9	812.	42.5	103.	25.8	6.25	0.312	0.91
3	3.	863.	28.	82.9	808.	33.2	103.	32.4	6.25	0.248	0.79
4	4.	854.	28.	82.0	800.	31.0	103.	37.4	7.89	0.170	0.89
5	5.	848.	28.	82.0	794.	35.0	104.	42.0	7.89	0.152	0.89
6	6.	853.	28.	82.0	797.	31.0	104.	46.4	7.89	0.137	0.70

Note: a) Glucose concentration in the nutrient feed was 38.7 mM/l.

b) Cell concentration in the filtrate was essentially zero.

(1) NaOH addition per liter at nutrient feed.

(2) Calculated using Eq. (23).

(3) Taken from smoothed curve of $Y_{P/S}$ (calculated by Eq. (31)) versus time.

Table XV. Transient High Density Experimental Run TD.

Sample number	time (hr.)	filtrate flow rate (ml/hr)	bleed flow rate (ml/hr)	NaOH flow rate (ml/hr)	nutrient flow rate (ml/hr)	lactate concentration (mM/l)	NaOH[1] addition (mM/l)	cell concentration in bleed (OD)	cell concentration in filtrate (OD)	α (mM/l glucose /OD)	specific growth[2] rate, μ (hr^{-1})	lactate yield[3] constant, $Y_{P/S}$ (mM lactate/ mM glucose)
0	0					43.2		10.7	0.	6.86	0.857	2.
1	1.	1125	28.0	88.	1065	62.3	82.7	18.2	0.	6.86	0.504	1.64
2	2.	1123	28.0	100	1051	49.0	94.2	27.0	0.	6.86	0.340	1.15
3	3	1116	28.0	107	1037	34.1	104.	35.8	0.	6.86	0.249	0.96
4	4	1110	28.0	109	1029	23.6	107.	43.0	0.	6.86	0.206	0.54
5	5	1094	28.0	111	1011	17.1	111.	50.4	0.	6.86	0.173	0.42
6	6	1069	28.0	110	987	13.9	112.	54.4	0.	6.86	0.156	0.35
7	7	1061	28.0	110	979	11.0	113.	62.8	0.04	6.86	0.134	0.29
8	8	1052	28.0	107	973	9.6	111.	68.0	0.24	6.86	0.123	0.25

Note: Glucose concentration in the nutrient feed was 37.9 mM/l.

(1) NaOH addition per liter of nutrient feed.

(2) Calculated Using Eq. (23).

(3) Taken from smoothed curve of $Y_{P/S}$ (calculated by Eq.(31)) versus time.

Table XVI. Transient High Density Experimental Run TE.

Sample number	time (hr.)	filtrate flow rate (ml/hr)	bleed flow rate (ml/hr)	NaOH flow rate (ml/hr)	nutrient flow rate (ml/hr)	lactate concentration (mM/l)	NaOH[1] addition (mM/l)	cell concentration in bleed (OD)	cell concentration in filtrate (OD)	α (mM/l glucose /OD)	specific growth[2] rate, μ (hr^{-1})	lactate yield[3] constant, $Y_{P/S}$ (mM lactate/ mM glucose)
2	0	1028	90	96.5	1051	65.4	92.1	20.2	.13	7.09	0.440	1.60
3	1	1030	90	96.5	1043	57.0	92.8	26.2	.05	7.09	0.342	1.52
4	2	1041	90	97.2	1034	52.8	94.4	28.8	.05	10.4	0.208	1.43
5	3	1043	90	97.2	1036	49.5	94.2	30.4	.05	10.4	0.197	1.34
6	4	1042	90	98.2	1044	44.6	94.4	32.2	.05	10.4	0.187	1.26
7	5	1041	90	100.	1031	43.2	97.5	33.6	.05	10.4	0.179	1.17
8	7	1026	90	100.	1026	35.3	98.1	35.4	.20	10.4	0.168	1.0

Note: Glucose concentration in the nutrient feed was 37.9 mM/l.

(1) NaOH addition per liter of nutrient feed.

(2) Calculated using Eq. (23).

(3) Taken from smoothed curve of $Y_{P/S}$ (calculated by Eq.(31)) versus time.

Table XVII. Transient High Density Experimental Run TF.

Sample number	time (hr.)	filtrate flow rate (ml/hr)	bleed flow rate (ml/hr)	NaOH flow rate (ml/hr)	nutrient flow rate (ml/hr)	lactate concentration (mM/l)	NaOH[1] addition (mM/l)	cell concentration in bleed (OD)	cell concentration in filtrate (OD)	α (mM/l glucose /OD)	specific growth[2] rate, μ (hr^{-1})	lactate yield[3] constant, $Y_{P/S}$ (mM lactate/ mM glucose)
0	0					-		8.0	-	9.00	0.657	2.0
1	1	772	90	73.6	788	75.1	93.8	13.2	0.17	9.00	0.399	1.86
2	3	770	90	71.8	788	61.6	91.5	18.9	0.05	9.00	0.278	1.58
3	4	769	90	72.7	786	55.0	92.8	21.7	0.04	9.00	0.242	1.45
4	5	763	90	72.7	780	50.2	93.2	23.3	0.03	9.00	0.226	1.33
5	8	775	90	78.1	787	37.5	99.8	30.3	0.03	6.61	0.233	1.07
6	13.3	768	90	82.7	775	21.4	107.5	40.4	0.02	6.61	0.174	0.61
7	25.	736	90	81.8	747	18.6	110.3	46.2	0.01	6.61	0.152	0.51

Note: Glucose concentration in the nutrient feed was 38.4 mM/l.

(1) NaOH addition per liter of nutrient feed.

(2) Calculated using Eq. (23).

(3) Taken from smoothed curve of $Y_{P/S}$ (calculated by Eq. (31)) versus time.

Table XVIII. Transient High Density Experimental Run TI.

Sample number	time (hr.)	filtrate flow rate (ml/hr)	bleed flow rate (ml/hr)	NaOH flow rate ml/hr)	nutrient flow rate (ml/hr)	lactate concentration (mM/l)	NaOH[1] addition (mM/l)	cell concentration in bleed (OD)	α (mM/l glucose /OD)	specific growth[2] rate, μ (hr^{-1})	lactate yield[3] constant, $Y_{P/S}$ (mM lactate/ mM glucose)
0	0					19.9		9.90		0.881	2.0
1	1	948	28	77.3	899	58.5	86.3	16.5	6.77	0.528	1.68
2	2	966	28	84.5	909	57.1	93.4	24.0	6.77	0.364	1.43
3	3	973	28	88.2	913	49.9	97.1	30.8	6.77	0.284	1.20
4	4	976	28	91.0	913	41.9	100	39.6	6.77	0.220	0.97
5	5	980	28	94.0	914	32.4	104	44.0	6.77	0.198	0.83
6	6	983	28	95.4	916	30.9	105	50.0	10.2	0.115	0.97
7	7	977	28	89.2	916	39.8	98.	54.0	10.2	0.107	1.31
8	8	968	28	85.0	911	48.4	93.7	58.4	10.2	0.099	1.27
9	9	971	28	88.0	911	37.9	97.3	62.2	10.2	0.093	0.94
10	11	960	28	97.3	911	30.9	108.	78.8	5.34	0.140	0.57
11	12	980	28	96.5	911	21.2	107.	86.8	5.34	0.127	0.48
12	13	989	28	98.2	919	16.8	108.	93.6	5.34	0.118	0.42
13	14	989	28	97.5	919	15.0	107.	96.8	5.34	0.114	0.40
14	15	990	28	97.5	920	15.4	107.	108.	5.34	0.102	0.45
15	19	990	28	95.4	920	25.7	104.	128.	5.34	0.086	0.71
16	24	990	28	95.0	920	19.7	104.	128.	10.4	0.045	0.47
17	25	988	28	95.0	921	13.0	104.	123.	10.4	0.046	0.36
18	26	983	28	95.0	921	12.4	104.	125.	10.4	0.046	0.33
19	28	988	28	95.0	921	10.3	104.	127.	-	0.069	0.30
20	33	988	28	95.0	921	9.9	104.	140.	-	0.063	0.25
21	38	995	28	102.0	921	7.1	112.	146.	-	0.060	0.20

Note: a) Glucose concentration in the nutrient feed was 40.0 mM/l.
b) Cell concentration in the filtrate was essentially zero.

(1) NaOH addition per liter of nutrient feed.

(2) Calculated using Eq. (23).

(3) Taken from smoothed curve of $Y_{P/S}$ (calculated by Eq.(21)) versus time.

Table XIX. Transient High Density Experimental Run TJ.

Sample number	time (hr.)	filtrate flow rate (ml/hr)	bleed flow rate (ml/hr)	NaOH flow rate (ml/hr)	nutrient flow rate (ml/hr)	lactate concentration (mM/l)	NaOH[1] addition (mM/l)	cell concentration in bleed (OD)	cell concentration (viable count/ml)	viable count/OD	α (mM/l glucose /OD)	specific growth[2] rate, μ (hr^{-1})	lactate yield[3] constant, $Y_{P/S}$ (mM lactate/ mM glucose)
0	0	591	-	60.	531	7.1	114	146	-	-	7.3	0.035	0.2
1	6	591	4.	60.	535	-	113	172	-	-	7.3	0.030	-
2	11	600	1.6	60.	540	-	112	201	-	-	7.3	0.025	-
3	17	597	1.4	60.	537	-	113	217	-	-	7.3	0.009	-
4	23	600	1.8	60.	540	-	112	226	-	-	15.	0.009	-
5	28.7	598	2.	60.	540	-	112	242	-	-	15.	0.008	-
6	35	590	2.	61.	531	-	117	257	1.99×10^{11}	7.75×10^{8}	15.	0.008	-
7	41	593	1.4	60.	533	-	113	265	2.14×10^{11}	8.07×10^{8}	-	0.008	-
8	47	594	-	60.	534	9.2	113	270	2.10×10^{11}	7.78×10^{8}	-	0.007	.25

Note: a) Glucose concentration in the nutrient feed was 40.0 mM/l.
b) Cell concentration in the filtrate was essentially zero.

(1) NaOH addition per liter of nutrient feed.

(2) Calculated using Eq (23).

(3) Taken from smoothed curve of $Y_{P/S}$ (calculated by Eq. (51)) versus time.

Table XX. Viscosity Measurements of Sample TJ8.

No dilution, OD = 270		2:1 dilution with buffer		5:1 dilution with buffer		10:1 dilution with buffer		supernatent of centrifuged sample	
shear rate ($sec^{-1} \times 10^{-3}$)	viscosity (centipoise)	shear rate ($sec^{-1} \times 10^{-3}$)	viscosity (centipoise)	shear rate ($sec^{-1} \times 10^{-3}$)	viscosity (centipoise)	shear rate ($sec^{-1} \times 10^{-3}$)	viscosity (centipoise)	shear rate ($sec^{-1} \times 10^{-3}$)	viscosity (centipoise)
9.32	6.34	6.95	1.93	6.83	1.52	10.9	1.53	7.78	1.85
7.17	5.74	8.67	2.19	8.79	1.52	12.5	1.58	9.69	1.97
9.80	5.20	10.1	2.30	9.84	1.61	10.9	1.47	11.2	2.12
11.2	5.00	12.0	2.39	10.8	1.70	9.90	1.44	12.3	2.08
12.6	4.60	13.2	2.42	12.1	1.76	11.6	1.47	13.5	2.05
11.0	5.05	11.6	2.33					14.6	2.06
9.29	5.42	10.3	2.27					9.65	2.05
7.52	5.83	8.59	2.17					8.79	1.98
5.58	6.52	7.20	1.90					7.75	1.83
		6.27	1.90					9.17	1.99
		5.30	1.93					9.50	2.04
		14.3	2.43						
		(Irreversible changes occurred due to shear)							
		15.6	2.59						
		16.4	2.60						
		4.90	2.43						
		3.97	2.49						
		4.07	2.43						
		5.20	2.35						
		6.47	2.22						
		8.52	2.47						
		10.4	2.54						
		10.6	2.59						

nutrient feed		sample washed twice and re-suspended in buffer to OD = 270	
shear rate ($sec^{-1} \times 10^{-3}$)	viscosity (centipoise)	shear rate ($sec^{-1} \times 10^{-3}$)	viscosity (centipoise)
8.85	1.25	5.62	4.06
9.95	1.34	7.53	3.89
11.0	1.42	9.19	3.68
11.7	1.46	10.8	3.54
13.0	1.52	11.7	3.40
14.0	1.73	13.0	3.40